

INFORMATION TO USERS

This manuscript has been reproduced from the microfilm master. UMI films the text directly from the original or copy submitted. Thus, some thesis and dissertation copies are in typewriter face, while others may be from any type of computer printer.

The quality of this reproduction is dependent upon the quality of the copy submitted. Broken or indistinct print, colored or poor quality illustrations and photographs, print bleedthrough, substandard margins, and improper alignment can adversely affect reproduction.

In the unlikely event that the author did not send UMI a complete manuscript and there are missing pages, these will be noted. Also, if unauthorized copyright material had to be removed, a note will indicate the deletion.

Oversize materials (e.g., maps, drawings, charts) are reproduced by sectioning the original, beginning at the upper left-hand corner and continuing from left to right in equal sections with small overlaps.

Photographs included in the original manuscript have been reproduced xerographically in this copy. Higher quality 6" x 9" black and white photographic prints are available for any photographs or illustrations appearing in this copy for an additional charge. Contact UMI directly to order.

**Bell & Howell Information and Learning
300 North Zeeb Road, Ann Arbor, MI 48106-1346 USA
800-521-0600**

UMI[®]

Morphologic Channel Response to Flood Events in a Salmon Spawning Stream

by: Brett Eaton. 

A Thesis Submitted in Partial Fulfillment of the
Requirements for the Degree of M.Sc. in Geography

Department of Geography
McGill University
Montreal (Qc)

Supervisor. Dr. M. Lapointe



National Library
of Canada

Acquisitions and
Bibliographic Services

395 Wellington Street
Ottawa ON K1A 0N4
Canada

Bibliothèque nationale
du Canada

Acquisitions et
services bibliographiques

395, rue Wellington
Ottawa ON K1A 0N4
Canada

Your file Votre référence

Our file Notre référence

The author has granted a non-exclusive licence allowing the National Library of Canada to reproduce, loan, distribute or sell copies of this thesis in microform, paper or electronic formats.

The author retains ownership of the copyright in this thesis. Neither the thesis nor substantial extracts from it may be printed or otherwise reproduced without the author's permission.

L'auteur a accordé une licence non exclusive permettant à la Bibliothèque nationale du Canada de reproduire, prêter, distribuer ou vendre des copies de cette thèse sous la forme de microfiche/film, de reproduction sur papier ou sur format électronique.

L'auteur conserve la propriété du droit d'auteur qui protège cette thèse. Ni la thèse ni des extraits substantiels de celle-ci ne doivent être imprimés ou autrement reproduits sans son autorisation.

0-612-50760-2

Canada

ABSTRACT

Changes in channel morphology in response to two flood events were measured within three reaches on the Sainte Marguerite River, Quebec. The first event was the spring freshet — peaking in mid-May, 1996— while the second event —peaking on July 20, 1996— was the largest flood on record for the region. The resultant channel adjustments can be classified as either bedform evolution —in which a clear, systematic pattern of adjustment is evident— or as bedform change, in which local hydraulic and sedimentologic conditions produce a seemingly random pattern of channel mobilization. Where bedform evolution has occurred, it is consistent with the existing paradigm for meander development. Sediment transport calculations based on the ‘inverse’ or ‘morphologic’ method were strongly correlated to reach average mobility ratios. The average rate of transport in response to the larger flood approached those reported by others for a braided system (Goff and Ashmore, 1994). Potential spawning zones within the three reaches were all subjected to significant net scour and/or fill following the second event; several potential spawning zones were significantly affected by the first event. The presence of bank protection upstream of a potential spawning zone seems to be a determinant in the severity of the impact by promoting erosion of these zones.

SOMMAIRE

Les changements morphologiques du chenal résultant de deux crues furent mesurés sur trois tronçons de la Rivière Sainte Marguerite (Québec). Le premier événement fut la crue printanière —qui atteigna son apogée à la mi-mai 1996— alors que le second événement, dont le point maximum fut atteint le 20 juillet 1996, représente la plus importante inondation qu’ait connue la région. Les ajustements du chenal résultant de ces événements peuvent représentés soit une évolution des éléments morphologiques du lit, lors de laquelle l’ajustement se reflète par un ré-arrangement spatial systématique et évident de ceux-ci; soit un changement des éléments morphologiques, lors duquel les conditions hydrauliques et sédimentologiques prédominantes résultent en une mobilisation aléatoire des éléments du chenal. Les calculs de transport sédimentaire basés sur la méthode “inverse” ou “morphologique” correspondent de très près aux ratios moyens de mobilité des tronçons. Le taux moyen de transport en réponse à la plus importante des deux inondations se rapproche de ceux décrits par d’autres auteurs pour des systèmes proglaciaux (Goff et Ashmore, 1994). Les aires de frai potentielles dans les trois tronçons furent tous soumis à une érosion et/ou une déposition nette considérable suite au deuxième événement; plusieurs aires de frai potentielles furent aussi affectées de façon significative par le premier événement. La présence de revêtement des berges en amont des aires de frai potentielles semble déterminer la sévérité des impacts de chaque événement en facilitant l’érosion de ces aires.

ACKNOWLEDGMENTS

I would like to thank a number of people for the financial support generously provided me to assist in the undertaking of this work. Primarily, support came from my supervisor, Dr. M. Lapointe and the Centre interuniversitaire de recherche sur le saumon atlantique (CIRSA) research group. Funding was also provided to me through the Department of Geography as a teaching assistant. For invaluable help in the field, I would like to thank all of the field assistants working with me at the CIRSA camp during the summers of 1995 and 1996. I am especially grateful for the outstanding contributions made to this project by Cindy Honeywill, Steve Driscoll and Nicole Couture. For intellectual stimulation and guidance, I would like to thank my supervisor, Dr. M. Lapointe, as well as Dr. N. Roulet.

TABLE OF CONTENTS

TABLE OF CONTENTS	IV
LIST OF FIGURES.....	VI
LIST OF TABLES.....	VII
1) INTRODUCTION	1
1.1) OBJECTIVES	3
1.2) LITERATURE REVIEW	4
1.2.1) CHANNEL MORPHOLOGY	4
1.2.2) MEANDER DEVELOPMENT.....	8
1.2.3) SALMONID SPAWNING HABITAT.....	12
1.2.4) CHANNEL SCOUR AND FILL.....	13
1.2.5) SEDIMENT TRANSPORT ESTIMATION	14
1.2.6) EXTREME FLOOD EVENTS.....	15
2) STUDY SITE	19
2.1) CHANNELIZED REACH OF THE SAINTE MARGUERITE RIVER	22
2.2) HISTORICAL CHANNEL CHANGES ILLUSTRATED BY AIR PHOTOS	22
2.3) CHANNEL RESPONSE TO CHANNELIZATION.....	24
2.4) CHARACTERISTICS OF THE THREE STUDY REACHES	24
3) METHODS	30
3.1) SURVEY DATA	30
3.2) SEDIMENTOLOGICAL DATA	31
3.3) SCOUR CHAINS.....	33
4) SPRING AND SUMMER FLOW CONDITIONS IN THE STUDY REACHES FOR 1996	34
4.1) DISCHARGE CONDITIONS	34
4.1.1) HYDROMETRIC STATION DATA ON THE NORTH-EAST BRANCH.....	34
4.1.2) DISCHARGE ESTIMATES AT THE STUDY SITES ON THE PRINCIPAL BRANCH	37
4.2) SHEAR STRESS AND STREAM POWER	39
4.2.1) ENTRAINMENT THRESHOLDS AND THE MOBILITY RATIO	41
5) PATTERNS OF MORPHOLOGICAL EVOLUTION	44
5.1) REACH 1	44
5.1.1) GENERAL BEDFORM RESPONSE	45
5.1.2) DETAILED MORPHOLOGIC CHANGES IN RESPONSE TO THE SPRING FRESHET	46
5.1.3) DETAILED MORPHOLOGIC CHANGES IN RESPONSE TO JULY 20 EVENT.....	51
5.1.4) SITE SPECIFIC INTERPRETATION OF MORPHOLOGIC CHANGES	54
5.2) REACH 2.....	55
5.2.1) GENERAL BEDFORM RESPONSE	56
5.2.2) DETAILED MORPHOLOGIC CHANGES IN RESPONSE TO THE SPRING FRESHET.....	56
5.2.3) DETAILED MORPHOLOGIC CHANGES IN RESPONSE TO JULY 20 EVENT	60
5.2.4) SITE SPECIFIC INTERPRETATION OF MORPHOLOGIC CHANGES	64
5.3) REACH 3	64
5.3.1) GENERAL BEDFORM RESPONSE	65
5.3.2) DETAILED MORPHOLOGIC CHANGES IN RESPONSE TO THE SPRING FRESHET.....	65
5.3.3) MORPHOLOGIC CHANGE IN RESPONSE TO JULY 20 EVENT	69
5.3.4) SITE SPECIFIC INTERPRETATION OF MORPHOLOGIC CHANGES	72

5.4) CHANGES IN VOLUMETRIC SEDIMENT STORAGE.....	72
5.4.1) <i>REACH 1</i>	72
5.4.2) <i>REACH 2</i>	75
5.4.3) <i>REACH 3</i>	76
6) PATTERNS OF CHANNEL ADJUSTMENT	78
6.1) CLASSIFICATION OF FLOOD SEVERITY	78
6.2) PATTERNS EVIDENT WITHIN THE REACHES	79
6.2.1) <i>REACH 1</i>	79
6.2.2) <i>REACH 2</i>	80
6.2.3) <i>REACH 3</i>	80
6.3) IMPACT OF FLOOD MAGNITUDE ON MORPHOLOGIC RESPONSE.....	80
6.4) GENERAL PRINCIPLES OF MEANDER DEVELOPMENT	82
7) SEDIMENT TRANSPORT ESTIMATES FROM MORPHOLOGIC CHANGES.....	86
7.1) SEDIMENT TRANSPORT ESTIMATES ALONG THE SAINTE MARGUERITE RIVER.....	89
7.1.1) <i>PAIRED EROSION AND DEPOSITION APPROACH</i>	89
7.1.2) <i>TOTAL EROSION/DEPOSITION WITH TYPICAL STEP LENGTH APPROACH</i>	89
7.1.3) <i>SEDIMENT BUDGET APPROACH</i>	93
7.1.4) <i>SUMMARY OF TRANSPORT ESTIMATES</i>	95
7.2) COMPARISON OF TRANSPORT ESTIMATES FROM THE SAINTE MARGUERITE AND SUNWAPTA RIVERS.....	97
8) IMPLICATIONS FOR SALMONID SPAWNING HABITAT STABILITY	100
9) CONCLUSIONS.....	106
REFERENCES	107
APPENDIX A: SEDIMENT TEXTURE VARIATIONS.....	114
A.1) REACH 1	114
A.2) REACH 2	117
A.3) REACH 3	121

LIST OF FIGURES

FIGURE 2.1.	LOCATION MAP, SAINTE MARGUERITE RIVER.	20
FIGURE 2.2.	CHANNELIZED REACH OF THE SAINTE MARGUERITE RIVER, 1950 AND 1995.	21
FIGURE 2.1.1.	VALLEY MORPHOLOGY OF THE CHANNELIZED REACH, 1990.	23
FIGURE 2.2.1.	CHANNELIZED REACH MORPHOLOGY IN PLANFORM, 1961 AND 1990.	25
FIGURE 2.4.1.	CHANNEL PLANFORM WITHIN AND UPSTREAM OF STUDY REACHES, 1995.	27
FIGURE 2.4.2.	REACH SEDIMENTOLOGY, AUGUST 1996.	28
FIGURE 4.1.1.	ANNUAL FLOOD FREQUENCY DATA FROM THE NORTH-EAST BRANCH, SAINTE MARGUERITE RIVER.	35
FIGURE 5.1.1.	DIGITAL ELEVATION MODELS, REACH 1, FOR THREE SUCCESSIVE SURVEYS.	47
FIGURE 5.1.2.	NET MORPHOLOGIC CHANGE, REACH 1, RESULTING FROM THE SPRING FRESHET.	48
FIGURE 5.1.3.	THALWEG AND CROSS-SECTIONAL ADJUSTMENTS, REACH 1, CAUSED BY THE SPRING FRESHET.	50
FIGURE 5.1.4.	NET MORPHOLOGIC CHANGE, REACH 1, RESULTING FROM THE JULY 20 FLOOD EVENT.	52
FIGURE 5.1.5.	THALWEG AND CROSS-SECTIONAL ADJUSTMENTS, REACH 1, CAUSED BY THE JULY 20 FLOOD EVENT.	53
FIGURE 5.2.1.	DIGITAL ELEVATION MODELS, REACH 2, FOR THREE SUCCESSIVE SURVEYS.	57
FIGURE 5.2.2.	NET MORPHOLOGIC CHANGE, REACH 2, RESULTING FROM THE SPRING FRESHET.	58
FIGURE 5.2.3.	THALWEG AND CROSS-SECTIONAL ADJUSTMENTS, REACH 2, CAUSED BY THE SPRING FRESHET.	59
FIGURE 5.2.4.	NET MORPHOLOGIC CHANGE, REACH 2, RESULTING FROM THE JULY 20 FLOOD EVENT.	61
FIGURE 5.2.5.	THALWEG AND CROSS-SECTIONAL ADJUSTMENTS, REACH 2, CAUSED BY THE JULY 20 FLOOD EVENT.	62
FIGURE 5.3.1.	DIGITAL ELEVATION MODELS, REACH 3, FOR THREE SUCCESSIVE SURVEYS.	66
FIGURE 5.3.2.	NET MORPHOLOGIC CHANGE, REACH 3, RESULTING FROM THE SPRING FRESHET.	67
FIGURE 5.3.3.	THALWEG AND CROSS-SECTIONAL ADJUSTMENTS, REACH 3, CAUSED BY THE SPRING FRESHET.	68
FIGURE 5.3.4.	NET MORPHOLOGIC CHANGE, REACH 3, RESULTING FROM THE JULY 20 FLOOD EVENT.	70
FIGURE 5.3.5.	THALWEG AND CROSS-SECTIONAL ADJUSTMENTS, REACH 3, CAUSED BY THE JULY 20 FLOOD EVENT.	71
FIGURE 5.4.1.	SEDIMENT STORAGE ZONES FOR ALL THREE REACHES.	73
FIGURE 5.4.3.	NET CHANGE IN SEDIMENT STORAGE OVER TWO EVENTS, REACH 2.	75
FIGURE 5.4.4.	NET CHANGE IN SEDIMENT STORAGE OVER TWO EVENTS, REACH 3.	76
FIGURE 6.3.1.	BED MOBILIZATION VERSUS MOBILITY RATIO.	81
FIGURE 6.4.1.	CHANNEL DYNAMICS MODERATED BY BANK PROTECTION.	83
FIGURE 7.1.1.	SEDIMENT TRANSPORT PER EVENT <i>VERSUS</i> PEAK SHEAR STRESS.	91
FIGURE 7.1.2.	SEDIMENT TRANSPORT PER EVENT <i>VERSUS</i> MOBILITY RATIO.	92
FIGURE 7.1.3.	SEDIMENT TRANSPORT PER METER OF WIDTH PER EVENT - ALL DATA.	96
FIGURE 8.1.	DISTRIBUTION OF NET SCOUR AND FILL IN POTENTIAL SCOUR ZONES IN ALL THREE REACHES.	103
FIGURE A.1.	BED AND SURFACE SEDIMENT TEXTURE DISTRIBUTIONS, REACH 1, BASED ON BULK SEDIMENT SAMPLES, PRIOR TO AND FOLLOWING JULY 20.	115
FIGURE A.2.	SURFACE TEXTURE DISTRIBUTIONS, REACH 1 & 2, BASED ON WOLMAN SAMPLES, PRIOR TO AND FOLLOWING JULY 20.	118
FIGURE A.3.	BED AND SURFACE SEDIMENT TEXTURE DISTRIBUTIONS, REACH 2, BASED ON BULK SEDIMENT SAMPLES, PRIOR TO AND FOLLOWING JULY 20.	119

LIST OF TABLES

TABLE 4.1.1.	RETURN PERIOD ESTIMATES FOR THE JULY 20, 1996 FLOOD EVENT.	36
TABLE 4.1.1.	ESTIMATED 1996 FLOOD DISCHARGES, REACH 1.....	38
TABLE 4.1.3.	RETURN PERIOD ESTIMATES FOR THE MAY 16, 1996 FLOOD EVENT.	39
TABLE 4.2.1.	REACH SCALE MEAN SHEAR STRESS AND STREAM POWER ESTIMATES FOR 1996 HIGH FLOW EVENTS.	41
TABLE 4.2.2.	EVENT SPECIFIC MOBILITY RATIOS.	43
TABLE 7.1.1.	SEDIMENT TRANSPORT ESTIMATES FOR THE SPRING FRESHET BASED ON PAIRED EROSION/DEPOSITION ZONES.	89
TABLE 7.1.2.	STEP LENGTHS APPLIED TO EROSION VOLUME ESTIMATES OF SEDIMENT TRANSPORT....	90
TABLE 7.1.3.	SEDIMENT BUDGET ESTIMATES OF AVERAGE AND MAXIMUM SEDIMENT TRANSPORT RATES.	94
TABLE 7.2.1.	SEDIMENT TRANSPORT ESTIMATES ON THE SAINTE MARGUERITE JULY 20 FLOOD AND SUNWAPTA RIVERS.....	98
TABLE 8.1.	PERCENT OF DESIGNATED SPAWNING ZONES SUBJECT TO NET EROSION, 1996.....	101
TABLE 8.2.	PERCENT OF DESIGNATED POTENTIAL SPAWNING ZONES AFFECTED BY EROSION OR DEPOSITION, 1996.	104
TABLE A.1.	BED AND SURFACE D50 AND D85, REACH 1, PRIOR TO AND FOLLOWING JULY 20, 1996.	114
TABLE A.2.	TEXTURAL MODIFICATIONS OCCURRING IN REACH 1 DURING THE JULY 20 FLOOD EVENT.....	116
TABLE A.3.	ARMOR RATIO, REACH 1, BASED ON SURFACE TEXTURE AND BAR HEAD BED MATERIAL.....	117
TABLE A.4.	BED AND SURFACE D50 AND D85 AND TEXTURAL MODIFICATIONS, REACH 2, PRIOR TO AND FOLLOWING JULY 20.....	120

1) INTRODUCTION

This work was undertaken as one of a number of projects initiated on the Sainte Marguerite River through the Centre interuniversitaire de recherche sur le saumon atlantique (CIRSA). It was one of several geomorphologic studies attempting to understand the geomorphic controls on the physical salmonid habitat on the Sainte Marguerite. In particular, the overall geomorphologic program focused on developing a more complete understanding of how the system has responded to environmental perturbations such as road building or logging and to elucidate the ramifications for salmonid habitat. Obviously, this is quite an ambitious task, requiring large quantities of data on parameters that are often difficult to quantify.

Given the goal of understanding the geomorphic processes responsible for determining the quality of salmonid habitat within the system, the projects were specified accordingly. For the work reported here, three study reaches were selected to represent a range of channel morphology and substrate, within which salmonid spawning and rearing habitat could be examined. Specifically, the spatial distribution of bed scour and bed form change/evolution within the riffle environment was to be examined by making detailed topographic surveys of the bed and through scour chains installed in the riffle zone. Riffle environments were the focus for this work because of their role in Atlantic salmon spawning, as well as their importance in controlling hydraulic habitat for juvenile rearing; the sedimentology and geomorphic stability of these bed elements is a key factor in the overall productivity of a salmon-bearing system such as the Sainte Marguerite River.

In addition to documenting the net scour and fill occurring within the riffle zones, a partial explanation of these patterns was to have been attempted using a map of shear stress calculated by a two-dimensional finite element model for fluid flow within the stream channel developed by other members of CIRSA. This model would have provided an approximate reconstruction of the peak shear stress conditions, which could likely have been related to the observed patterns of maximum scour. A detailed map of the reach topography was required to run this model, as were estimates of the upstream and

downstream peak water levels. The finite element model was to be run over a reach of approximately 400 m of river channel, in the middle of which was the study riffle.

However, the extraordinarily wet 1996 field season --which precluded much fieldwork before August and culminated on July 20 in the largest flood on record for the basin-- forced a reevaluation of the principal research questions. Reevaluation was necessary because the majority of the scour chains installed in the riffle environments were lost during the flood, before they could be recovered. Even if the chains had remained, there were now two events that had to be considered in an analysis of net scour and fill, which precludes meaningful conclusions about the actual patterns. As it was, 15% of the chains remained in place following the flood, of which most were found along the channel margins or in other lower energy environments. Measurements of bed mobilization occurring in the absence of net bedform change/evolution were therefore impossible to determine.

The utility of the finite element model in predicting net bedform response under these circumstances was very questionable; while it is reasonable to expect some relation between peak shear stress conditions and maximum depth of scour, it does not necessarily follow that peak shear stresses will be related to the patterns of large-scale bedform evolution.

Although it was still possible to run the finite element hydraulic model given the available hydraulic data, the extensive morphologic change presents a problem. That the bed has been substantially modified by the July 20 flood event invalidates the assumption implicit in the model that the bed constitutes a static boundary. In addition, limit conditions at the upstream and downstream boundaries become increasingly uncertain once the static bed condition has been violated. A good example of this pitfall is provided by House and Pearthree (1995), in which they have found that initial estimates of flood magnitude for an extreme event may have been far too high when made in an alluvial channel reach (2080 m³/s versus 750-850 m³/s from a 50 km² basin). They write that --for the Bronco Creek basin in Arizona--

“Dynamic adjustments that occur in the bed and banks of an alluvial stream during large floods may result in the final channel area being different from that associated with the peak discharge.

Furthermore, the attainment of maximum depth, stage, cross-sectional area, and discharge may not be synchronous. [Quick, 1991] Channel roughness may decrease during a flood, particularly if bars are removed or streamlined...the timing of the changes in roughness in relation to peak discharge is also unknown." (p. 3068)

1.1) OBJECTIVES

Given the data available --which consisted of very detailed topographic surveys bracketing two significant flood events in three reaches of the Sainte Marguerite River, as well as sedimentologic data in each reach-- a new focus was developed. Comparisons of the topography before and after the two significant flood events revealed systematic patterns of morphologic change. The changes were quantified by calculating the volumes of sediment eroded and deposited, and the patterns associated with these changes were revealed using a Geographic Information System (GIS). Flow conditions were then combined with the existing understanding of channel dynamics to explain the magnitude and spatial extent of these morphologic changes in each of the three reaches. The revised focus was to develop an understanding of the magnitude and spatial distribution of bedform evolution and change; the distinction between evolution and change is made below.

The term bedform evolution refers to a systematic trend of morphologic adjustment occurring during high flow events in response to the prevailing channel pattern. A typical example of this would be the growth of a point bar in a meandering system, in which the point bar will more or less continuously aggrade and propagate outward as the bank opposite retreats. Indeed, meander development and maintenance can be viewed in the context of an equilibrium channel pattern; one would expect an artificially straightened channel to progressively reestablish a meandering pattern, which would be an example of bedform evolution (Langbein and Leopold, 1968b).

Seemingly random patterns of net change in sediment storage can also occur. Rather than reflecting an overall tendency of the channel to evolve in response to channel scale characteristics of the fluid flow field, such changes in net storage are most likely caused by local and/or transient sedimentological and hydraulic conditions. These

changes to the bed can be viewed as stochastic variations--or noise--as they do not necessarily represent a temporally or spatially consistent pattern of form adjustment.

Based on this, one can distinguish between bedform evolution and bedform change; bedform evolution is driven by overall reach scale patterns of change, while bedform change is driven by local sedimentological and hydraulic conditions.

The July flood provides a unique opportunity to examine in detail the precise effects of an exceptional flood on channel morphology. **The revised objectives of this study are:**

1. to identify and compare patterns of morphologic channel adjustments in each of the three reaches for the exceptional July flood event as well as the more frequently occurring spring freshet,
2. to understand how the channel adjustments are related to event magnitude,
3. to make sediment transport calculations based on the observed morphologic changes, and
4. to identify the environmental factors controlling the stability of potential spawning zones on the Sainte Marguerite river.

In the coming chapters, maps of net erosion and deposition produced using a GIS are examined to identify the pattern and magnitude of net morphologic change. Then, the patterns exhibited are placed in the context of the existing paradigm for meander development. Sediment transport estimates are made using the calculated volumes of erosion and deposition. Then, the effects of the two flood events on potential spawning zones within the three reaches are also examined.

1.2) LITERATURE REVIEW

1.2.1) CHANNEL MORPHOLOGY

It is believed that channel form in alluvial rivers is closely related to the processes of fluid and sediment transport, which in turn are influenced by the resultant bedforms in a mutually reinforcing interaction (Keller and Melhorn, 1983; Church and Jones, 1982).

Channel bedforms are generally classified --or more precisely, defined-- by the processes theoretically producing them.

An alluvial river flows within a floodplain of its own sediment. This floodplain is composed primarily of sediment deposited within the channel as lateral accretions, though vertical accretions directly to the floodplain surface will also occur during overbank flood events (Wolman and Leopold, 1957; Leopold *et al.*, 1964; Desloges and Church, 1987). Lateral channel migration has been observed to occur with little net change in channel width; net bank erosion is generally equal to the net deposition occurring on the point bar opposite, thereby maintaining a relatively constant channel width (Wolman and Leopold, 1957). Channel meandering, the result of the lateral channel migration, is common in alluvial channels and can be geometrically described as a wave, the wavelength of which is scaled by the channel width (Leopold *et al.*, 1964; Keller and Melhorn, 1973; Hey, 1976).

Within the channel itself a number of different morphologic elements are apparent, independent of channel pattern. The fundamental morphologic units identified within the channel are the bar, pool and riffle.

Bars develop as the result of deposition of sediment within the channel, or by the deformation of the bed to form elements producing hydraulic resistance (Leopold *et al.*, 1964; Keller and Melhorn, 1973; Church and Jones, 1982; Ashmore, 1990). Divergence of flow is thought to cause the stalling of bedload sheets, which may accrete on to existing bars or form the nucleus for bar growth (Keller and Melhorn, 1973; Church and Jones, 1982; Leopold and Emmett, 1984; Ashmore, 1990; Ferguson, 1993).

The crest of the downstream edge of the divergence-associated sediment deposit forms the riffle, whereas the upstream deposit forms the bar (Church and Jones, 1982). Bars as observed in the field are rarely the products of a single event; rather, they are produced by the accumulation of a number of smaller "unit" bars. As such, most bars may be appropriately referred to as "complex" bars (Church and Jones, 1982).

Several types of unit bars were described by Church and Jones (1982), which may form the nucleus for development of a number of complex bar types. Unit bars are typified by an upstream sediment ramp along which sediment is transported and a

downstream avalanche face where deposition occurs. Vertical accretion occurs as well, when sediment in transport stalls before reaching the avalanche face (Church and Jones, 1982).

Several types of complex bar can be produced. Church and Jones describe five types of complex bar; they are 1) transverse and 2) medial bars --occurring in the middle of the channel and producing a bifurcation of the main channel-- 3) point bars--occurring along the inner bank of a meander bend-- 4) lateral bars --having the form of a point bar and the resultant thalweg sinuosity in the absence of meandering-- and 5) diagonal bars which traverses the channel diagonally. This classification is quite useful in its simplicity, and will be adopted for the current work.

An additional feature common to both point and lateral bars deserves mention: secondary or chute channels along the inner bank have been reported, the creation of which is attributed to the upstream exclusion of bedload (Church and Jones, 1982; Ferguson and Ashworth, 1991). To differentiate this form from the incipient braid mechanism of chute cutoffs (Ashmore, 1990; Ferguson, 1993), the term 'secondary channel' will be adopted herein.

Pools have received far less attention. These forms are relatively self-evident in the field, and are the product of bed erosion. It has been hypothesized that while bars are the products of divergent flow, pools are produced by scour associated with convergent flow (Keller and Melhorn, 1973; Richards, 1978; Church and Jones, 1982). It has also been hypothesized that pools are the products of cyclic development and decay of macro-turbulent eddies within the channel (Hey, 1976; Richards 1976a, Richards 1978). The role of vertical vortices in the generation of highly localized extreme bed erosion at points of great stream curvature may also be important (Mlynarczyk and Rotnicki, 1989). Work on small streams indicates that pools may also form where the flow pattern is modified by large organic debris or other non-alluvial elements (Keller and Swanson, 1979; Mosley, 1981; Beshta and Platts, 1986; Andrus *et al.*, 1988).

Riffles, however, are less easily classified than bars or pools. This is in part because riffles represent both a bed feature and a stage-dependent flow condition. This stems back to the use of the word "riffle" by fishermen to describe shallow, rapidly

flowing water with a roughened water surface (Leopold *et al.*, 1964). These flow conditions are most often associated with zones of thalweg shallowing, and the term riffle was adopted to describe these zones of locally elevated bed by Leopold *et al.*, (1964). However the definition of these bedforms is difficult to objectify as a result of the combination of topographic and stage-dependent hydraulic characteristics used to define them.

Keller and Melhorn (1973) describe riffles as occurring at the inflection between one bend and the next through divergent flow and deposition, producing a relatively shallow, symmetric cross-section. Others also believe that alternating convergence and divergence associated with secondary circulation cells is responsible for riffle formation (Hey, 1976; Richards, 1978; Church and Jones, 1982). Richards (1976b) argues that riffles are indeed shallower and wider, on average, than pools lending support to the convergence/divergence hypothesis.

Given that riffles are implicitly the product of deposition and are therefore often, if not always, associated with an extant bar deposit upstream, it is often difficult to distinguish between submerged bar and riffle. In fact, any such distinction is to some degree an artifice of the classification scheme. However, the distinction made by Church and Jones (1982), in which the downstream edge of the bar-riffle depositional unit is determined to be the riffle and the upstream accumulation of sediment is determined to be the bar is a useful conceptual framework. Within this framework, riffles can be viewed as the primary elements for hydraulic resistance, while bars act primarily as sediment storage elements (Church and Jones, 1982; Church 1994).

Other workers have made various attempts to develop objective criteria for identifying riffles and pools. A brief review of these attempts is presented by Richards (1976a), following which it is proposed that the exponents of the at-a-station hydraulic geometry are the most appropriate criteria for distinguishing riffles and pools. This hydraulic definition is an integral part of the velocity reversal hypothesis of pool-riffle development and maintenance, and is therefore based on a theoretical process-form relation (Keller, 1971; Lisle, 1979; Carling, 1991; Clifford and Richards, 1992; Keller and Florsheim, 1993; Sear, 1996). A more practical field technique based simply on the

bed topography and an objective threshold for cumulative elevation changes between one bedform and the next has been proposed (O'Neill and Abrahams, 1984).

It should be noted that there is another scale at which bedforms may be classified; the scale of the megaform. It has been observed that zones of sedimentation, consisting of bar assemblages and areas of local braiding, may develop in response to non-equilibrium conditions of sediment transport and storage (Church, 1983). A review of the relevant literature is presented by Nicholas *et al.*, (1995).

To summarize, the terminology for fluvial forms will be drawn from the above literature; specifically, the classification of complex bars resulting from development of unit bars summarized by Church and Jones (1982) will be adopted. Riffles will be likewise taken to refer to the downstream edge of sediment deposition along the thalweg, which act primarily as elements of hydraulic resistance as opposed to sediment storage, and which therefore have a definite association with the local flow conditions. Pools are rather self-evident forms, though it should be noted that vertical vortex scour or flow deflection scour may be important in the local depths of scour within the pools. Other features, such as bedload sheets, avalanche faces and secondary channels will be described using the terminology adopted by Church and Jones (1982) because of its wide use in other, subsequent literature.

1.2.2) MEANDER DEVELOPMENT

There has been extensive discussion in the literature regarding the initiation and maintenance of meanders in alluvial channels. Workers initially posited that secondary circulation within the channel controlled the spatial location of erosion and deposition involved in the natural meander activity (Leliavsky, 1955; Prus-Chacinski, 1954). An attendant issue is the development and maintenance of the riffle-pool sequence, which is intimately linked to channel pattern.

Langbein and Leopold (1968a) have examined the nature of bedforms within alluvial channels, and came to the conclusion that gravel bars --and therefore the attendant riffle-pool sequence-- can be well described by kinematic wave theory. This initial work

suggests that the transport rate of sediment within the channel is controlled by the spacing of the mobile particles, with the result that accumulations of sediment will tend to form.

The same authors have explicitly described channel meandering as a stable equilibrium channel pattern, resulting from the tendency of a river to minimize the variance of shear stress and friction. Field observations have been presented to support this position; it is argued that the channel depth, slope and velocity adjust to attain a condition of minimum variance of shear stress and bed friction. It is argued on the basis of the collected field data that the meandering pattern is more stable than a straight channel pattern as a result.

Subsequent work has suggested that planform convergence and divergence control the location of erosion and deposition, and thereby channel pattern (Keller and Melhorn, 1973, Church and Jones, 1982). It is argued that the convergent flow occurring in pools during formative discharges result in erosion and therefore maintenance of its relatively low average elevation, whereas the flow divergence typical of the riffle environment results in deposition.

Based on the observed similarity in the spacing of the riffle-pool units in both meandering and straight channels, Keller and Melhorn proposed that the regular spacing of riffle-pool elements limits the scale of meander development, noting that the meander wavelength seldom exceeds twice the riffle-pool spacing of 5 to 7 channel widths. This raises the ultimately sensible point that the channel pattern and longitudinal form must be closely tied. That the riffle-pool spacing seems to be independent of the occurrence of meandering does imply a limitation to the spatial dimensions of meander bends.

A more direct approach was taken by Hooke (1975), who assumed that bed geometry adjusts to transport exactly the incident sediment flux. This is achieved through progressive erosion or deposition, which modifies the local hydraulic conditions until they are sufficient to transport the sediment arriving at that point. This reflects the view of channel adjustment proposed by Keller and Melhorn (1973) who wrote "development of the shoals may be considered as a metamorphosis resembling a feedback mechanism in which process and form evolve in harmony." Hooke reported that the sediment transport field is ultimately responsible for the development of the observed channel pattern.

Secondary flow is downplayed as a mechanism shaping the channel pattern. Instead, Hooke asserts that the radius of curvature for the meanders controls the occurrence of flow separation along the downstream edge of the point bar, and therefore the sediment transport field. It is argued that the meandering pattern is inherently stable, and will tend to reestablish a meandering form following a perturbation through the interaction between bend curvature, flow separation and sediment deposition.

The importance of the radius of curvature is further explored by Hickin (1974), and by Hickin and Nanson (1983). Meander scrolls were examined to determine the rate and direction of channel migration on the Beaton River, British Columbia. It was found that, typically, meanders developed to the point where the ratio of the radius of curvature to the channel width (R_c/w) took a value close to 2.11, with a standard deviation of only 0.13. It was concluded from this that the value of 2.11 for R_c/w represented a value for which flow resistance reached a minimum value.

Hey (1976) came to the conclusion that meander wavelength was a function of the channel width only, with the form

$$(1) \quad \lambda = 4\pi w,$$

where λ is the meander wavelength, and w is the channel width. This is based on the supposition that meander wavelength is dominated by the existence of two helicoidal flow cells within the channel, which are responsible for a pattern of alternating channel bars. Following this argument, one comes to the conclusion that meandering is an inherent property of the fluid, and would be a function of bed material only insofar as it determined the channel cross-sectional geometry and therefore the width.

Support for this comes from several studies that have established the existence of two helical flow cells. Bathurst, Thorne and Hey (1979) measured the primary and secondary flow components at various discharges within the River Severn. The secondary circulation pattern is dominated by a skew induced secondary cell, while a smaller cell of opposite rotation may exist against the outer bank. Thorne and Hey (1979) report that the cell of opposite rotation is not a relic cell from the previous bend, but rather a result of the interaction of the skew-induced cell and the outer bank. It was further reported that the helicoidal cell associated with a bend was displaced from below as a cell

of opposite rotation developed at the entrance to the next bend. The result was a set of vertically stacked cells at the inflection point between the two bends.

Parker (1976) contradicts the supposition that meandering initiation is a function of the flow conditions; he posits, first of all, that meandering and braiding are the products of essentially the same mechanism, and second that the mechanism responsible for initiation of submerged channel bars is the result of sediment transport and bed friction. In the model for bed development put forward by Parker, secondary circulation is not a component. However, it is conceded that secondary circulation seems to play a significant role in the further development and maintenance of the meander, following its initiation by submerged bar deposition. Once thalweg sinuosity has been established, the feedback mechanisms alluded to above contribute to meander-development to the equilibrium condition for which R_c/w takes on the appropriate value (2.11 on the Beaton River, for example). Therefore, the mechanisms for meander initiation described by Parker are not inconsistent with the model for meander equilibrium form based on the fluid flow structure.

Begin (1981) further elucidates the secondary mechanism of post-initiation development. A functional relation between R_c/w and the force per unit area exerted on the channel bank was developed based on the conservation of momentum as the fluid is accelerated centripetally around the bend. From this relation, it was found that R_c/w values between 1.3 and 4.1 produced a maximum force per unit bank area. This is supported by the field evidence provided by Hickin (1974) for which maximum rates of channel migration occurred when R_c/w was approximately 2.11. The model developed by Begin includes bed material composition, however, thereby explaining how R_c/w can be determined by the texture of the alluvium.

To summarize, meander development and maintenance is related to a number of interdependent factors. In a spatial sense, the meander wavelength is adjusted to very nearly twice the riffle-pool spacing. In this way, it may seem likely that wave-like properties determine the ultimate meander form by controlling the riffle-pool spacing. However, the meander wavelength has also been related to the fluid structure alone.

1.2.3) SALMONID SPAWNING HABITAT

Salmonid spawning habitat, the quality of which is critical to the success of the fish population, is strongly influenced by the mobility of the streambed. Spawning is typically observed to take place behind riffle crests, which are areas of inflow to the bed (Stuart, 1953; Milhous, 1982). The circulation of water through the gravel maintains an appropriate dissolved oxygen concentration and evacuates waste products produced by the developing eggs.

Several studies of subsurface flow in alluvial channels confirm that aquifer recharge is associated with the riffle environments; Bencala *et al.*, (1984) and Bencala (1984), reported that water was transferred through the sub-surface from one pool to the next by flow paths sub-parallel to the riffle. Subsequent investigation reported that stream water recharged the surrounding aquifer in riffle zones, while the aquifer discharged to the stream in the vicinity of pools. Furthermore, these flow paths persisted over a range of stream discharges and aquifer conditions (Harvey and Bencala, 1993).

The burial depth of the eggs is typically between 10 and 50 cm (Milhous, 1982; Lisle, 1989). The spawning is thought to occur in a fairly narrow range of gravel sizes (Milhous, 1982). For example, Platts *et al.*, (1979) report that Chinook salmon spawned in gravels with median diameter of 7 to 20 mm.

Another important feature of the substrate, besides its mean size, is the amount of fine sediment. Material carried in suspension will often infiltrate the existing gravel matrix, thereby reducing the gravel permeability, the dissolved oxygen concentration and posing a physical barrier to the emergence of fry from the gravel (Vaux, 1962; Phillips, 1971; Koski, 1972; Beshta and Jackson, 1978; Carling and McCahon, 1987). Siltation of spawning grounds has been observed to produce 100% egg mortality rates, indicating the significance of infiltration of fine sediment (Turnpenny and Williams, 1980).

Entrainment of the channel bed during a flood event may improve spawning habitat by flushing the fine particles from the gravel matrix (Adams and Beshta, 1980; Carling, 1987), or it may adversely affect it by introducing fines to lower levels in the

substrate (Lisle, 1989; Nawa and Frissell, 1993). There is also the direct threat of scouring the bed to the depth of the egg burial, especially in the more geomorphically active streams of the Pacific Northwest (Lisle, 1989; Nawa and Frissell, 1993).

1.2.4) CHANNEL SCOUR AND FILL

It was reported by Leopold and Emmett (1984) that scour depths were not a function of location within the riffle-pool morphologic unit, nor of channel curvature. However, scour and fill can vary across the channel --being higher within the thalweg-- as well as downstream (Neill, 1969; Laronne *et al.*, 1994).

The patterns of scour and fill reportedly reverse as the flow level changes, thus areas scoured at flood stage tend to fill at low flow and areas filled at flood will scour at during low flow (Andrews 1979). Leopold *et al.*, (1966) related the measured scour in a sand bed river to the square root of the peak specific discharge, though it is believed that the reported functional relation was a function of the migrating bedforms (Colby, 1964; Foley, 1978). Carling (1987) examined scour in a gravel bed river, and found that this relation significantly underestimated scour depths.

Hassan (1990), using both magnetically tagged tracer particles and scour chains confirmed that scour and fill depths are functionally related to discharge, and that the relative magnitudes of scour and fill were related to morphology. In general, for most sections during most events, the thalweg scour depths were higher than those on the bar. though a strong relation between scour or fill depths and bar/thalweg designation did not seem to exist. Hassan (1990) concluded that "the changes in the burial, scour, and fill depths indicate that the filling and scouring process is sporadic and has spatially a highly differential pattern which changes between events, during and event across the channel and downstream." (p. 355) In addition, the data collected did not fit the functional relations proposed by Carling (1987) and Leopold *et al.*, (1966), indicating that the relation between discharge and the channel bed is site specific to some degree.

1.2.5) SEDIMENT TRANSPORT ESTIMATION

Many equations based on relating shear stress or some equivalent measure of fluid force to sediment transport rates have been proposed, though a generally applicable equation has not yet been developed (Reid and Frostick, 1994). A review of various bedload formulae was undertaken by Gomez and Church (1989), from which it was concluded that none of the twelve bedload transport formulae examined were adequate predictors of sediment transport rates; typically, order of magnitude errors in prediction of transport rates were observed. The data against which the various formulae were tested came from four sets of field data representing as close to equilibrium transport as possible and from three sets of flume data. The failure of these formulae is in large part due to the complexity of the entrainment threshold for heterogeneous gravel beds.

However, event-scale transport rates may be calculated from net changes in sediment storage within the channel (Popov, 1962; Hubbel, 1964; Neill, 1971, 1987; Church *et al.*, 1987; Carson and Griffiths, 1989; Lane *et al.*, 1995; Ashmore and Church, 1995). This alternate technique has been called the “morphologic” or “inverse” method.

The method described by Ashmore and Church (1995) is based on a general statement of continuity of mass as follows:

$$(2) \quad \partial q_{bx} / \partial x + \partial q_{by} / \partial y + (1-p) \partial z / \partial t + \partial C_b / \partial t = 0$$

Where z is the bed elevation, q_b is the transport per unit width of bedload, x and y represent the downstream and transverse directions, C_b is the concentration of transported sediment (by bed area) and p is the porosity. By integrating across the channel, this equation can be reduced to a finite difference form for changes along the channel direction:

$$(3) \quad \Delta Q_b / \Delta x + (1-p) \Delta A_b / \Delta t = 0, \text{ or } (1-p) \Delta V + (Q_{bo} - Q_{bi}) \Delta t = 0$$

and

$$(4) \quad \Delta V = V_i - V_o$$

Q_b is the sediment transport rate, A_b is the sediment deposit/scour cross-section for the channel, and $\Delta V = \Delta A_b \Delta x$ is net volumetric change in storage of sediment within the reach of length Δx .

According to Ashmore and Church, this finite difference equation can be used to calculate the change in sediment transport within a reach based on storage changes. Note, however, that an input sediment transport rate is required to use this method in producing downstream estimates of sediment transport. In addition, any component that is carried through the reach without interacting with the morphology is not recorded. This type of behavior is a function of both the time scale at which changing morphology is recorded, and of the sediment transport mode.

Other, simpler methods are based on estimates of the step length for gravel transport, that is, the distance between centroids of erosion and those of deposition (Neill, 1971; Church *et al.*, 1987; Neill, 1987; Carson and Griffiths, 1989; Goff and Ashmore, 1994; Lane *et al.*, 1995). This step length morphological method has been applied to both meandering and braided channels.

1.2.6) EXTREME FLOOD EVENTS

The literature pertaining to the geomorphic impacts of rare flood event is, by definition, sparse. Given the nature of such events, the data is usually insufficient to accurately quantify the impact because there is little by way of pre-flood information. Observation of the change in channel pattern from air photos is common practice in such cases (Desloges and Church, 1992), or reliance upon previously existing cross-sectional information (Miller, 1990). As such, the available data are often inadequate to determine the net vertical component of change or --if cross-sectional data is used-- the extent of planform adjustment.

From what data are available, however, there seem to be several typical responses to large floods. The first, most obvious adjustment is a widening of the channel, often by 2 or 3 fold. Such widening is often observed in arid and/or alpine environments, where there is sparse riparian vegetation (Warburton, 1994; Huckleberry, 1994). This widening is often associated with a shift in channel pattern from a single thread meander to a braided channel (Desloges and Church, 1992; Warburton, 1994).

Warburton (1994) reported a cycle of channel pattern change from a single thread to a braided pattern on a proglacial meltwater stream. The initial shift from single thread

to braided pattern occurred in response to a flood event, while the subsequent return to a single thread pattern occurred more gradually.

Desloges and Church (1992) previously described such a process of sudden shift in channel pattern, followed by a gradual relaxation. The authors report on the effects of two extremely large events on the Noeick River, British Columbia, resulting from glacial outburst flooding. The events described were approximately 2.4 times larger than the maximum probable meteorological flood. The channel response to the first flood was predictably an overall widening of the channel, with significant areas of braiding. This channel widening/braiding occurred on a forested flood plain. The second event produced only minor redistribution of sediment made available by the scouring effects of the first. It was concluded that a new equilibrium, a new regime, had been established during the brief but powerful first event, thereby explaining the relatively minor effects produced by the second. In this way, the channel had undergone a step change in regime, which would likely be followed by a gradual return to a morphology similar to that existing previously. The authors write "that regime adjustments can occur rapidly in alluvial channels, and that the 'equilibrium' between alluvial morphology and the governing conditions change in such a way that stream power increases out of proportion to the increase in sediment supply or grain size. In the reverse circumstances, however, a long period of non-regime adjustment is required." (p. 362).

Miller (1990) examined channel response to various large floods in the Central Appalachian region. It was noted by the author that "despite the abundance of literature describing geomorphically effective floods, there are relatively few studies that attempt to provide quantitative information on what threshold conditions, if any, distinguish floods that are effective from those that are not." (p. 120). The term "geomorphically effective" refers to floods that cause substantial reworking of the river floodplain of a type and magnitude that could not be accomplished by a number of lesser events. Miller reported that, in the Central Appalachians, the size and intensity of the rainfall event are not sufficient to predict the effectiveness of a given event.

By examining several floods occurring in the region, Miller noted that the most geomorphically effective flood did not exhibit the highest rainfall intensity, nor the largest

cumulative precipitation amounts. Furthermore, the effectiveness of a given event was spatially variable, in general being much more effective in the steeper, confined valley tributaries than in the larger channels. Miller attempted to identify some criteria for a threshold using unit stream power. He wrote:

“these results suggest a trend, but they do not establish a clear threshold suitable for predictive purposes: unit stream power values exceeding 1000 W/m^2 were calculated for sites where geomorphic impacts were negligible, and severe erosion was observed near sites with calculated values as low as 45 W/m^2 . It is noted that the erodability of the bed must be considered...the highest values were associated with a bedrock canyon.”

However, Miller continues,

“for valleys wider than about 200 m, evidence discussed in this paper clearly shows a trend towards increasing severity of erosion with increasing values of unit stream power. Narrower valley reaches are less sensitive to unit stream power, in part because they are more likely to have resistant boundaries and in part because the channel more often runs parallel to the valley margins and there are fewer opportunities for the central core of the flow to cross from the channel onto the adjacent valley floor. To the extent that a threshold value of unit stream power can be associated with severe channel erosion, 300 W/m^2 appears to be a reasonable minimum estimate of that threshold.” (p. 132).

It was reported by Miller that an event occurring on June 21 to 24, 1972, on the eastern seaboard of the United States in which 269 mm of rain fell in 12 hours, did not produce significant floodplain modification; only local channel widening and scattered examples of floodplain erosion were observed.

This concept of a threshold for severe flood impact on alluvial channels was further examined by Magilligan (1992). An approximate minimum threshold for potentially catastrophic channel modifications was identified, corresponding to approximately 100 N/m^2 or 300 W/m^2 , which concurs with that proposed by Miller (1990) for a geomorphically effective extreme event. Magilligan (1992) reported that such threshold values were typically attained by floods ranging from 2 to 18 times the 100 year flood discharge.

The susceptibility of a given region to catastrophic floods has been examined; this involves both physiographic and climatic aspects. (Baker, 1988). While climate is obviously very important in determining flood susceptibility, it is constrained by the local physiographic conditions such as soil permeability, drainage density, vegetation and hillslope gradients which controls the hydrologic response of the drainage basin to precipitation inputs (Baker, 1988).

The extent and persistence of the channel changes are also controlled by local physiographic conditions. Nolan and Marron (1985), for example, report that in California, the interaction between hillslopes and the channel influence the severity of channel modification due to a large flood, as well as the time required for channel recovery. More generally Gupta (1983) reported that the persistence of the effects of large floods was primarily related to the (in)ability of the "normal" regime to rework the material introduced during the large event. It is proposed that the material introduced by the large flood and bedforms formed during it may be treated as lag features; a condition of disequilibrium between the channel form and the flow regime will persist until the next high magnitude event. Arid environments generally permit flood related channel alterations to persist much longer than in humid environments (Harvey, 1984).

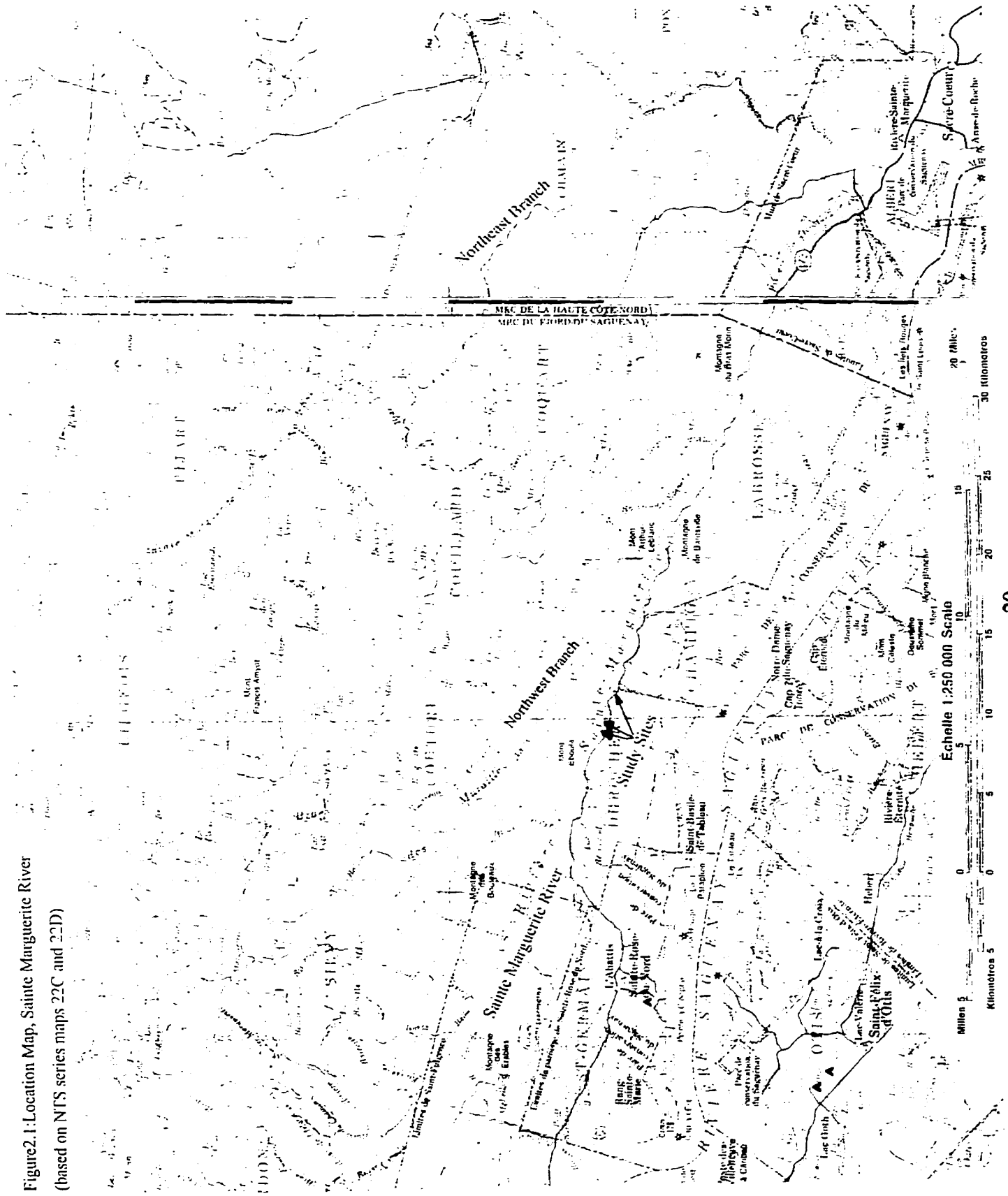
2) STUDY SITE

Research was carried out on the Sainte Marguerite river, located in the Saguenay region of the province of Quebec (Figure 2.1). This river consists of two main branches, the North-East branch and the Principal branch, which drain a total area of 2135 km². The river exhibits a variety of substrate types, ranging from predominantly sandy reaches to lag deposits of glacially transported boulders. However, a cobble-gravel bed is common throughout much of the river course. Atlantic salmon spawn at various locations on the Sainte Marguerite, and the related sport fishery plays a prominent role in the local economy.

Three study sites were selected on the upper section of the Principal branch, which drains approximately 285 km². This section of the Principal branch was altered during construction, in the early 1960's, of highway 172 along the northern edge of the Saguenay fjord. The three study reaches are located within a section of channel that was subjected to extensive channelization, which consisted of re-routing the river channel through the neck of the existing meanders, thus creating a straighter channel of higher gradient. Air photo images are presented for the years 1950 and 1995 for the channelized reach, highlighting the impact of the road construction on the system and the location of the three study reaches (figure 2.2). There is a general trend of downstream fining of sediment texture and channel gradient reduction throughout the channelized reach, a point that is illustrated later. The study reaches cover a range of sediment textures and channel slopes.

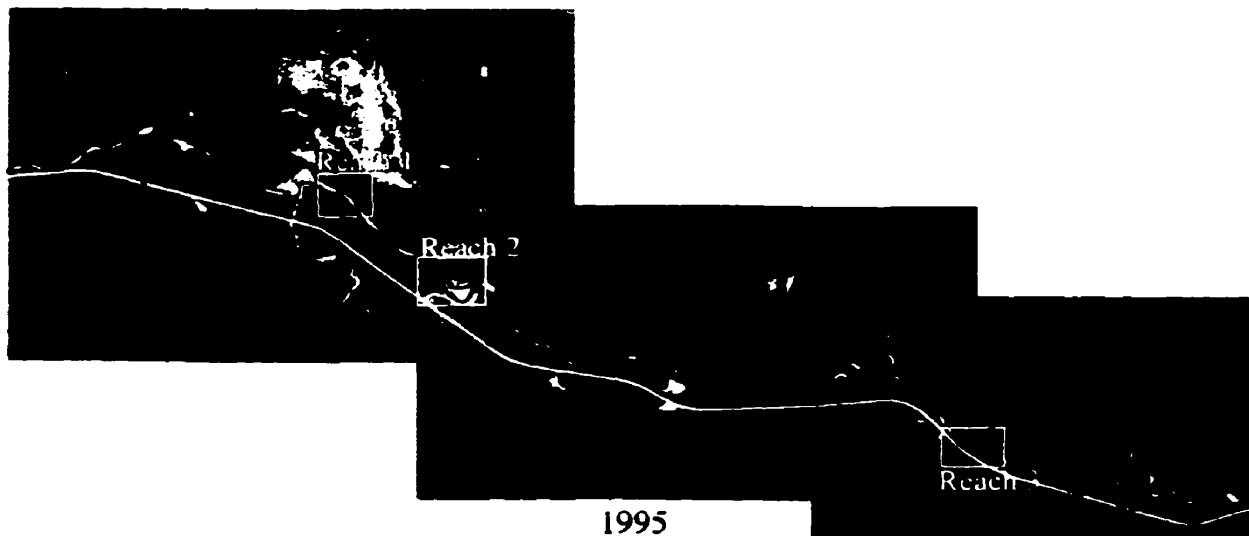
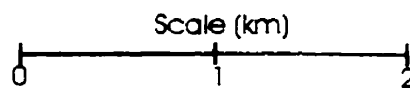
The study sites were located within the channelized reach to illustrate the morphological response to floods of different magnitudes in reaches of contrasting substrate, slope and pattern.

Figure 2.1: Location Map, Sainte Marguerite River
(based on NTS series maps 22C and 22D)





1950



1995

Figure 2.2 Channelized Reach of the Ste. Marguerite River, 1950 and 1995
 air photos: 1950: A12492-396, 1995: Q95402-219, Q95422-132 and 130

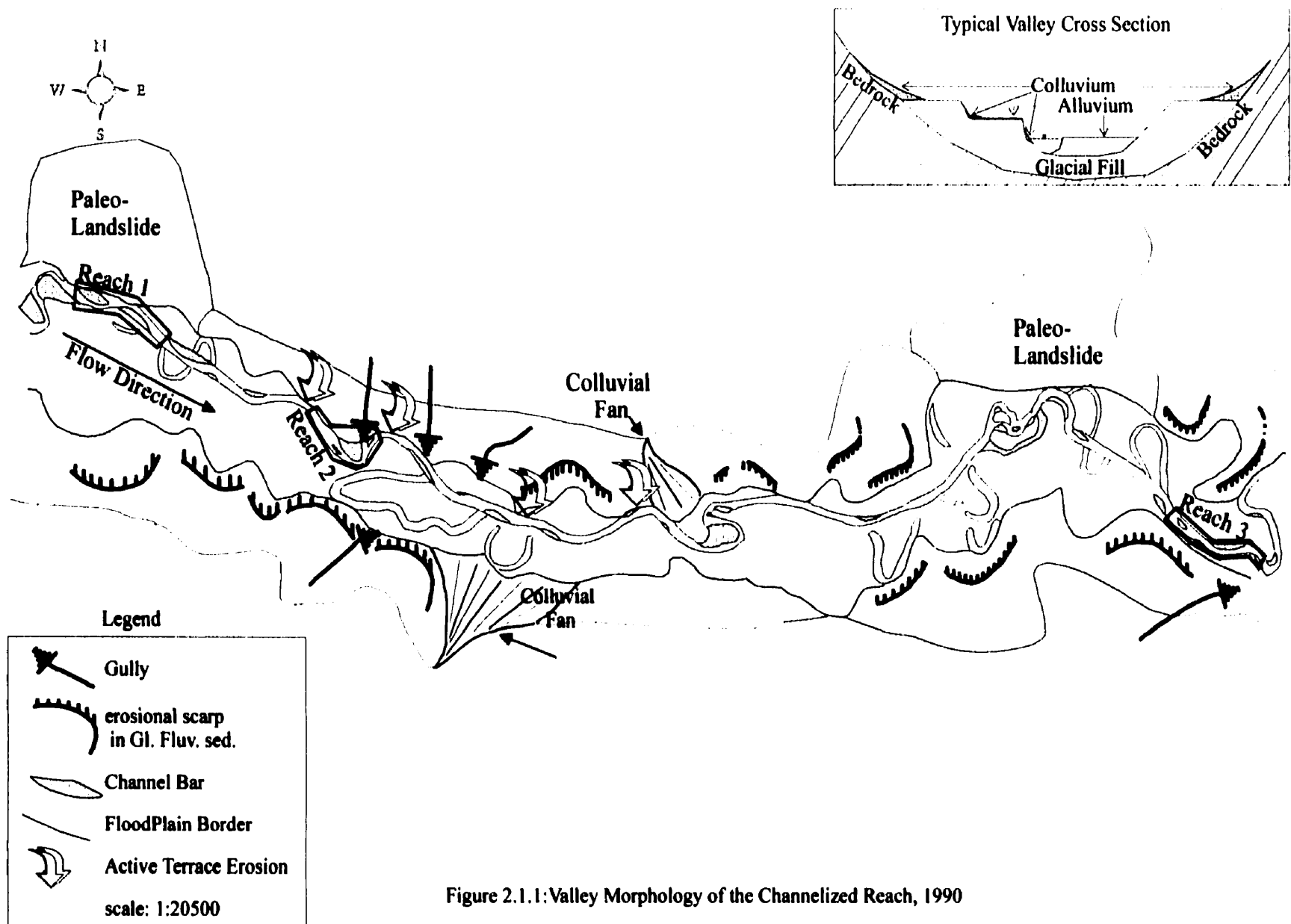
2.1) CHANNELIZED REACH OF THE SAINTE MARGUERITE RIVER

During the 1960's, a highway linking Tadoussac and Chicoutimi was constructed, sections of which were built upon the floodplain of the Sainte Marguerite River. To protect the highway from flooding and to minimize the number of bridges that needed to be built, a fairly long section of the river was channelized; this section of river is illustrated in figure 2.1.1. Within this stretch of river, all meanders were bypassed by man made channels cutting through the neck of the meander. This resulted in a straighter, steeper channel which would theoretically flood its banks less frequently than in its previous state. The channelization also had the effect of physically distancing the river from the highway, theoretically reducing the direct threat of erosion to the roadway.

The valley sides exhibit a number of terraces cut into sandy glacio-fluvial material, with evidence of past fluvial erosion at various elevations, indicating progressive down-cutting into the fill material (figure 2.1.1). The glacial sediments are subject to gully erosion in a number of places, which likely constitute a significant sediment input to the channel. The river floodplain also encroaches on a number of colluvial fans and inactive paleo-landslides. The landslides are to some extent vegetated, and do not seem to be active at present (figure 2.1.1). The contemporary floodplain is defined at its borders by scarps in the glacial materials caused by fluvial erosion.

2.2) HISTORICAL CHANNEL CHANGES ILLUSTRATED BY AIR PHOTOS

A comparison of the channelized reach morphology between 1961 --just after the beginning of channelization-- and 1990 provides some indication of the activity over the last three decades (figure 2.2.1). Some areas underwent rapid and extensive channel change, while most of the channelized reach has remained relatively stable. Measurements of net terrace erosion and point bar growth made using a zoom transfer scope (Driscoll, 1996, internal report) are presented on figure 2.2.1 as well, to provide some indication of the magnitude of net channel adjustment over this time period.



2.3) CHANNEL RESPONSE TO CHANNELIZATION

The imposed channel alteration have produced increased rates of bank and terrace erosion during the past three decades, and presumably higher rates of local sediment transport as well. Note, however, that over most of the channelized reach channel alterations have been fairly minor.

In part this lack of activity at the downstream-most end of the channelized reach is due to the existence of a local base level control at the confluence of the Principal and the Northwest branches downstream of the channelized reach. A coarse alluvial fan has been deposited at the mouth of the steeper Northwest, creating a boulder rapid channel section downstream, within which significant vertical erosion is improbable under the current runoff regime. Upstream of the fan, the main channel exhibits a tortuously meandering pattern which progressively grades into the gravel bed pattern observed in the upstream study reaches; this transition from sand to gravel bed can be seen in figure 2.2 just downstream of reach 3.

Additionally, coarse material supplied to the river during the historical erosion of the glacio-fluvial fill --as well as through present-day bank retreat-- may protect the bed from degradation. While this sediment is not a lag deposit, it does reduce channel activity through its relative immobility.

2.4) CHARACTERISTICS OF THE THREE STUDY REACHES

The three reaches selected for this study exhibit a range of sedimentological, morphological and channel slope characteristics (figure 2.4.1); sedimentological data on figure 2.4.1 was derived from bulk samples taken at the bar heads in each of the reaches. Sediment sampling methodology is described in chapter 3. There are no tributaries to the Sainte Marguerite in the stretch of river between the upstream- and downstream-most reaches, and therefore the discharge through each of the reaches is essentially the same.

The upstream site --reach 1-- has the highest channel gradient, and the coarsest sediment. The channel is relatively straight, with two lateral bars (bars 1 and 2, figure

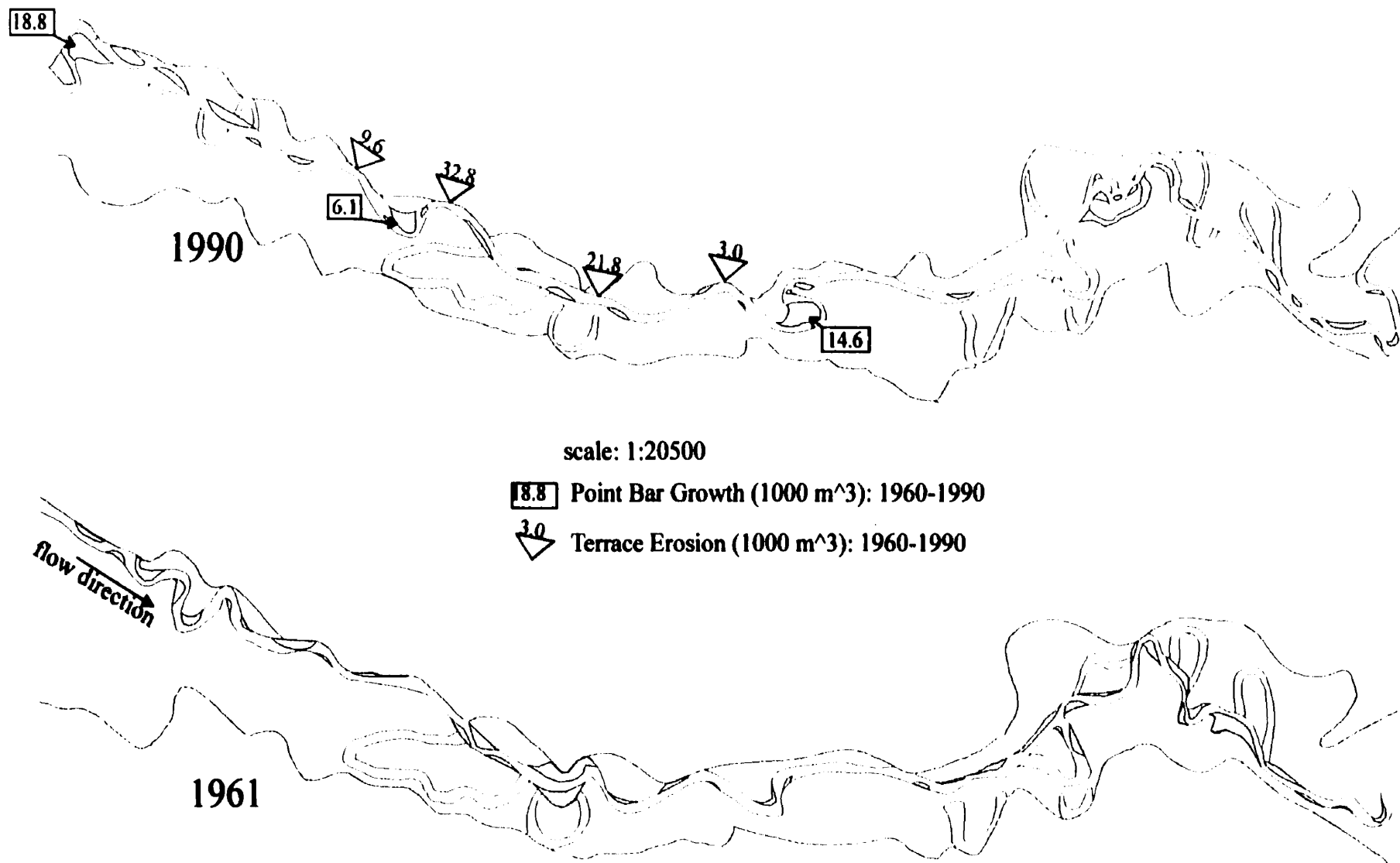


Figure 2.2.1: Channelized Reach Morphology in Planform, 1961 and 1990

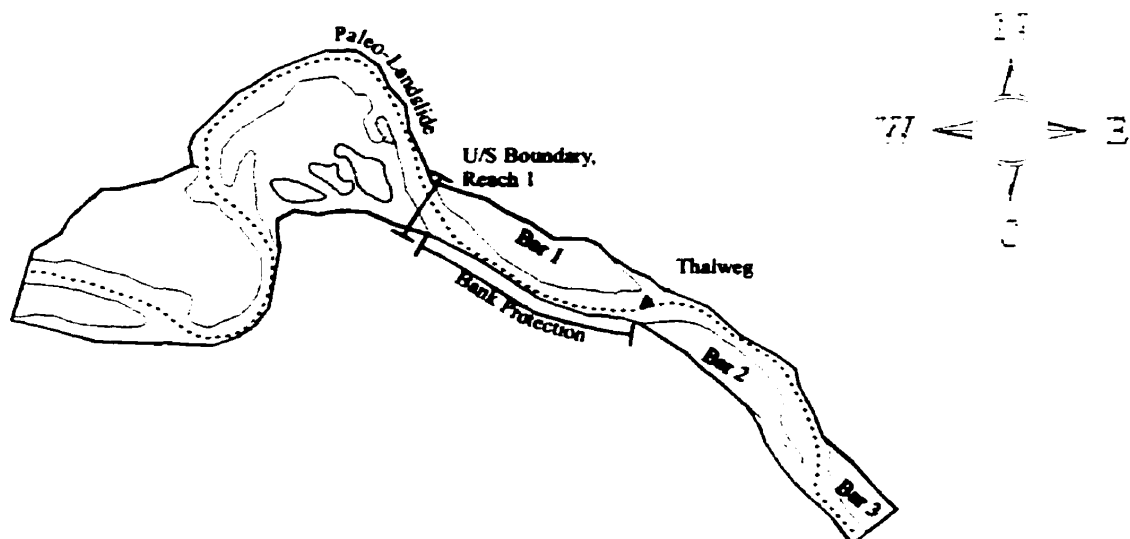
2.4.1). Upstream of the reach is a complex point bar, which stores a large amount of sediment.

Reach 2 is 500 m downstream of reach 1, and exhibits similar sedimentological characteristics and channel slope (figure 2.4.1). A terrace at the upstream reach limit supplies large amounts of gravelly sand to the reach, which is reflected in the greater range of substrate size. The reach morphology is dominated by a central point bar (bar 2); the adjacent cut bank has been protected by rip rap.

The third reach is almost 4 km downstream, and has a much lower channel gradient. It is located just upstream of the transition from gravel bed to a sand bed channel pattern. The upstream boundary is located just below a loose, bouldery weir-like structure built across the channel. The “weir” was likely emplaced in the 1970’s to mitigate potential bed incision adjacent to the highway, or possibly to provide temporary sediment storage upstream. The segment of the reach downstream of the weir is fairly straight, and contains a lateral bar of fine gravel (bar 1), and a medial bar just downstream (bar 2). Downstream, a meandering pattern develops; there is a fine gravel point bar (bar 3), followed by a sandy point bar (bar 4).

Reach sedimentology was characterized by bulk samples taken at the bar heads, grid-by-number samples upon the bar surface at several other locations, and by field sketches of the planimetric variations in sediment texture made upon detailed topographic maps based on reach surveys. Sediment sampling methods are described in chapter 3, and the sediment texture data is fully presented in Appendix A. Reach-scale sedimentology is summarized in figure 2.4.2. Based on limited point sampling combined with visual surveys, these maps illustrate the main patterns of bed material textures in the study reaches.

There is little sedimentological variation within reach 1 (figure 2.4.2). Several zones of fine material exist at the upstream boundary, primarily along the channel margins. Finer material is also found at the confluence of the main and secondary channels near the tail of bar 1, at the head of bar 2 in the lee of the bank protection and at the tail of bar 2. The surface material is also finer than average within the secondary channel which traverses bar 1 and within the main channel in the pool opposite bar 2.



	reach 1	reach 2	reach 3
length (m)	355	392	374
bankfull width (m)	38	58	28
water surface slope (at or above bankfull)	0.0028	0.0026	0.001
D50 _{subsurface} (mm)	19 - 39	9 - 32	5.6 - 19
D85 _{subsurface} (mm)	70 - 80	31 - 91	21 - 31
D50 _{surface} (mm)	41 - 64	18 - 59	12 - 19
D85 _{surface} (mm)	75 - 102	32 - 101	28 - 31
Armor Ratio based on D50 _(surface/subsurface)	1.2 - 3.1	1.9 - 3.3	1.0 - 2.1
Channel Pattern	wandering with lateral bars	acute meander with medial bar upstream	wandering, with point, lateral and medial bars.
Bank Protection	u/s lateral bar only	point bar only	right bank up to first point bar
Terrace Input	no	at u/s and d/s boundaries	no
Other	Complex point bar u/s of reach		weir at upstream boundary

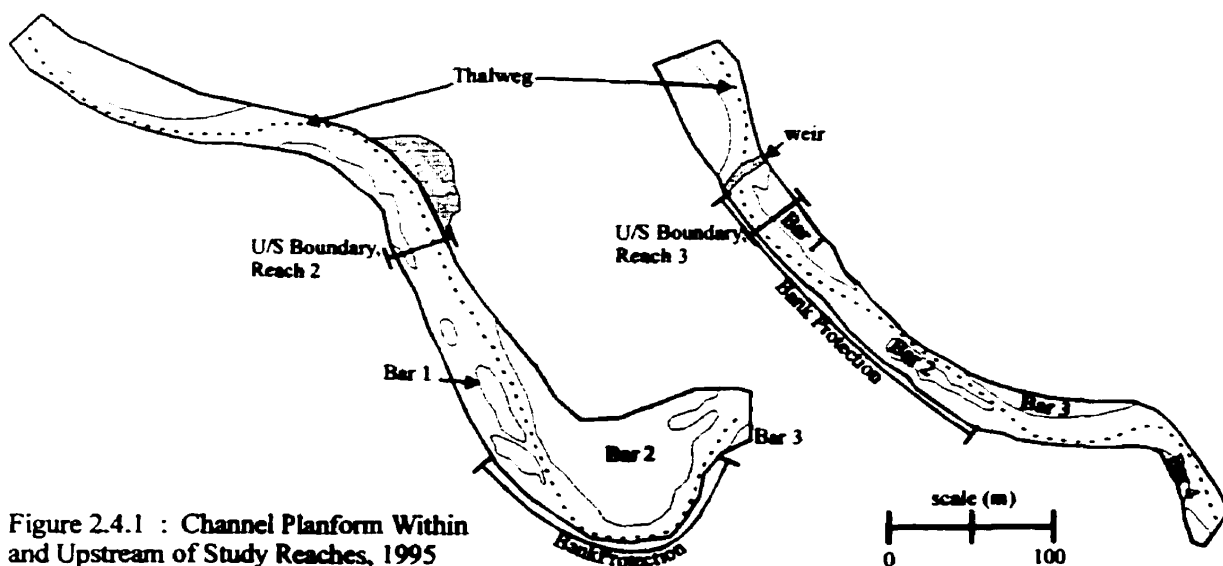
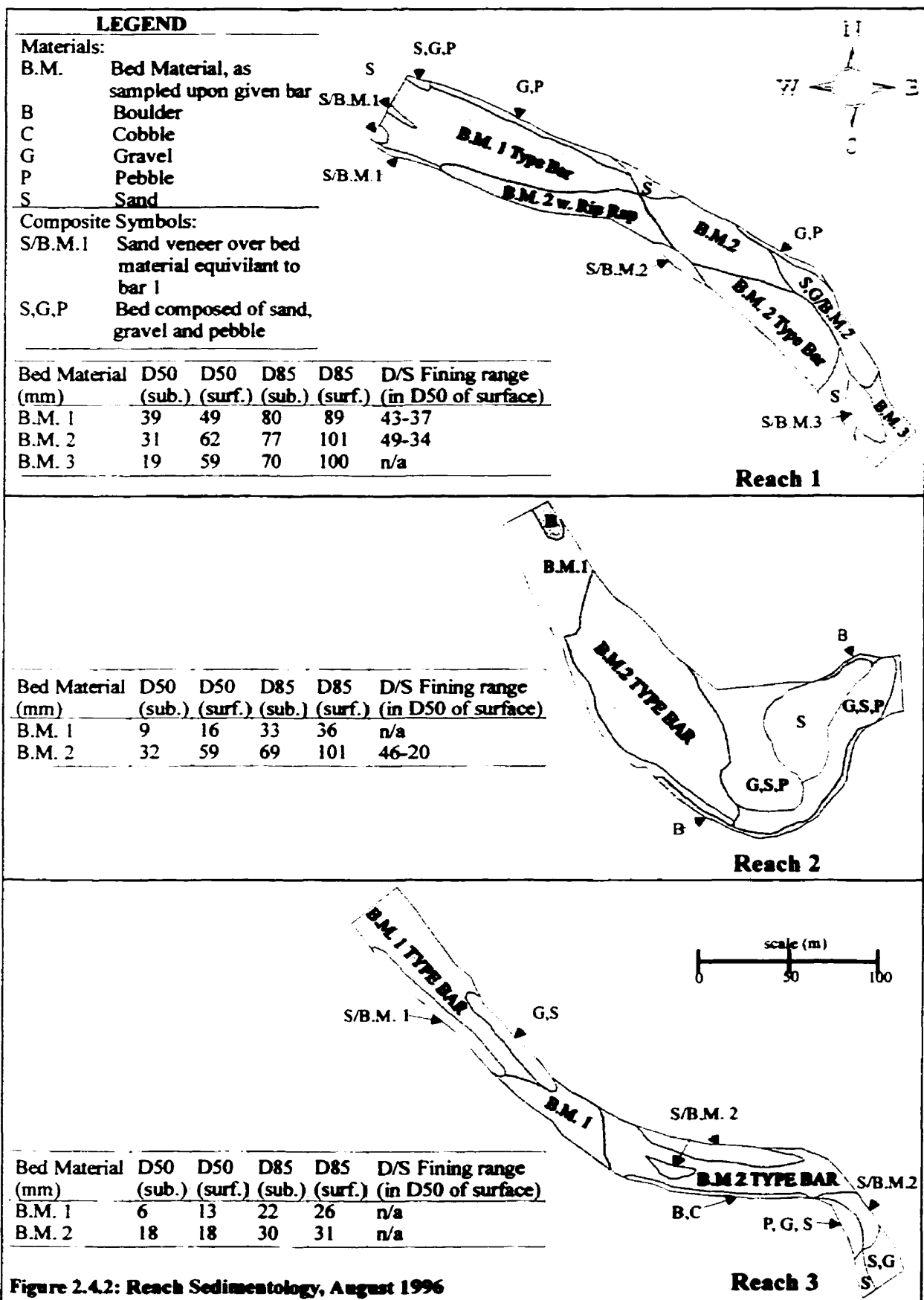


Figure 2.4.1 : Channel Planform Within and Upstream of Study Reaches, 1995



The surface texture is coarser than average within the channel adjacent to the bank protection as the coarse, angular boulders emplaced along the banks are incorporated into the bed.

Reach 2 exhibits a more variable distribution of surface sediment textures. Upstream of the point bar, the material is relatively fine, though it is still primarily gravel. Large, stable boulders supplied by the eroding terrace characterize the pool at the upstream end of the reach. The head of the point bar has a texture similar to the main channel in reach 1. The downstream half of the point bar quickly grades into fine gravel and sand and finally to sand.

Reach 3 has a fairly fine gravel substrate over much of the bed. A sand and fine gravel substrate dominates the bed downstream of the inflection between bar 3 and 4. A sand veneer covers the bed in the thalweg opposite bar 1, and a fine gravel substrate typifies the secondary channel running along the left bank of bar 1. Sand also forms a veneer over the top of bar 3. The cut bank opposite bar 3 exhibits a lag of boulders and cobbles at its base.

3) METHODS

3.1) SURVEY DATA

The morphology of the three reaches was surveyed three times, bracketing two distinct flood events. Surveying was performed with a Total Station, which is a high accuracy electronic theodolite incorporating a laser-based distance measuring unit (an EDM), and using a penta-prism --which reflects the laser beam from the EDM-- mounted on a telescoping rod, in place of the usual stadia rod. This allowed for very precise, very rapid collection of topographic data. Data was stored digitally by the Total Station, and subsequently downloaded directly onto a PC. The equipment allowed for the collection of upwards of 1000 data points per day by a team of two surveyors. No data reduction was required; the data was recorded in x,y,z form using a UTM coordinate system.

Typical survey point spacing varied from less than 1 meter to almost 5 meters, depending on the topographic complexity. Survey points were located in an approximate grid --allowing for the location of many points in areas of relative complexity and of fewer points in flatter, less complex areas-- to maintain a consistent survey coverage.

Semi-permanent bench marks used to initiate the survey were initially established using differential Global Positioning System technology, accurate to a few cm (accuracy depends on the satellite constellation on the given day). Differential GPS differs from GPS in that it requires two stations, recording simultaneously, to and produce position measurements relative to one another, which substantially increases the accuracy. These bench marks were used to initialize the Total Station in each reach; subsequent bench marks were established using the Total Station. Temporary bench marks used in the two years of survey were either metal rods inserted up to three feet into the gravel bed or wooden stakes inserted about 1 foot into the bed.

This raw survey data was subsequently imported into GRASS --a raster-based geographic information system-- with which digital terrain models were created with a horizontal resolution of one decimeter, and vertical resolution of one centimeter. The

digital terrain models were developed in GRASS using an inverse-distance weighting procedure based on the nearest three data points. This procedure was the most conservative interpolation algorithm available in GRASS, and best reflected the method of data collection (which assumed linear interpolation based on a triangular irregular network). The interpolation procedure was chosen to minimize its effect on the digital terrain model. A triangular irregular network interpolation routine was not available in GRASS.

While the survey instruments had a precision of one or two centimeters, the nature of the bed surface --which consisted of gravel with a b-axis approaching 181 millimeters for the coarsest particles-- limited the accuracy with which the surface could be resolved. Uncertainty in the vertical position of a given survey data point is conservatively estimated to be at most 5 cm. Given this natural limitation on the possible measurement accuracy, the raster --which has a vertical resolution of 1 cm-- should be more than adequate for identifying any changes that have occurred. The digital elevation models became the raw data for all subsequent GIS analysis.

3.2) SEDIMENTOLOGICAL DATA

Reach sedimentology has been characterized using a number of standard methods. Grid-by-number samples (Leopold *et al.* 1964; Church *et al.* 1987) were taken following each flood event at various points in reaches 1 and 2; the sediment texture in reach 3 is too fine for this method to be reliable. A single grid-by-number (or Wolman) sample consisted of b-axis measurements for 100 stones, collected over a 5 by 5 m grid. The stones were templated in the field using hand-held aluminum templates. Typically, three samples were taken on a given bar. Samples were located --as precisely as possible-- along the direction of gravel transport so as to provide some indication of the down bar pattern of fining, rather than lateral patterns of sediment texture variation. The first sample was typically located at the bar head adjacent to the exposed riffle upstream, the second sample at the bar toe, and the last sample on the patch of coarsest sediment found on the downstream 1/5 of the bar.

Bulk samples (Church *et al*, 1987) of the bed surface and subsurface were taken at bar heads in the reaches. In reaches 1 and 2, bulk samples were taken after both high flow events. These samples were taken within the 5 by 5 m bar head zone also sampled by grid-by-number. In reach 3, bulk samples were taken at the bar heads following the July 20 event only; flow conditions did not permit samples to be taken before this. Bulk samples of the surface material (a.k.a. armor, pavement) were taken by first identifying the largest stone in the sample zone and then skimming all material on the surface with a shovel to the depth of this stone. A square sampling area was chosen to limit possible sampling bias. Care was taken during the skimming to minimize the loss of fines during the sampling. Sample sizes taken in this way were approximately 125 kg. The estimated precision for the size percentiles for samples of this size, assuming a maximum particle size of 128 mm is between 2 and 5% (Church *et al*, 1987).

The subsurface material (a.k.a. bed material, sub-pavement) was sampled in the same location as the surface material. Once the surface had been removed during the surface sampling, an approximately rectilinear volume of sediment was excavated to a depth of 30 cm, totaling about 200 kg. The estimated precision for the size percentiles for samples of this size, assuming a maximum particle size of 128 mm is between 1 and 2% (Church *et al*, 1987).

Bulk samples of the surface and subsurface were sieved in the field down to 16 mm; a split of about 5 kg was taken from the remaining sediment, which was transported back to the field station where it was dried for at least 24 hours at 40 degrees Celsius. It was then sieved at one-phi intervals down to 63 microns.

A more general description of the reach overall was made by mapping the sedimentological variations within the reach upon an existing topographic map of the reach. Sediment textures were qualitatively related to existing sediment samples in the vicinity by way of comparative judgments of the texture. Where necessary, the material was described by the applying descriptive terms based on the sediment caliber such as boulder, cobble, pebble, gravel or sand. Where this material appeared to be a veneer over the typical bed material, it was noted as well.

3.3) SCOUR CHAINS

Scour chains provide information on the mobility of the channel that is not available from comparisons of topographic surveys. Maximum scour depths were measured using scour chains installed at various locations in the three reaches during the 1995 field season.

Scour chains were installed --following previously established procedures focused on minimizing bed disturbance (M. Church, pers. comm. 1995, Laronne et al. 1994, Nawa and Frissell 1993)-- in the channel bed behind riffle crests. Installation was accomplished by driving a steel pipe into the gravel, inserting the chain and then removing the pipe, leaving the chain in the bed. Typically, 30 minutes to an hour were required for the installation of a single chain to a depth of 50 cm.

The chains were recovered using a metal detector to relocate them, and then --if they were buried-- using a shovel to remove the fill material. Using a metal detector allowed the chains to be recovered relatively quickly and efficiently, thus reducing the labor required.

Unfortunately, no interesting data came out of this work. High flow levels during June and July 1996 prevented the recovery of the chains following the spring flood. During low flow conditions in August 1996, only 15% of the chains were recovered; extremely high flow conditions during the July 20 flood event had scoured out all of the chains near the thalweg, leaving only those located along the channel margins.

4) SPRING AND SUMMER FLOW CONDITIONS IN THE STUDY REACHES FOR 1996

4.1) DISCHARGE CONDITIONS

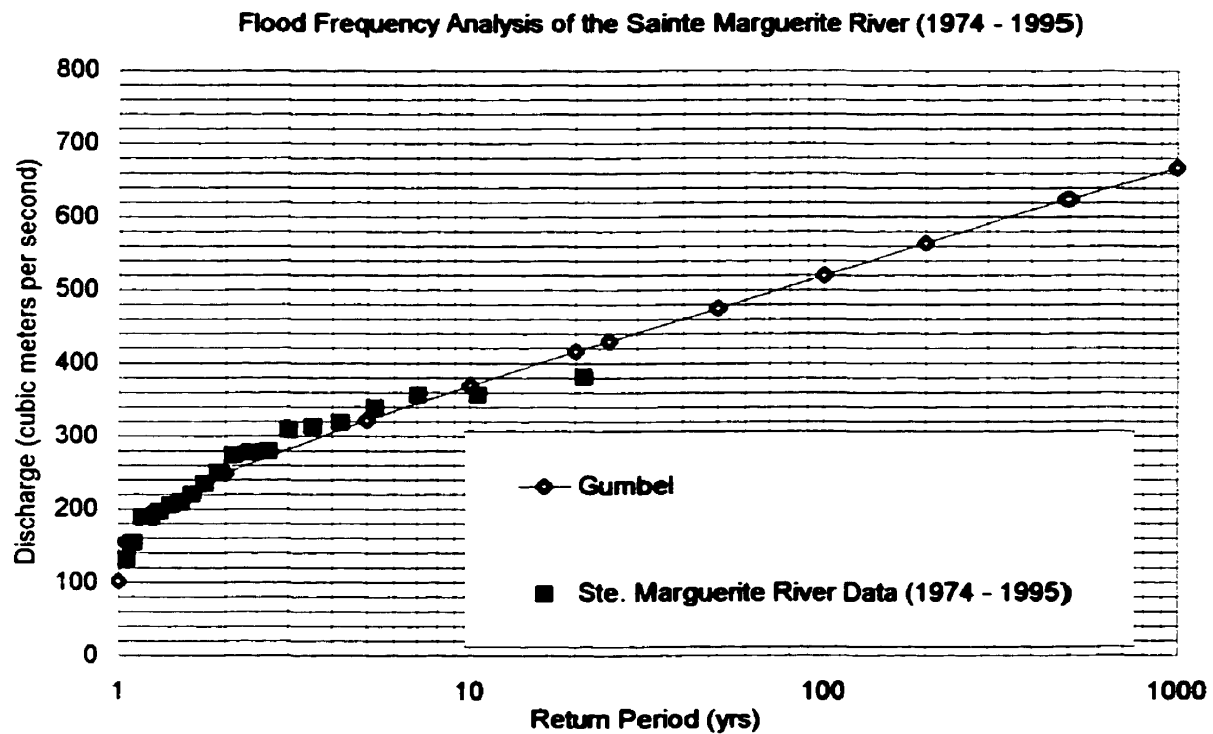
4.1.1) HYDROMETRIC STATION DATA ON THE NORTH-EAST BRANCH

Three significant flood events occurred within the Sainte Marguerite basin during the spring and summer of 1996. The first peak was minor while the second was reported to have a decadal scale recurrence according to local inhabitants; both were generated by rain-on-snow events typical of the spring snowmelt. The third event was generated by a summer storm, producing some of the most severe flood damage in Canadian history for the Saguenay region. The data available for reconstruction of these three event magnitudes in the Sainte Marguerite basin are limited.

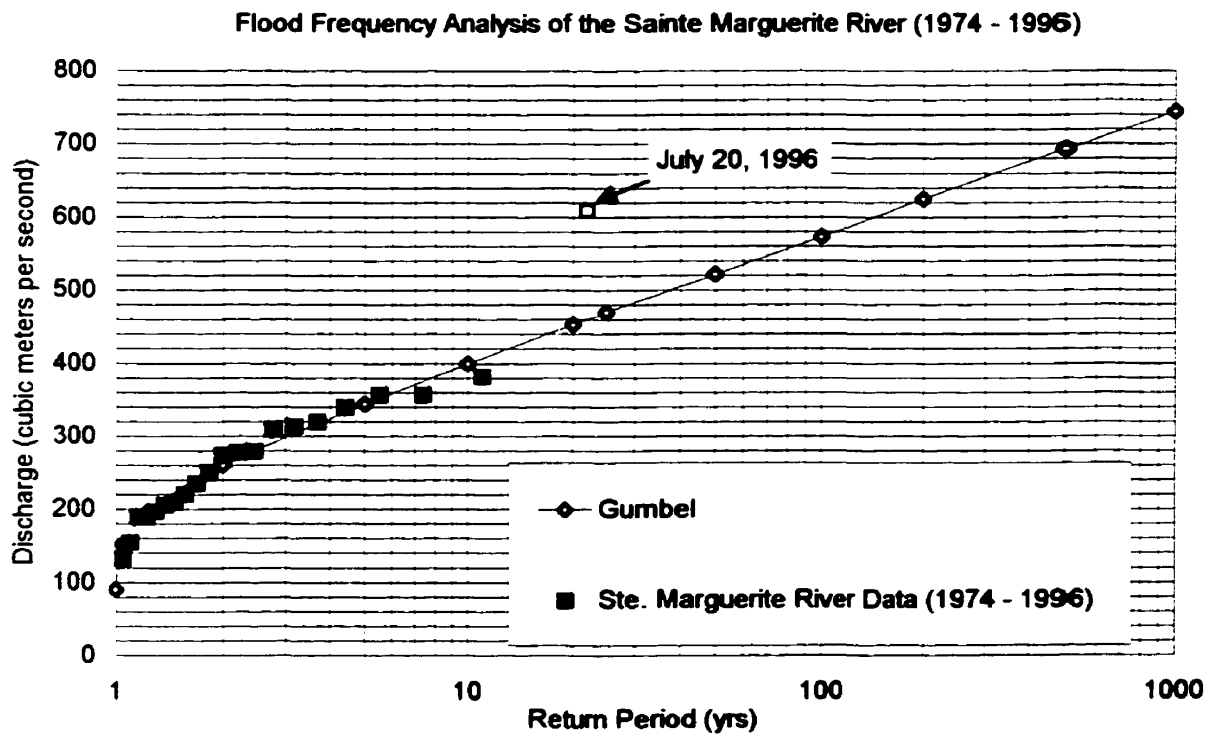
On the principal branch of the Sainte Marguerite River, there are no time series data on river stage or discharge. A hydrometric gauge was installed during the summer of 1996, following the data collection period for this study, but not in time to record the flood events. However, a gauge has been maintained near the mouth of the North-East branch of the river since 1974 (Water Survey of Canada station No. 02RH047).

The basin area at the North-East gauge is approximately 3.5 times that at the study sites on the Principal branch. Unfortunately, no data are available for the North-East gauge during the period from May 14 to July 16, 1996, during which the second peak of the spring freshet occurred. However, the gauge was operational on July 20, 1996, when the largest flood on the 22-year record occurred. The relative recurrence periods of the two spring and the July peak flows can be estimated from these records for the Sainte Marguerite River at the study sites.

The flood frequency relation based on the maximum annual daily discharges is presented in figure 4.1.1. A Gumbel type distribution, fit to the data using the British Columbia Ministry of Environment flood frequency analysis program, FFAME, is shown, as are the data points to which it was fit.



A.



B.

Figure 4.1.1. Annual Flood Frequency Data From the North-East Branch, Sainte Marguerite River
 A. Gumbel distribution fit to all data, excluding the July 20, 1996 event
 B. Gumbel distribution fit to all data, including the July 20, 1996 event

The extreme event occurring on July 20, 1996 affects the distribution significantly, and the distribution was fit to data sets including and excluding this event, providing a range of possible return periods for a given event. Log-Normal, Pearson type III and Log Pearson Type III distributions were also applied to both data sets, but they were much more sensitive to the inclusion of the July 20, 1996 event (see Table 4.1.1).

The first peak of the 1996 spring freshet occurred on April 27; the mean daily discharge recorded on the North-East was 245 m³/s --which-- based on the Gumbel distribution, would have a return period of about 1.8 to 1.9 years. The following peak, occurring on May 16, was reportedly much larger than the preceding one (with a return period on the order of a decade), though stage data is not available for this time period at the North-East gauging station. Return period estimates for this event are presented in the following section. The flood occurring on July 20th attained a peak of 609 m³/s on the North-East, which was larger than any previously reported event; the return periods given by the four different distributions which were fit to the two data sets (one including, the other excluding the July 20, 1996 event) are presented in table 4.1.1.

Table 4.1.1. Return Period Estimates for the July 20, 1996 Flood Event.

Distribution Type	Return Period for the July 20, 1996 Event	
	A. Excluding the July 20, 1996 event from the data set. (years)	B. Including the July 20, 1996 event in the data set. (years)
Gumbel	398	160
Log-Normal	34,000	92
Pearson Type III	1,000,000	83
Log Pearson Type III	79,600	85

The Gumbel distribution produces the most conservative and consistent estimates of the return period; the July 20 event would have a return period of between 398 and 160 years.

4.1.2) DISCHARGE ESTIMATES AT THE STUDY SITES ON THE PRINCIPAL BRANCH

CIRSA staff recorded water levels within reach 1 at several different periods during the spring and summer of 1996. Workers in the field directly surveyed water levels on April 25, 1996 at both the upstream and downstream limits of reach 1. The April 25 data corresponds roughly to the first peak of the spring freshet and should have a return period of about 1.8 years, based on the record from the North-East gauging station (on the North-East, the discharge on April 25 was 239 m³/s, versus 244 m³/s on April 27).

The larger peak of the spring freshet occurred on about May 15, 1996. The maximum water elevation was recorded at the upstream end of reach 1 during this event. The downstream boundary was not accessible during this period of high flow. Workers in the field on May 27 documented apparent high water line markers on a sandy bank near the downstream boundary, which were consistent with the upstream water level observed and the water surface slope measured on April 25.

Following the extraordinary July 20 event, maximum stage indicators were observed and recorded at the upstream boundary of reach 1; no markers were evident near the downstream reach boundary.

Given this information, average hydraulic radii were calculated in reach 1 for each of the three events and slope-area estimates of the flood discharges were computed. The results are presented in table 4.1.1. Manning's equation was used to produce estimates of the average velocity based on the water surface slope data, and applied over the reach average cross-sectional area to produce a discharge estimate. Manning's n estimates were based on grain size data from samples of the surface layer taken at the bar heads within the reach using Strickler's law. Error estimates were derived based on the uncertainty of the estimate of hydraulic radius, the water surface slope, the cross-sectional area and Manning's n.

Table 4.1.1. Estimated 1996 Flood Discharges, Reach 1.

Event	R (m)	S	n_{Manning}	V (m/s)		A (m ²)	Q (m ³ /s)	
				ave.	std. err.		ave.	std. err.
April 25	0.67	0.0028	0.029	1.39	18.4%	26.10	36	22.3%
May 16	1.48	0.0028	0.029	2.35	16.4%	60.94	143	20.2%
July 20	1.98	0.0028	0.029	2.85	16.2%	86.16	246	18.8%

Uncertainties in peak stage estimates are under 5 cm and are negligible compared to the other sources of error in the slope-area calculations. The uncertainty for the hydraulic radius term was based on the standard deviation for a number of profiles traversing the channel extracted from the digital elevation models in GRASS, as was the uncertainty for the cross-sectional area. The uncertainty in the water surface slope was taken to be the difference between the water surface slope measured on April 25 during a moderately high discharge, and those observed on May 26 and 27, during much more moderate discharges. Since entry and exit cross-sectional areas were approximately equal, no velocity head correction was made and the energy slope was assumed to be identical to the water surface slope. Uncertainty in n was taken to be the difference between the values estimated from the highest and the lowest D50 for the surface material using Strickler's law. Estimates of $D50_{\text{surface}}$ were derived from either the bulk surface or the Wolman samples. The value of n used for the calculation was based on an average value for $D50_{\text{surface}}$ at the head of each bar within the reach as measured by the bulk sampling technique.

There is no way to estimate accurately the over-bank water losses, and these have not been accounted for. The estimates presented above are for the discharge carried by the channel itself, though it is likely that minor secondary channels on the floodplain were also active, especially during the July 20 event. However, water leaving the channel can have little effect on the dynamics within the channel, which is the focus of the present work, and therefore these losses have been ignored.

Given the discharge estimates from the slope-area method at the study sites and the data from the gauge on the North-East branch of the Sainte Marguerite River, it is possible to make an estimate of the return period for the May 16, 1996 event. The ratio of the discharges occurring on July 20, 1996 at the study sites and at the gauge on the North-East were used to estimate the discharge occurring at the gauge on the North-East Branch on May 16. This estimate was subsequently used to derive a return period for this event. Table 4.1.3 presents the return period estimates derived from four different distribution types based on data sets including/excluding the July 20, 1996 event.

Table 4.1.3. Return Period Estimates for the May 16, 1996 Flood Event.

Ratio of July 20, 1996 Discharges (North-East/Study Site Location)		2.47 : 1
Discharge, May 16 1996 (Study Site Location)		143 m ³ /s
Estimated Discharge, May 16 1996 (North-East Branch)		353 m ³ /s
Distribution Type	Return Period for the May 16, 1996 Event	
	A: Excluding the July 20, 1996 Event from the Analysis (years)	B: Including the July 20, 1996 Event in the Analysis (years)
Gumbel	7.9	5.6
Log-Normal	10.0	5.3
Pearson Type III	10.1	5.3
Log Pearson Type III	9.0	5.3

Based on this analysis, the return period for the May 16, 1996 event seems to be between 5 and 10 years. The results are consistent among the various distributions, though the Gumbel distribution exhibits the least sensitivity to the July 20, 1996 event.

4.2) SHEAR STRESS AND STREAM POWER

There are several measures of the flow strength by which one can characterize each of these flow events besides the discharge; two of the most useful quantities are shear stress and stream power. Reach average shear stress and stream power have been estimated approximately --based on the reach topography, which determines the hydraulic radius, the cross-section for flow and the slope, and observed or interpreted peak water levels-- using the usual 1D uniform flow approximations

$$(5) \quad \tau_o = \rho g R S_w \text{ and } \omega = \rho g Q S_w / w$$

where τ_0 is the reach average shear stress exerted upon the wetted perimeter, ρ is the density of water, g is the acceleration of gravity, R is the hydraulic radius, S_w is the water surface slope (taken here to approximate the energy gradient) ω is the average specific stream power and w is the average bankfull channel width.

As mentioned above, workers in the field observed water levels in reach 1 during the three flood events. In reach 2, the water level at the upstream and downstream boundaries was surveyed on April 25 during the early spring, near bankfull event. The slope measured at this time was applied to the other two events as well. In addition, the downstream water levels were reconstructed for the May 15 and July 20 floods based on a survey of physical evidence of the peak water levels. The same physical parameters were calculated for this reach as for reach 1; that is, the hydraulic radius for each event, the cross-sectional area for flow, and the water surface slope.

Upstream and downstream flow levels within the third reach were surveyed, also on April 25, providing an estimate of the water surface slope. However, the flow depth during the May 15 and July 20 events could not be reconstructed from physical evidence. Instead, the reach average water depths for each event were solved iteratively by imposing a known discharge (those reported above for reach 1) and using the observed water surface slope and Manning's Law. From this information, reach average shear stress was calculated, as was specific stream power for all three reaches. Table 4.2.1 presents the results of these calculations, including the estimated errors for the calculated parameters. Errors for the morphological parameters were based on the sample standard deviation (both R and w estimates for the reach come from a number of estimates equally spaced throughout the reach). The error in the water surface slope was taken as the difference in measured slope between a relatively high flow (April 25, 1996) and a more moderate one (May 26/27, 1996). The error estimates for the discharge were calculated above.

Table 4.2.1. Reach Scale Mean Shear Stress and Stream Power Estimates for 1996 High Flow Events.

Reach 1	R (m)	S	τ (Pa)		Q (m ³ /s)	w (m)	ω (W/m ²)	
			ave.	std. err.			ave.	std. err.
April 25	0.67	0.0028	18	19.2%	36	37.84	26	42.0%
May 16	1.48	0.0028	41	16.9%	143	37.84	104	39.9%
July 20	1.98	0.0028	54	16.4%	246	37.84	178	38.6%
Reach 2	R (m)	S	τ (Pa)		Q (m ³ /s)	w (m)	ω (W/m ²)	
			ave.	std. err.			ave.	std. err.
April 25	0.59	0.0026	15	21.5%	36	58.35	16	41.2%
May 16	1.53	0.0026	38	13.7%	143	58.35	61	39.1%
July 20	2.11	0.0026	53	14.3%	246	58.35	105	37.8%
Reach 3	R (m)	S	τ (Pa)		Q (m ³ /s)	w (m)	ω (W/m ²)	
			ave.	std. err.			ave.	std. err.
April 25	1.04	0.0010	10	19.6%	36	28.48	12	41.7%
May 16	2.04	0.0010	20	18.0%	143	28.48	49	39.6%
July 20	2.77	0.0010	27	17.6%	246	28.48	85	38.3%

There is a progressive increase in both shear stress and unit stream power over the three events occurring in 1996. In addition, both shear stress and unit stream power decrease from reach 1 to reach 3 for the same event, reflecting the decreasing channel gradient. Since they involve discharge in additions to flow depth and slope, the estimate errors are larger for unit stream power than for shear stress for all reaches. As a result, shear stress will be used as the main index of flow strength in subsequent analyses.

4.2.1) ENTRAINMENT THRESHOLDS AND THE MOBILITY RATIO

From the reach scale estimates of shear stress, one can calculate a mobility ratio for each reach, giving some indication of the relative level of bed disturbance to be expected. The mobility ratio is the ratio of the stress imparted upon the bed to the force required to initiate transport of the bed material. Typically, it is the entrainment of the median particle on the surface of the bed that is critical for entrainment of the bed overall. The mobility ratio can be expressed as

$$(6) \quad \tau_o / \tau_{c(D50)}$$

where τ_o is the shear stress exerted upon the bed and $\tau_{c(D50)}$ is the shear stress required to mobilize the D50 of the surface material. For simplicity, the values of τ_o here are reach average values ($\tau_o = \rho g R S_w$, as presented earlier) and do not represent the maximum shear stresses occurring within the reach which are very difficult to estimate from reach-scale hydraulic measures. It was decided to use the surface D50 estimates from the bar heads in each of the reaches, where the bulk samples of the surface were located. However, the bar heads represent the coarsest alluvial material within the reach; they represent the coarsest regularly mobile substrate in the reach. Therefore, the mobility ratio calculated in this way does not represent a ratio of shear stress at a given location to the threshold for the entrainment of the bed material at that location; rather, it represents a relation between the reach average shear stress and the stress necessary to mobilize the material located at the bar heads within the reach. Andrews (1984) and Ferguson and Ashworth (1991) use similar reach-averaged mobility ratios to compare transport conditions between different river reaches.

It follows that mobility ratios calculated in this way must be interpreted carefully. A ratio less than 1 does not imply that the flow conditions cannot produce transport anywhere; rather, bed entrainment will occur in zones of higher than average shear stress only. The purpose of this ratio is to scale the flow strength by the material forming the bed of the reach and thus highlight inter-reach contrasts in substrate mobility along river systems. The more typical application of this ratio requires an estimate of the shear stress and bed entrainment threshold at the same point (Dietrich *et al.*, 1989) ; this data is not available for the present study.

The non-dimensional critical shear stress for entrainment of a gravel bed for a given sediment size class can be estimated by the equation

$$(7) \quad \tau_{ci}^* = \tau_i / \{(\gamma_s - \gamma_f) D_i\}$$

The value of τ_{ci}^* is important; it was therefore decided to use rather conservative estimates of τ_{ci}^* . Ashworth and Ferguson (1989) have examined the critical threshold for movement in three rivers, and have estimated the critical entrainment thresholds on a size by size basis. The three rivers used in this study are the Alt Dubhaig, the Feshie (both in

Scotland) and the Lyngsdalselva (Norway). The results from data from all three rivers took the form

$$(8) \quad \tau_{ci}^* = 0.089(D_i/D_{50surf})^{0.74}$$

where $D50_{surf}$ is the surface median substrate size. This generally agrees with the results reported by others (Andrews, 1983; Parker *et al.*, 1982), and from this relation, one can estimate the critical threshold for sediment transport based on the D50 of the surface material using a value of τ_{ci}^* of 0.089. This value is conservative: other studies have reported values of τ_{c50}^* of 0.05 to 0.06.

The results of the calculations made in this way are presented below in table 4.2.2.

Table 4.2.2. Event Specific Mobility Ratios.

Reach	D50 ¹ _{surface} (mm)	Crit. Shear Stress (Pa)	Mobility Ratio		
			April 25	May 16	July 20
1	46	65	0.29	0.63	0.85
2	41	38	0.27	0.71	0.98
3	25	35	0.29	0.57	0.77

1: median surface size is estimated from bulk samples of the surface material at the bar heads within the reaches

It should be kept in mind that these mobility ratios are reach average estimates, therefore one would expect far less than average activity on the channel margins and much more than average activity in the thalweg. This ratio is used here simply as a convenient method of scaling the flow strength by the bed material caliber for inter-reach and inter-event comparison.

5) PATTERNS OF MORPHOLOGICAL EVOLUTION

Morphologic change differed between the three reaches and also between flow events. The primary tool used for analysis of bedform evolution and/or change was GRASS, in which digital terrain models were manipulated to reveal the spatial distribution and volume of net erosion and deposition within the reaches.

5.1) REACH 1

This reach is near the upstream limit of the channelized section of the Sainte Marguerite River, and consists of two lateral bars in a relatively straight length of channel. Immediately upstream is a complex morphological unit consisting of two very large point bars, which developed following channelization (figures 2.2 and 2.4.1).

The river channel response to a flow event capable of producing gravel transport has been classified as either bedform change or as bedform evolution. As discussed at length in chapter 1, bedform change represents localized changes in sediment storage, which are primarily related to site-specific conditions. Bedform evolution is the change in sediment storage that can be related to an overall pattern of channel adjustment to the imposed flow conditions and constrained by the channel boundary conditions (i.e. bank material type, vegetation, anthropogenic effects, etc.).

There are several general evolutionary response types that have been observed by comparing the changes in planform, longitudinal section and in cross-section within the reach. The three flow events bracketed by these three surveys are grouped into two time periods. The first two surveys encompass the small flood occurring in April as well as the significantly larger flood in May. The changes due to the flood in July are illustrated by the third survey.

The first two floods are considered --by necessity-- together; it can be assumed that the much larger flood occurring in May was responsible for the preponderance of the geomorphic work. In any case, both flood peaks were part of the spring freshet, and will thus be treated as a single event. The flood occurring in July is considered in isolation.

5.1.1) GENERAL BEDFORM RESPONSE

The primary tool used to display the detailed reach morphology and analyze the subsequent channel modifications was the raster-based GIS package, GRASS. Raw survey data was imported into GRASS, from which a digital elevation model (DEM) was constructed using an inverse distance weighting procedure, applied to the nearest three survey points. The specific characteristics of the DEM are presented in section 3.1. The digital elevation models are presented in figure 5.1.1. Potential salmon spawning zones are indicated on this figure; these zones were defined to extend upstream of well developed riffle crests for 1 bankfull channel width, having a maximum width equal to the water surface width during low to moderate discharges. These zones are further discussed in chapter 8.

Over the course of the spring freshet, bedform response was localized, although a net evolutionary tendency was evident. Bar head deposition occurred upon bar 1, where a unit bar appeared on the June, 1996 survey (point A, figure 5.1.1). Along the avalanche face on the left flank of bar 1, net deposition occurred; the bar advanced downstream as well. Other significant changes include erosion of the right edge of bar 1 near the bar head and bed scour on and upstream of riffle 2 near the bar tail (R2, figure 5.1.1). The right bank adjacent to bar 1 was protected by rip rap prior to the spring flood of 1994.

On bar 2, net accretion occurred across the bar top and in the adjacent channel. The cut bank opposite bar 2 was eroded and the pool beginning at the bend apex scoured vertically and grew laterally.

The second flood, that of July 1996, caused more extensive change within the reach, concomitant with its larger size. An overall streamlining of bars 1 and 2 is evident. The secondary channel along the left bank of bar 1 has been filled significantly, reducing its cross-sectional area. Unlike the freshet, no downstream component of bar growth seems to have occurred during this event. Erosion in the thalweg upstream of the crest of riffle 2 has continued.

Bar 2 has responded in a fashion similar to that observed during the spring freshet. Both cut bank retreat and pool extension have occurred, as has deposition upon the bar top and the adjacent channel. However, the locus of deposition has shifted downstream and formed a steep avalanche face along the downstream margin of bar 2.

5.1.2) DETAILED MORPHOLOGIC CHANGES IN RESPONSE TO THE SPRING FRESHET

The digital elevation models bracketing the spring freshet were used to identify the precise patterns of net morphologic change, and to calculate the volumes of discrete zones of erosion/deposition. The digital elevation models, referenced to common semi-permanent bench marks in the reach were subtracted one from the other, and the resultant raster map was separated into positive and negative residual components, corresponding to either erosion or deposition occurring in response to a given flood event. The maps of erosion and deposition are presented in figure 5.1.2, with local scour or fill volume estimates overlain.

The pattern of bedform response to the spring freshet is strikingly coherent, and can be grouped into discrete associations of deposition and erosion (figure 5.1.2). A unit bar of approximately 24 m^3 of sediment was deposited at the head of bar 1. Adjacent to this is a related deposit of material in the head of the secondary channel, where close to 21 m^3 of sediment has been deposited.

One hundred and sixty-eight cubic meters of sediment have been deposited along the length of the avalanche face at the tail of bar 1, producing a net downstream component of bar growth. Net erosion of the right edge of bar 1 near the bar head has also occurred --with a volume of 148 m^3 -- opposite the recently protected cut bank (rip rap emplaced in 1993).

At the upstream end of the reach, 148 m^3 have been eroded from the right edge of bar 1, while 7 m^3 were eroded from the bar top and 12 m^3 were eroded from the left bank, for a total of 167 m^3 . Advance of the avalanche face towards the left bank and downstream has resulted in a net deposition of 168 m^3 . Since the locus of deposition is

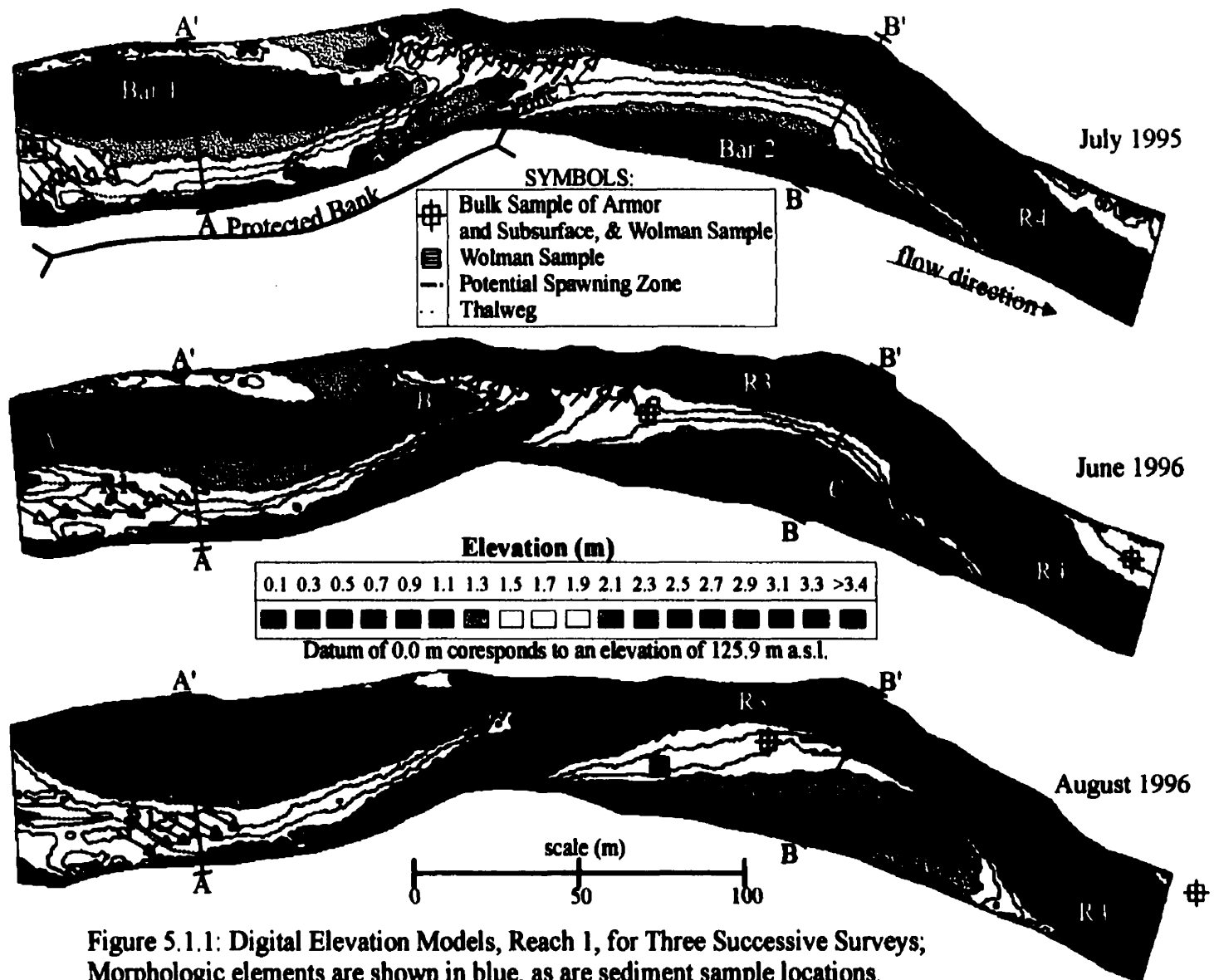


Figure 5.1.1: Digital Elevation Models, Reach 1, for Three Successive Surveys; Morphologic elements are shown in blue, as are sediment sample locations.

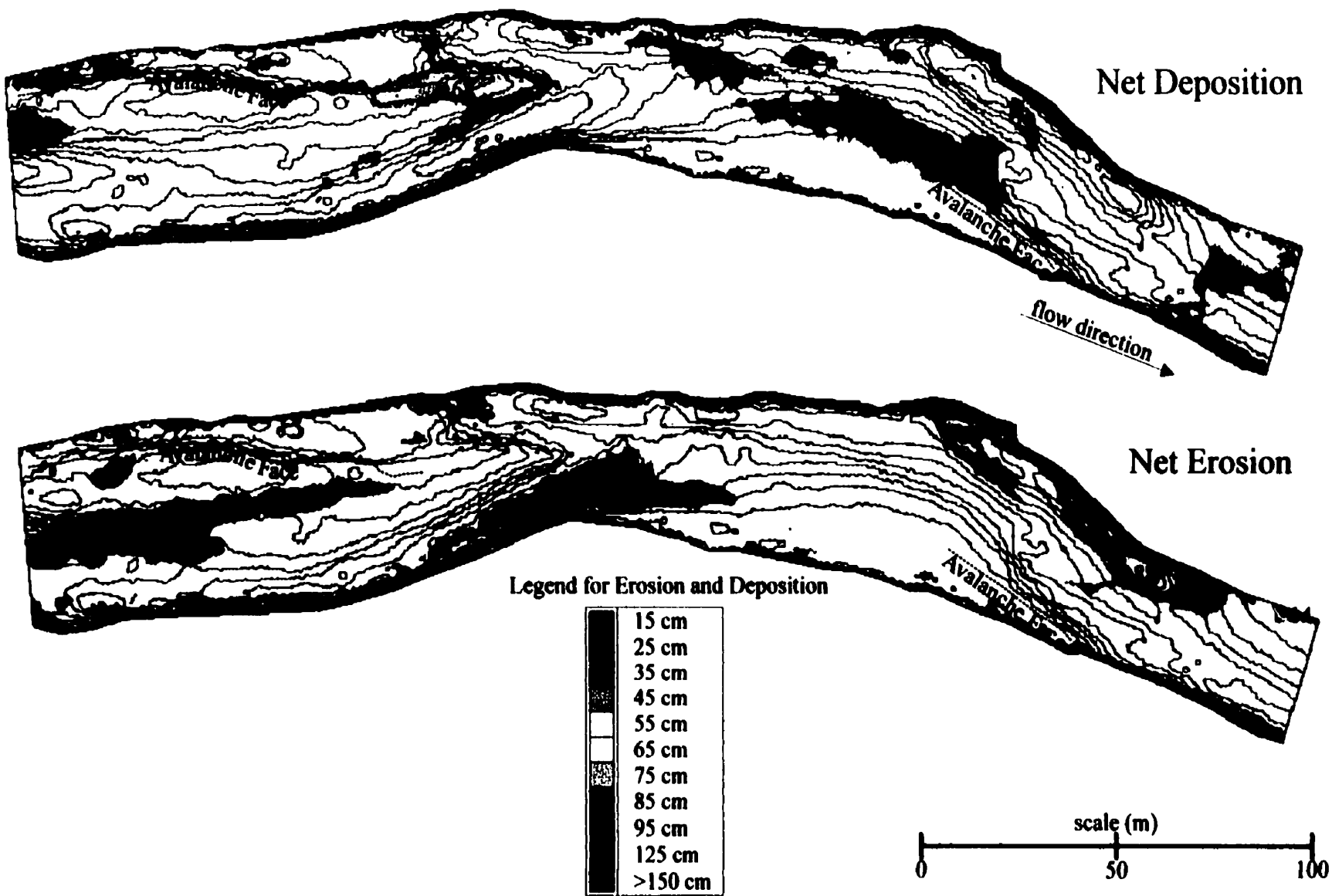


Figure 5.1.2: Net Morphologic Change, Reach 1, Resulting from Spring Freshet. Maps of net morphologic change for reach 1, Volumes of change in cubic meters are shown in red. June 1996 bed contours are overlain. Key features of previous survey shown in blue.

situated on the channel centerline, directly downstream from the main site of erosion, it is reasonable to link these changes.

Adjacent to the tail of bar 1, the channel bed has scoured, with a net volumetric change of 102 m^3 . Sediment deposited upon the top of bar 2 has a net volume of 107 m^3 . These two zones can similarly be linked as a source and subsequent sink of sediment.

At the tail of bar 1, near the left bank, net erosion of 44 m^3 has occurred, paired with a net deposition of 45 m^3 within the channel downstream of riffle 2. These two zones are likewise thought to represent paired erosion/deposition zones.

Transects were extracted from the digital elevation models to illustrate the adjustments to the cross-sectional and thalweg profiles occurring during the flood. Figure 5.1.3 illustrates these adjustments. The pattern of erosion along the bar face and deposition upon the avalanche face is illustrated by cross-section A:A', through the centroid of bar 1 (see Fig. 5.1.1).

The thalweg long profile shows a net downstream shift of the crest of riffle 2, near the tail of bar 1 (figure 5.1.3). Net erosion behind the crest and deposition downstream of it has occurred. The deposition just downstream of riffle 2 is part of a more extensive band of deposition extending across bar 2; the entire band of sediment has a volume of about 152 m^3 (figure 5.1.2).

Significant erosion has occurred along the unprotected cut bank opposite bar 2, where 191 m^3 of bank and bed erosion has occurred at the pool head as the pool deepens and extends laterally. Just downstream of this, 188 m^3 of bed erosion occurred as the pool extended downstream. Figure 5.1.3 illustrates the extension of the pool opposite bar 2 (between riffles 3 and 4), while cross-section B:B' indicates a widening and deepening of the pool. The preponderance of the bank retreat has occurred downstream of B:B', and therefore does not show up on Figure 5.1.3 C.

Riffle 4 has been significantly altered by the downstream extension of the last pool. Although the riffle crest has not shifted downstream, the bed upstream has degraded.

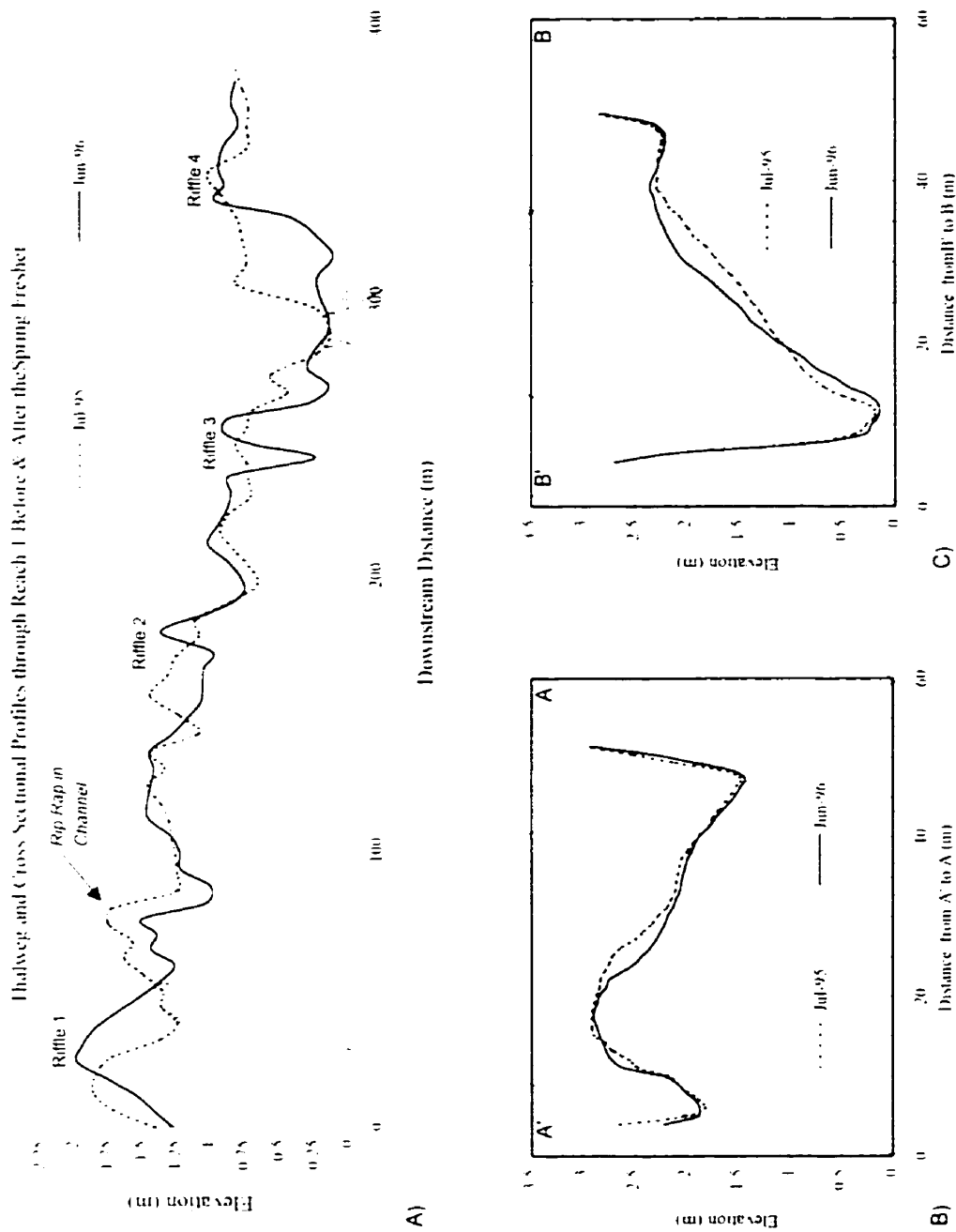


Figure 5.1.3. Thalweg and Cross Sectional Profiles through Reach 1, caused by the Spring Freshet

A) Thalweg Profiles Before and After the Spring Freshet

B) Cross Sections Before and After the Spring Freshet along profile A-A' on Figure 5.1.1

C) Cross Sections Before and After the Spring Freshet along profile B-B' on Figure 5.1.1

Datum of 0.0 m corresponds to an elevation of 125.9 m a.s.l

5.1.3) DETAILED MORPHOLOGIC CHANGES IN RESPONSE TO JULY 20 EVENT

The second flood event of 1996 was much larger than the first, and produced much greater morphologic change. However, it is interesting to note that the patterns of deposition and erosion are qualitatively similar to the previous one (figure 5.1.4).

The primary depositional environment on bar 1 is again the left bank avalanche face, which has continued infilling the secondary channel, with very little downstream component of bar growth; the total depositional volume is approximately 810 m³ (figure 5.1.4).

The right edge of bar 1 near the bar head has been eroded in an overall process of bar streamlining. There is a substantial volume of net erosion (139 m³), though it is clear that this is part of a much larger scour zone extending upstream beyond the reach boundary. Downstream, there has also been extensive erosion of the right flank of bar 1, which forms a continuous zone of erosion along the channel centerline, including riffle 2 and the left flank of bar 2 (there has been 525 m³ of erosion in this continuous scour zone, figure 5.1.4).

The cross-section A:A' shown in figure 5.1.5 through the centroid of bar 1 again illustrates an overall pattern of erosion on the bar face and deposition behind the bar crest, resulting in a net shift of the bar crest towards the left bank; the thalweg has widened in the main channel, and the bar face has steepened somewhat. These morphologic changes were not apparent in response to the first event (A:A', Fig. 5.1.3), and suggest that the difference in the flood magnitude has altered the local hydraulics.

The thalweg profile shows a downstream displacement of riffle 1 in response to the growth of the pool just upstream and outside the reach. Significant scour of the bed has occurred adjacent to the bank protection, between riffles 1 and 2. The crest of riffle 2 has shifted further downstream. Riffle 3 has also aggraded; the aggradation is part of an

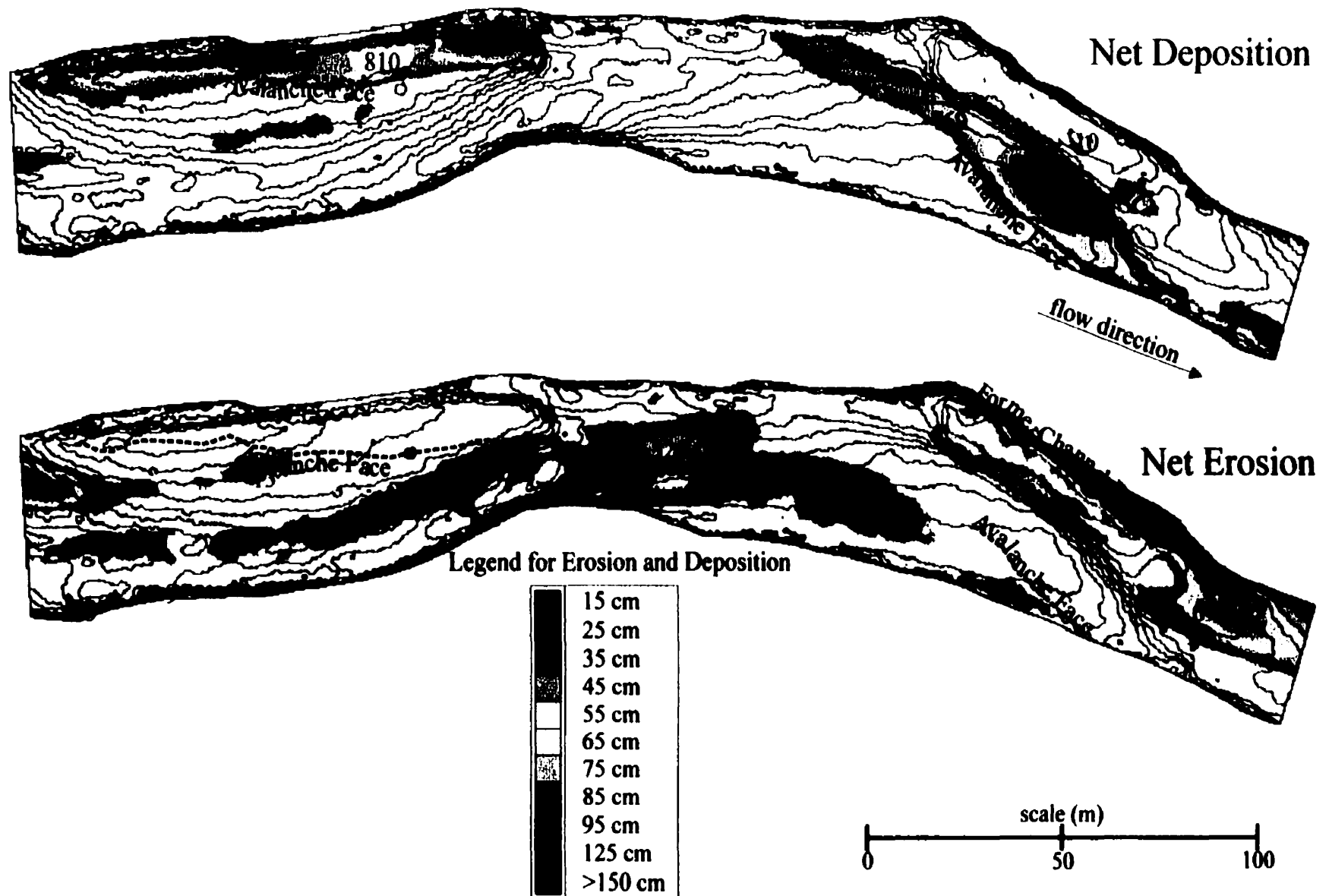


Figure 5.1.4: Net Morphologic Change, Reach 1, Resulting from July 20 Flood Event. Volumes of change in cubic meters are shown in red. August 1996 bed contours are overlain in black. Blue dashed lines indicate June 1996 avalanche face crest and former channel bank locations.

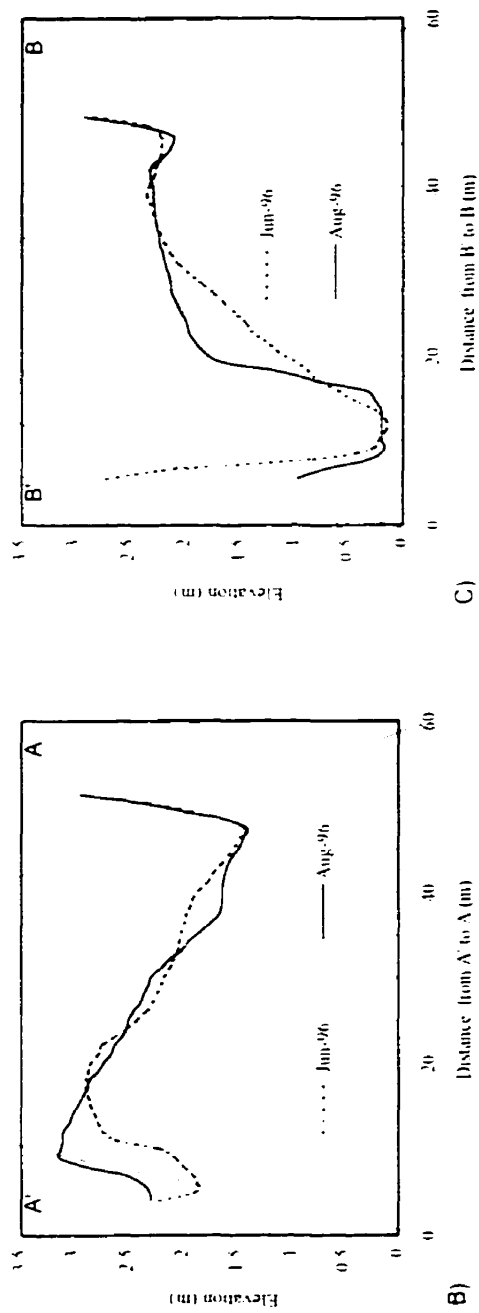
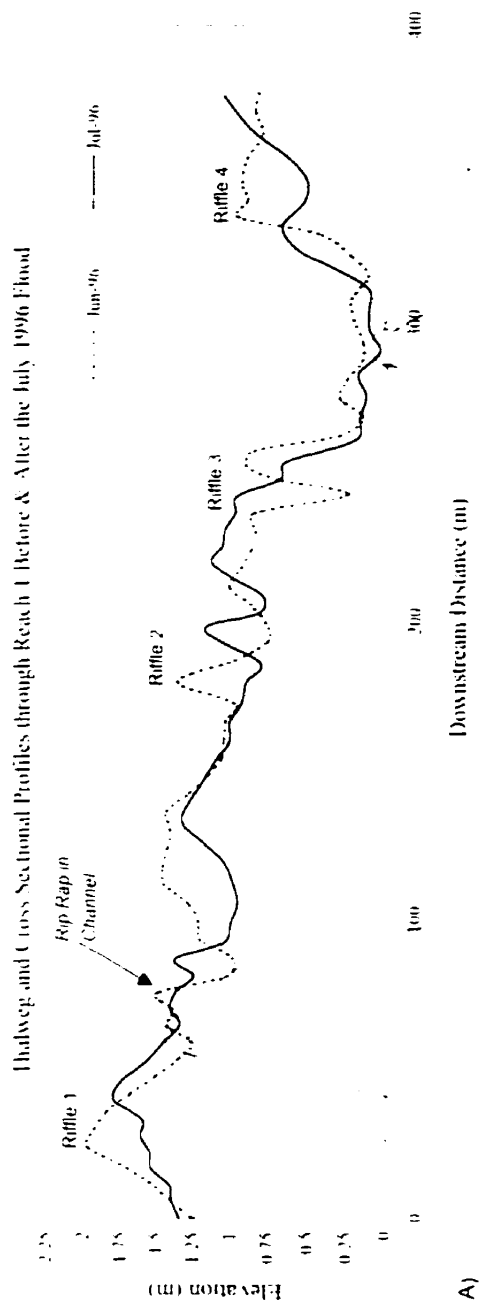


Figure 5.1.5 Thalweg and Cross Sectional Adjustments, Reach 1, caused by the July 20 Flood Event

A) Thalweg Profiles Before and After the July 20 Flood Event

B) Cross Sections Before and After the July 20 Flood Event along profile A' A' on Figure 5.1.1

C) Cross Sections Before and After the July 20 Flood Event along profile B' B' on Figure 5.1.1

Datum of 0.0 m corresponds to an elevation of 125.9 m a.s.l

overall band of sediment being deposited for the most part across the left edge and downstream face of bar 3 (Fig. 5.1.4).

Large-scale deposition has continued along the left edge of bar 2, though the locus of deposition has shifted downstream, extending the avalanche face along the downstream margin. The volume of this unit of deposition is about 769 m³. The cross-section B:B' through the centroid of bar 2 illustrates the degree to which the bar face has advanced towards the left bank and steepened (figure 5.1.5).

The thalweg profile (figure 5.1.5) shows both upstream and downstream extension of the last pool. The map of net erosion clearly indicates the extent of bank and bed erosion downstream of riffle 3. The bank has retreated at the same time as pool extension has occurred; the total erosional volume is 697 m³.

Again, basic observations about the spatial arrangement of erosion and deposition sites can be made. The bulk of material forming the 810 m³ deposited along the avalanche face on bar 1 is obviously from the left cut bank upstream of reach 1 (figure 2.4.1). If one assumes that all the eroded sediment downstream of the 32 m³ site in the main channel and along the right bank is not incorporated into the deposit on bar 1, one finds that at least 586 m³ (32 + 6 + 9 + 525 + 14) are exported to the downstream bar. However, the volume deposited upon bar 2 is 779 m³ (769 + 10), indicating a discrepancy of 193 m³. It is clear that the transport distance for bedload during this event is significantly larger than for the previous one, making it more difficult to balance scour and fill within the reach.

5.1.4) SITE SPECIFIC INTERPRETATION OF MORPHOLOGIC CHANGES

A general pattern of morphologic response within reach 1 can be identified for both flood events. While the total volumes of sediment eroded and deposited vary with the flood magnitude, the spatial patterns remain consistent. The response of bar 1 in reach 1 has been controlled primarily by the protected cut bank facing it. Bank protection reduces the sediment supply from the bank and restricts the natural pattern of meander growth. As a result, there is a consistent trend of erosion of the bar face and the adjacent

bed, as well as deposition in the lee of the bar crest. This produced a migration of the bar away from the protected bank and downstream.

During the first event, net erosion of 148 m^3 has occurred on the right side of the bar. In addition, there has been a net erosion of about 102 m^3 from the adjacent riffle downstream (R2, Figure 5.1.1), which is also a direct result of the sediment supply limitation induced by the bank protection. During the second event, there is a similar pattern of alternate bar erosion and riffle degradation, with a net volumetric change of 557 m^3 . The loci of bar and riffle erosion have remained unchanged, though the spatial extent and total volume varied with flood magnitude.

The patterns of deposition are likewise quite similar, although again of different magnitude and spatial extent. Both involve the advance of the bar 1 downstream and towards the left bank. The net deposition occurring during the first event is about 189 m^3 versus 810 m^3 for the second.

In contrast to the situation upstream, the bank facing bar 2 has not been protected. The patterns here are also consistent for the two events; deposition has occurred as a band of sediment across the left bar face and in the zone between riffles 2 and 3, while the cut bank has predictably retreated and the pool has grown deeper and more laterally extensive.

The consistency of the patterns of erosion and deposition within this downstream part of the reach suggest an evolution trend towards a more stable, meandering pattern (Langbein and Leopold, 1968b; Hooke, 1975). This is hardly surprising, considering that this section of channel has been channelized, thus imposing a higher channel gradient.

5.2) REACH 2

The second study reach is located roughly 500 meters downstream of the first; it has a slightly lower gradient and a somewhat finer substrate (figure 2.4.1). This site has been characterized by a high rate of cut bank retreat subsequent to channelization; the right cut bank was protected in 1993. Figure 5.2.1 illustrates several morphologic features of note that will be touched upon briefly. The channel has divided around a low

amplitude mid-channel bar, (bar 1). Bar 2 --the point bar-- is composed of coarse gravel on the upstream side and grades to predominantly sand on the downstream side. The lobate shape of the gravel accumulations on the point bar surface are obvious (points Lobe 1, Lobe 2, Lobe 3), and indicate rapid rates of bar accretion.

Pools were located at points A, C and D in 1995. The pool at point C, located at the point of maximum flow attack on the protected bank, was very steep-sided and quite deep. The other two pools were not as deep and were characterized by much more gradually sloping edges.

5.2.1) GENERAL BEDFORM RESPONSE

During the freshet, bars 1 and 2 changed only slightly. The pools, while slightly modified by the flood, remained in essentially the same locations.

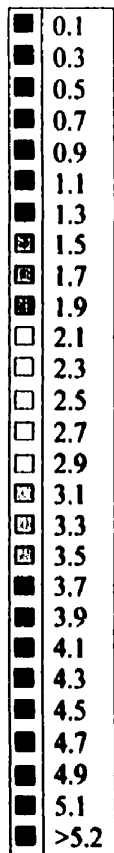
However, the July 1996 flood altered the reach extensively. Bar 1 was incorporated into the head of bar 2, and the thalweg shifted over to the right bank. Bar 2 was also modified. An incipient chute cutoff channel formed across the bar; the gravel lobes on the bar top have advanced, reflecting a net accumulation of sediment on bar 2.

5.2.2) DETAILED MORPHOLOGIC CHANGES IN RESPONSE TO THE SPRING FRESHET

There seems to be little coherent pattern to the net change resulting from the spring freshet (figure 5.2.2). There are a number of small pockets of erosion or deposition; there are, however, several key patterns indicative of systematic channel response.




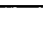
The most striking feature is the downstream extension of bar 1, resulting in a net fill of approximately 198 m^3 . The cross-section (A:A') shown in figure 5.2.3 through bar 1 shows clearly the vertical bar growth that has occurred. A shifting of the left branch of the main channel around bar 1 towards the point bar has caused erosion of the head of bar 2, with a net scour volume of 84 m^3 . The thalweg profile (figure 5.2.3) shows very little alteration of the bed configuration upstream of riffle 2.

Elevation (m)



Datum of 0.0 m corresponds to an elevation of 121.4 m a.s.l.

SYMBOLS:

	Bulk Sample of Armor and Subsurface, & Wolman Sample
	Wolman Sample
	Potential Spawning Zone
	Thalweg

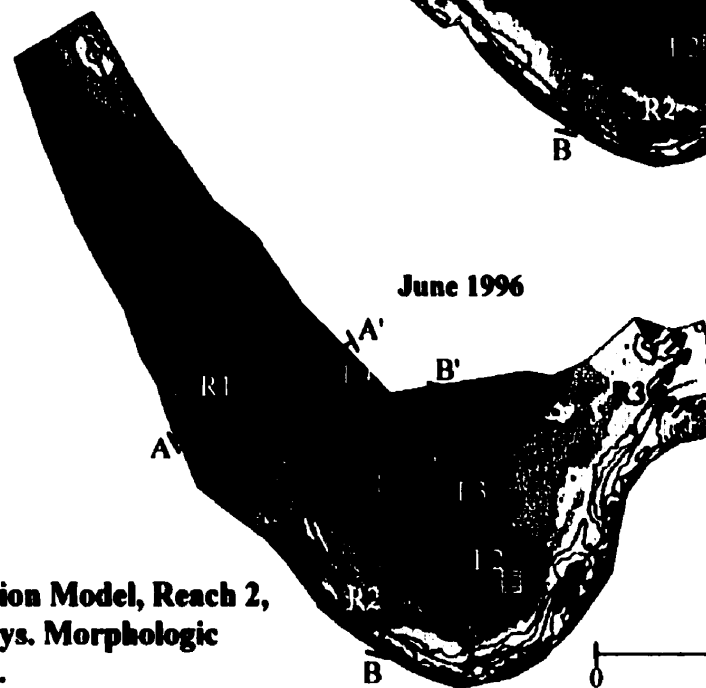
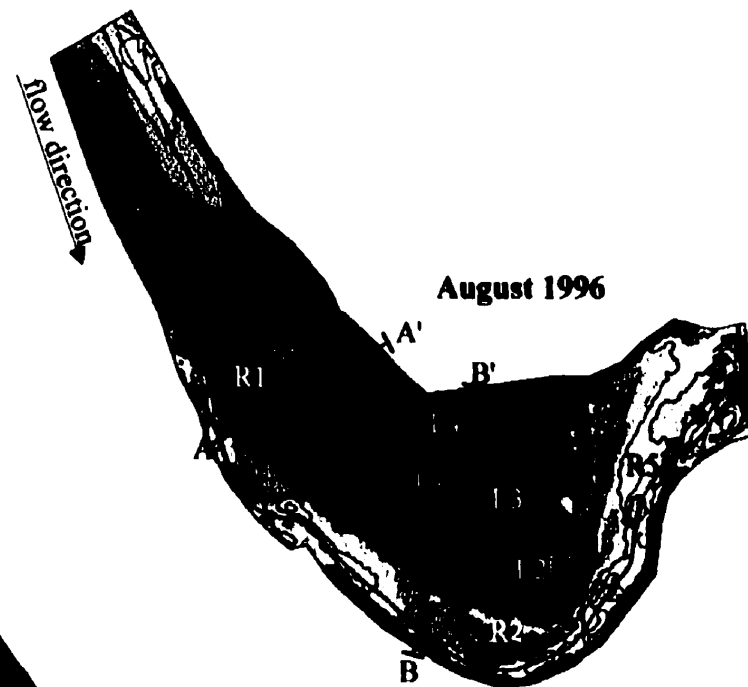
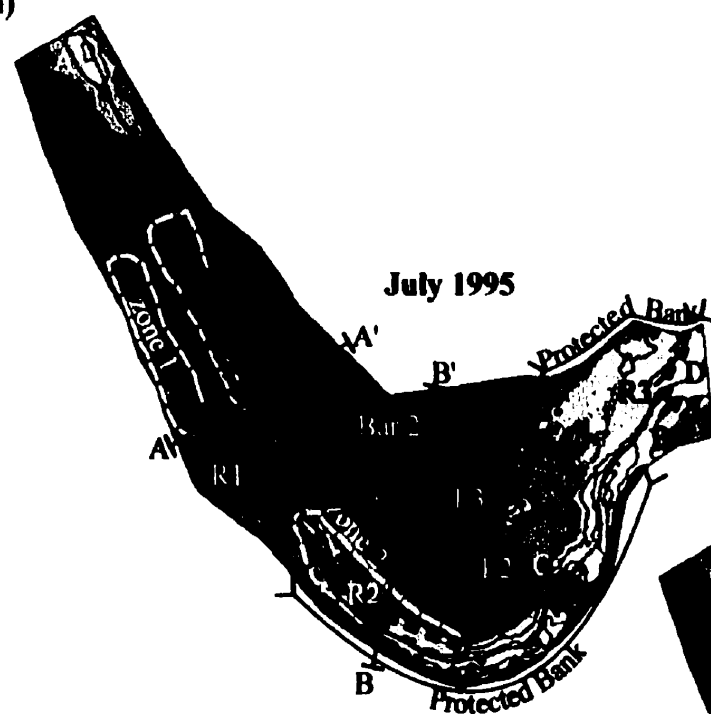
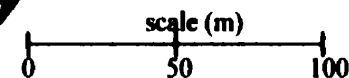


Figure 5.2.1: Digital Elevation Model, Reach 2, for Three Successive Surveys. Morphologic elements are shown in blue.



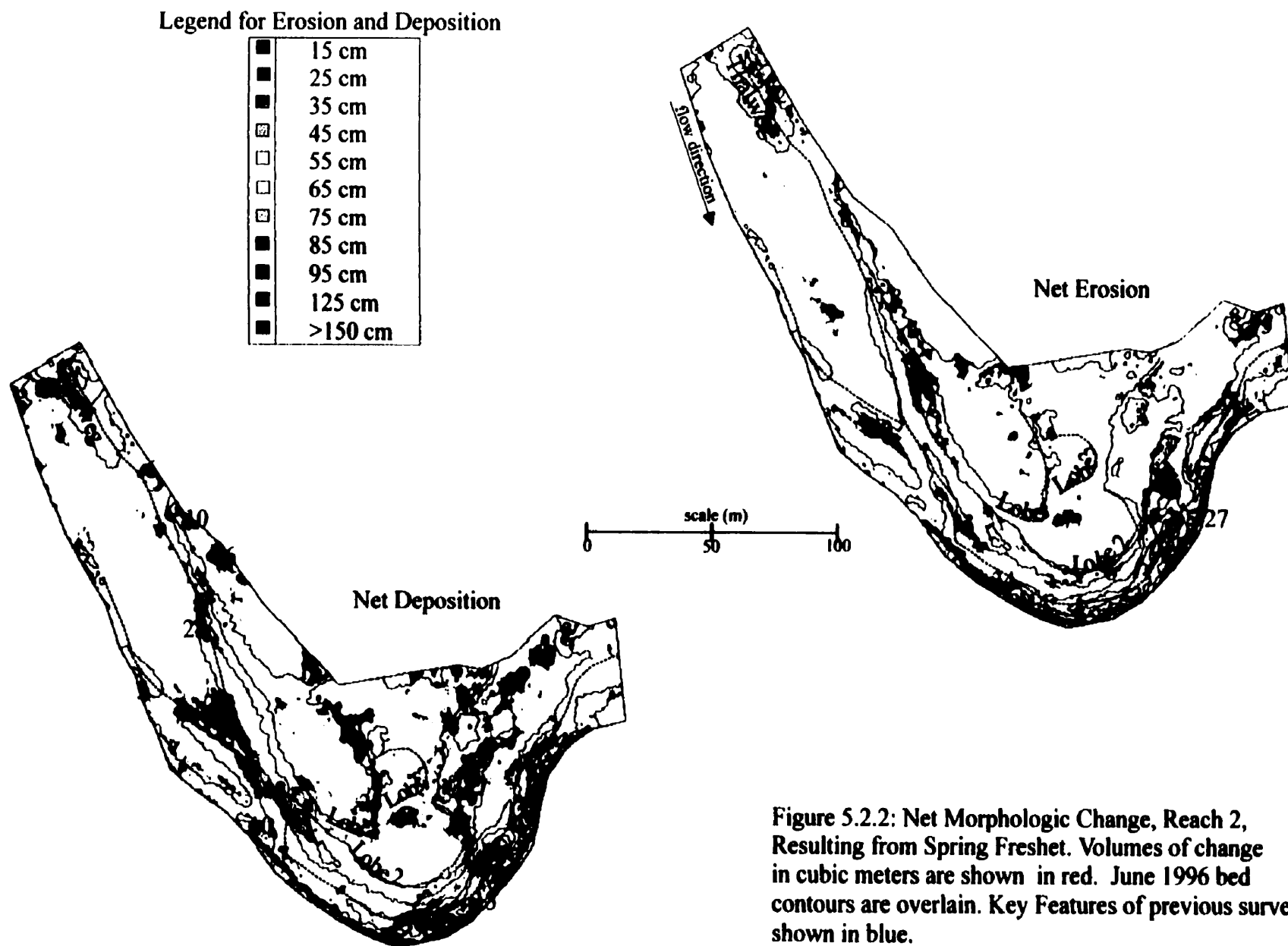


Figure 5.2.2: Net Morphologic Change, Reach 2, Resulting from Spring Freshet. Volumes of change in cubic meters are shown in red. June 1996 bed contours are overlain. Key Features of previous survey shown in blue.

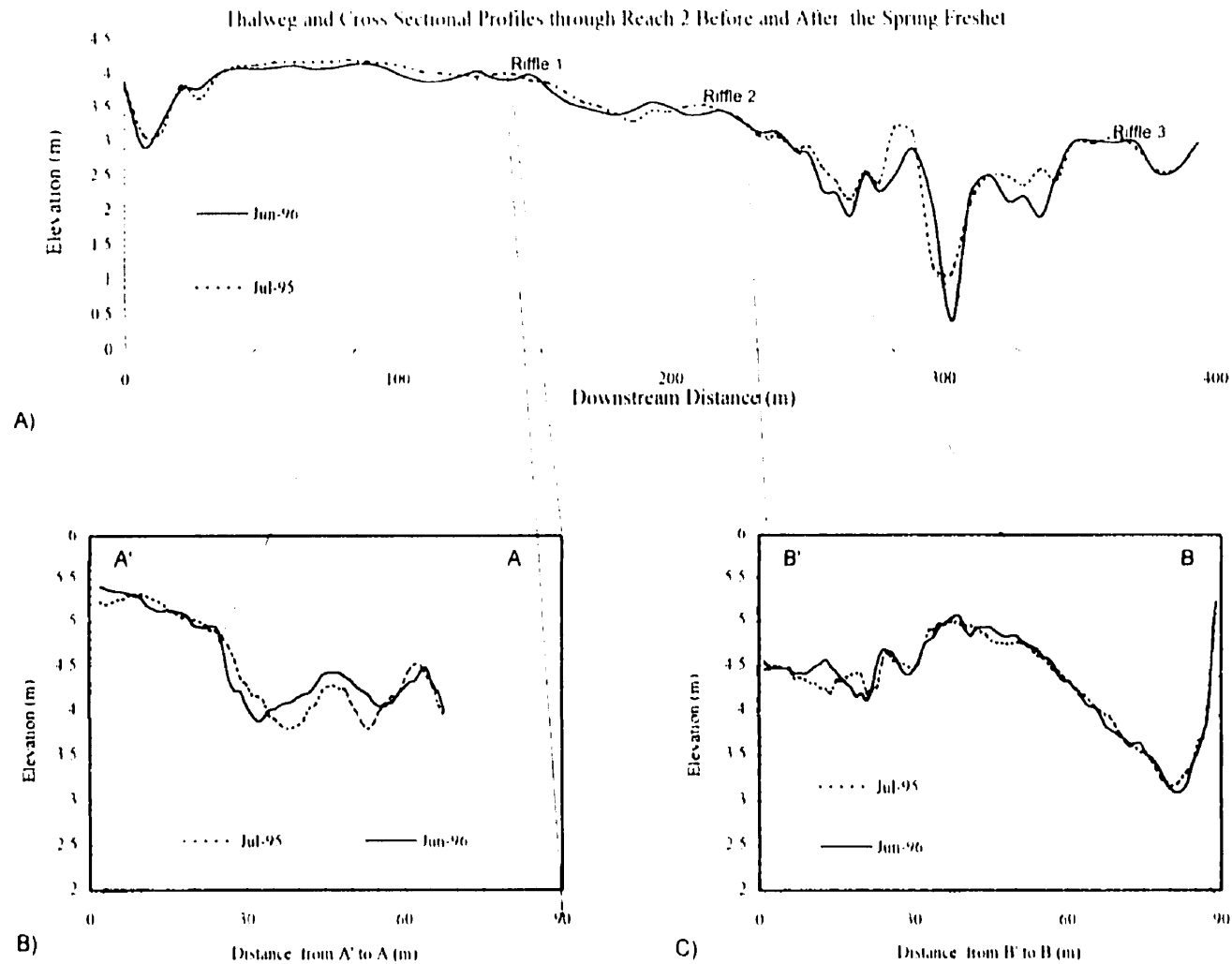


Figure 5.2.3: Thalweg and Cross Sectional Adjustments, Reach 2, caused by the Spring Freshet

A) Thalweg Profiles Before and After the Spring Freshet

B) Cross Sections Before and After the Spring Freshet along profile A:A' on Figure 5.2.1

C) Cross Sections Before and After the Spring Freshet along profile B:B' on Figure 5.2.1

Datum of 0.0 m corresponds to an elevation of 121.4 m a.s.l.

There is a clear pattern of advance of the sediment lobe 1 across the bar 2 with a total volume of deposition of about 70 m^3 ($25 + 31 + 14$). The cross-section B:B' through bar 2, however, illustrates that for the most part, the right edge of bar 1 and its crest have remained essentially unchanged following the flood (figure 5.2.3).

There is also evidence of advance of lobe 2, though this is part of a larger region of deposition. This larger region consists of deposition in the sandy, low energy area on the downstream edge of bar 2. The entire region underwent a net volumetric deposition of about 317 m^3 . Net erosion has also occurred in deeper water in this area, with a net scour of about 75 m^3 . Along the base of the rip rap along the right bank there has also been a tendency for erosion to occur.

Consistent pairings of erosion/deposition zones are more difficult to establish in this reach than in reach 1. However, the erosion along the head of bar 2 (76 m^3) likely supplied the sediment deposited upon the face of gravel lobe 1 (70 m^3). Net erosion along the base of the protected bank upstream of pool C accounts for 70 m^3 of sediment, while 69 m^3 of sediment has been deposited, suggesting that only very localized scour and fill have occurred in the area.

5.2.3) DETAILED MORPHOLOGIC CHANGES IN RESPONSE TO JULY 20 EVENT

The pattern of bedform response to the July flood is more coherent. As discussed before, this flood was quite a bit larger than the spring freshet events, and mobilized a much larger volume of sediment.

At the upstream limit of the reach, a large volume of sediment has been eroded as pool A has grown deeper and more elongated along the left bank (figure 5.2.4). This unit of erosion also includes significant erosion of the bed along the left bank upstream of bar 2. The total volume of erosion is 497 m^3 . The downstream extension of this pool is clearly apparent on the thalweg profile on figure 5.2.5.

A large volume of sediment has also been deposited at the head of bar 2. The left channel branch has been completely filled in, as bar 2 has advanced towards the center of the channel, incorporating the body of bar 1. The crest of the mid-channel bar (bar 1) has

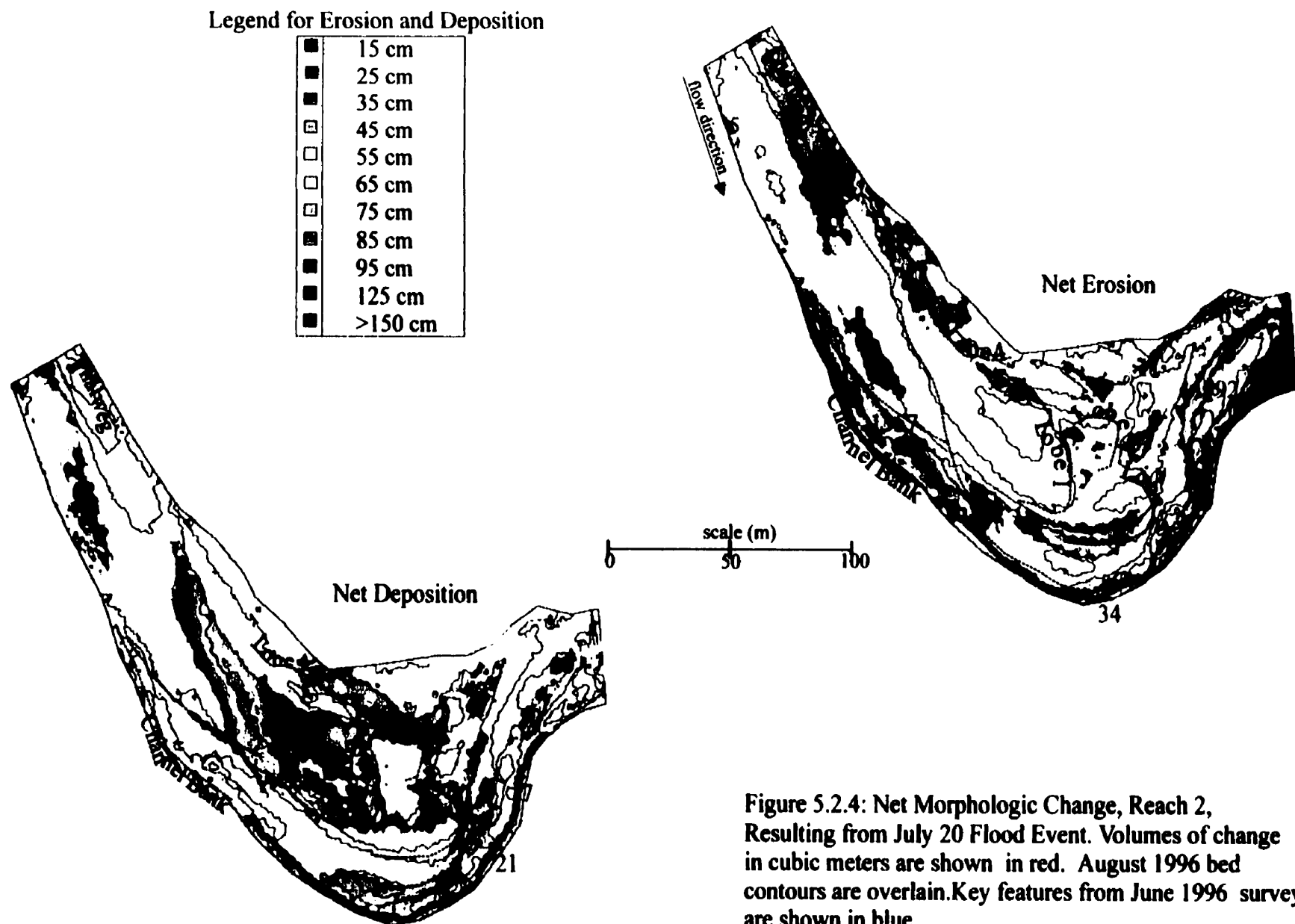


Figure 5.2.4: Net Morphologic Change, Reach 2, Resulting from July 20 Flood Event. Volumes of change in cubic meters are shown in red. August 1996 bed contours are overlain. Key features from June 1996 survey are shown in blue.

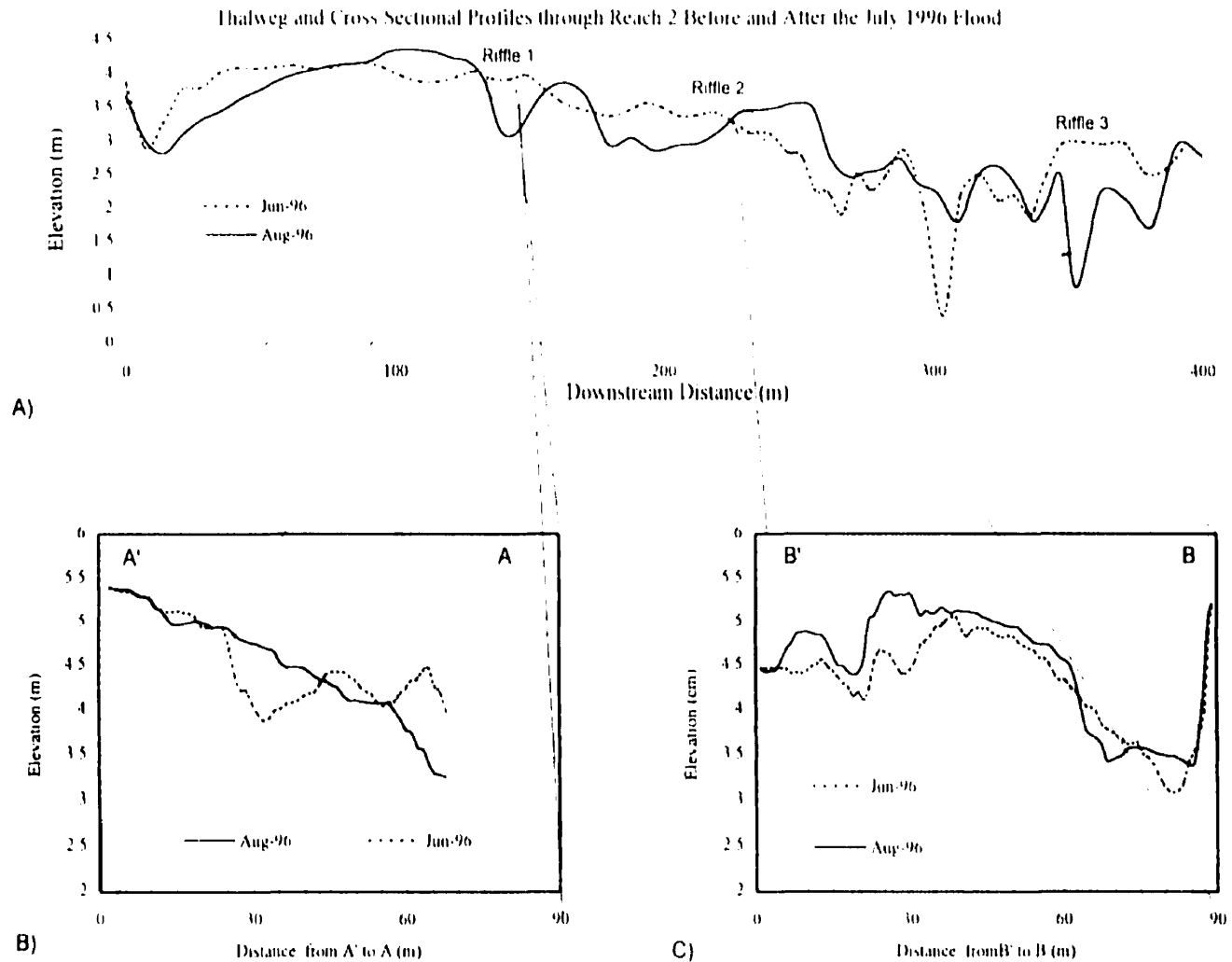


Figure 5.2.5. Thalweg and Cross Sectional Adjustments, Reach 2, caused by the July 20 Flood Event
 A) Thalweg Profiles Before and After the July 20 Flood Event
 B) Cross Sections Before and After the July 20 Flood Event along profile A-A' on Figure 5.9
 C) Cross Sections Before and After the July 20 Flood Event along profile B-B' on Figure 5.9
 Datum of 0.0 m corresponds to an elevation of 121.4 m a.s.l.

also been eroded, producing 45 m^3 of scour. At the same time as the point bar encroached on the mid-channel bar, there has been massive erosion of the channel bed and banks on the right-hand side of the channel, just upstream of the protected banks. The overall shifting of the thalweg towards to right bank appears clearly in cross-section A:A' in Figure 5.2.5.

Deposition was not limited to the left-hand chute around bar 1 but was also significant on the point bar, bar 2. There has been a net accumulation of sediment on the bar face and top, and large-scale lateral propagation of lobes 1, 2 and 3. A new lobe (lobe 4) has also developed, albeit a much smaller one, on the left side of an incipient chute cutoff involving 48 m^3 of scour. Advance of lobe 4 has formed the left bank of the incipient chute cutoff.

The channel bed adjacent to the left bank has been eroded at the upstream limit of the rip rap as the bank itself retreats. However, once the bank protection is encountered, the bed quickly changes from a pattern of degradation to one of aggradation in the vicinity of riffle 2. Erosion occurs on the left edge of bar 2 at the bend apex, forming a quasi-continuous band of erosion with that occurring adjacent to the left bank upstream.

At the downstream limit of the bank protection, erosion has once again attacked the right bank and bed. Riffle 3 has been significantly eroded, and the pool downstream has deepened and extended.

There has been both erosion and deposition within the low energy environment in the lee of bar 2. Also, the large pool between riffle 2 and 3 has been filled considerably.

Given the complex nature of the morphologic changes occurring in this zone and the much larger transport distances associated with this flood, there is little to be learned from attempting to analyze the patterns of net changes in storage in terms of paired erosion/deposition zones; the reach is insufficiently long for this to be reliable, which is further complicated by the complex pattern of net storage changes.

5.2.4) SITE SPECIFIC INTERPRETATION OF MORPHOLOGIC CHANGES

The response to the two events is quite different within reach 2. The first event produced a scattered pattern of erosion and deposition, with some consistent spatial organization. However, the extant morphology remained essentially unaltered. The primary response was a downstream advance of bar 1 --a medial bar-- with a net deposition of about 198 m³. In addition, lobe 1 advanced as sediment accumulated on bar 2. The primary zone of deposition was, however, on the downstream edge of bar 2. Erosion was focused along the left bank, near the head of bar 2, and in the vicinity of the pool at the upstream end of the reach. Erosion associated with the downstream growth of bar 1 also occurred.

In contrast, the July 20 event produced substantial morphologic adjustment. Bar 2 extended laterally and upstream, incorporating bar 1 and filling the left channel around bar 1. Erosion focused on the channel bed and unprotected banks on the right margin of bar 1.

Significant accretion of gravel to the point bar face (bar 2) and top has occurred; the previously identified gravel lobes have all advanced, producing a net shift of the bar crest inward, towards the left bank. Along the right bank, erosion site shifted, from the bank and bed upstream of the protection, to the face of bar 2 opposite the protection, and diminishes around the right edge of lobe 2.

The net result of the July 20 event was to streamline the bar morphology and to deepen the existing pools. The general configuration and position of the riffles has been altered as well. This contrasts with the limited morphologic alterations produced by the spring freshet.

5.3) REACH 3

This reach is located at the downstream end of the channelized section of the Sainte Marguerite, its bed is composed of fine gravel and sand. Its slope is less than half that for reaches 1 and 2 (Figure 2.4.1). It represents a transition point from a gravel bed to

a sand bed morphology. The upstream boundary of this reach is several tens of meters below a low partly permeable weir traversing the channel.

The primary morphologic elements within the reach are a lateral bar (bar 1), just below the weir, composed primarily of fine gravel, a medial deposit of similar material just downstream (bar 2), a point bar of fine gravel grading into sand at its tail on the left bank (bar 3), and a small sandy point bar on the right bank (bar 4) (figure 5.3.1). Riffles exist downstream of bar 1 (R1) and bar 2 (R2), and near the tail of bar 3 (R3) (figure 5.3.1).

5.3.1) GENERAL BEDFORM RESPONSE

Following the spring freshet, there has been some readjustment of the existing riffles (figure 5.3.1). Most significantly, riffle 2 has undergone net deposition and migrated downstream. Riffle 3 has been eroded and its crest has migrated downstream; however, the morphologic configuration has remained relatively unchanged.

The more powerful July 20 event has had a more significant impact on the morphology. Erosion has eroded a significant portion of bar 1 and obliterated bar 2; point bars 3 and 4 have undergone lateral and vertical accretion. Riffle 1 was destroyed, while riffle 2 migrated downstream significantly as part of a larger deposit of sediment upon bar 3. Riffle 3 has translated downstream and been somewhat eroded upstream of the riffle crest.

5.3.2) DETAILED MORPHOLOGIC CHANGES IN RESPONSE TO THE SPRING FRESHET

There is little pattern to the net deposition occurring within this reach (figure 5.3.2, and cross-sections A:A', B:B' and C:C' on figure 5.3.3). A plug of sediment with a volume of 45 m³ was deposited within the left bank branch of the main channel, near riffle 2. There have also been linear deposits of finer material in the sand bed section of the channel --along the right bank, downstream of riffle 3-- resulting in a net aggradation of point bar 4.

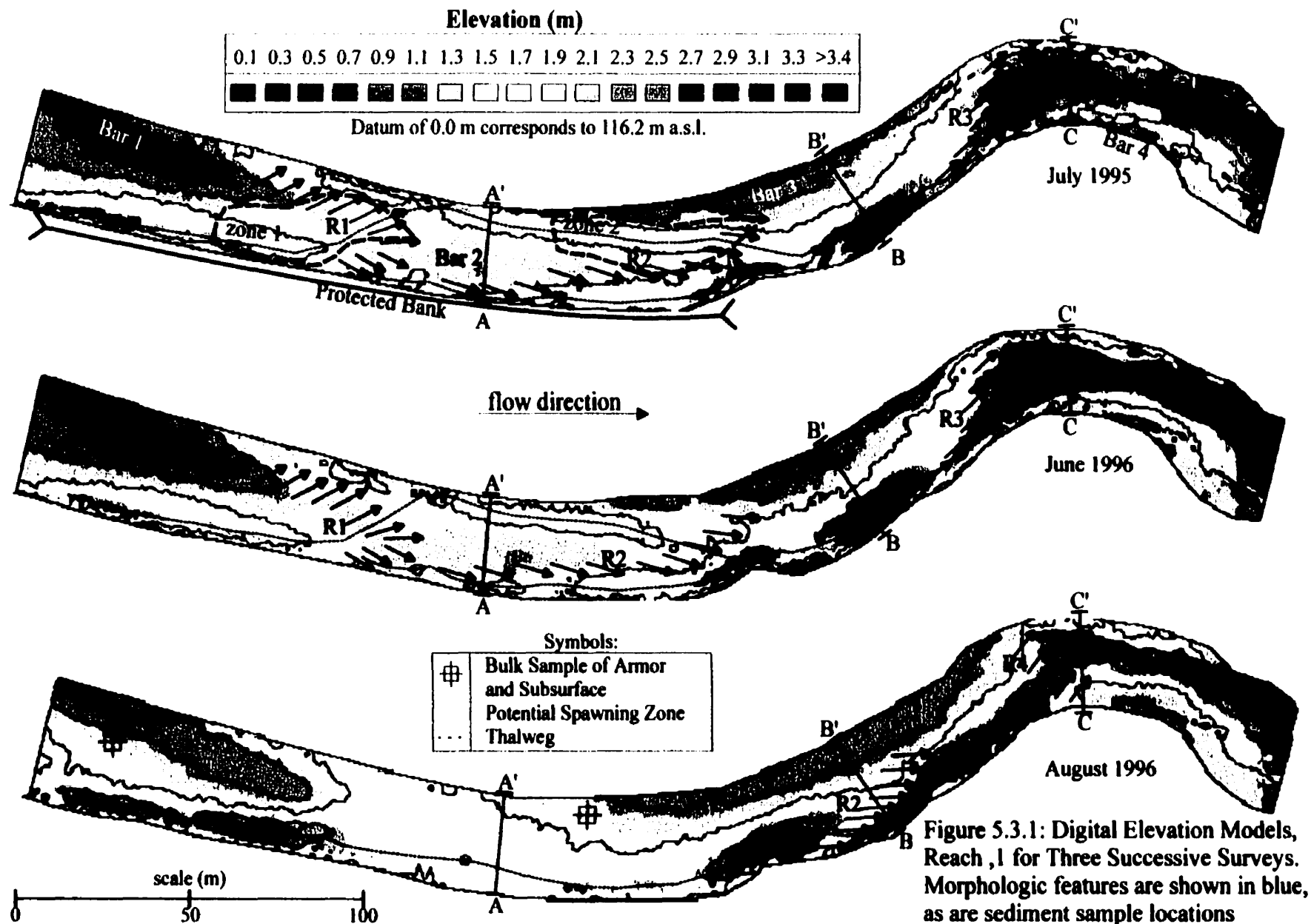


Figure 5.3.1: Digital Elevation Models, Reach 1 for Three Successive Surveys. Morphologic features are shown in blue, as are sediment sample locations

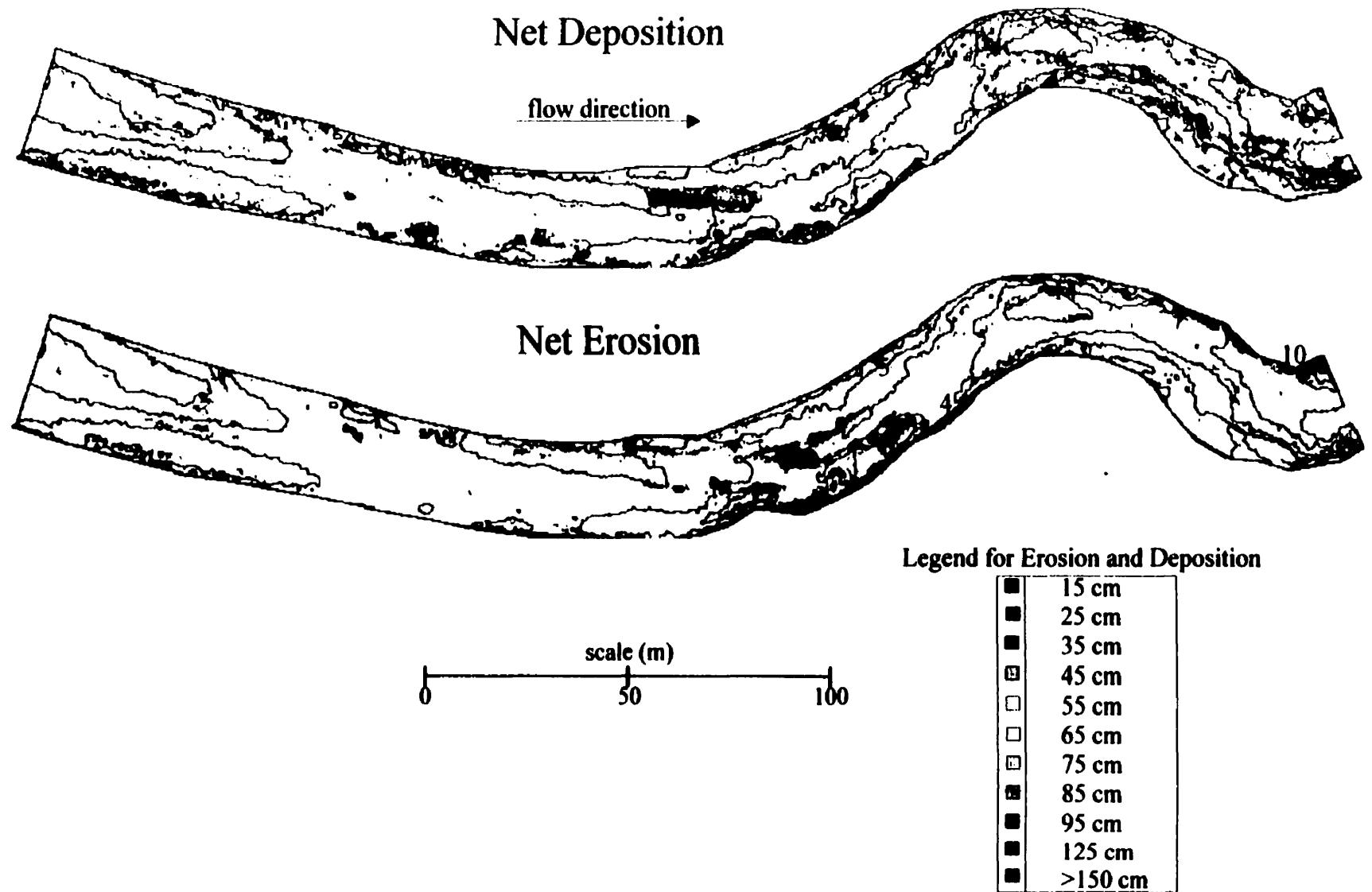


Figure 5.3.2: Net Morphologic Change, Reach 3, Resulting from Spring Freshet. Volumes of change in cubic meters are shown in red. June 1996 bed contours are overlain in black.

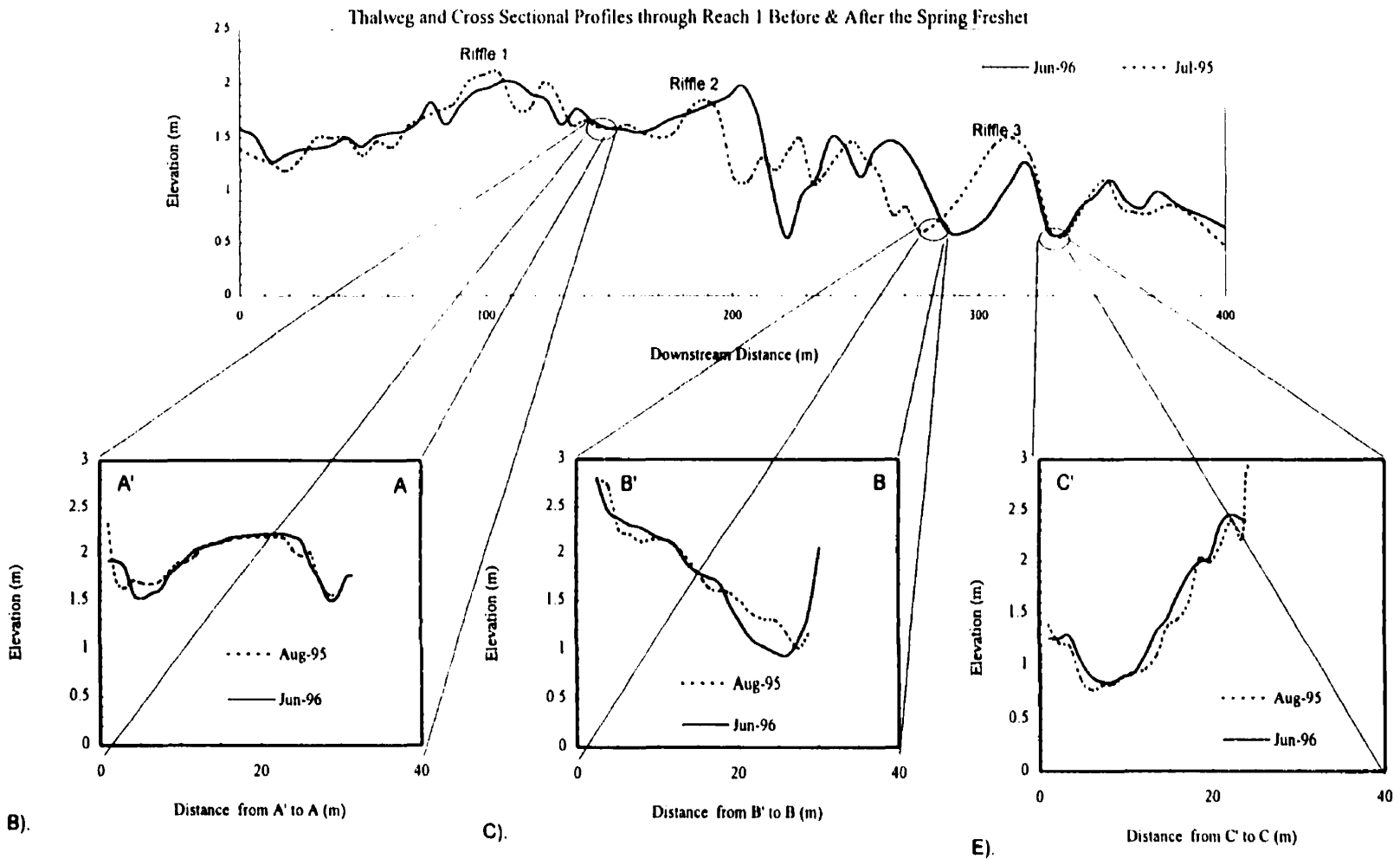


Figure 5.3.3: Thalweg and Cross Sectional Adjustments, Reach 3, caused by the Spring Freshet

A). Thalweg Profiles Before and After the Spring Freshet

B). Cross Sections Before and After the Spring Freshet along profile A:A' on Figure 5.3.1

Datum of 0.0 m corresponds to an elevation of 116.3 m a s l.

C). Cross Sections Before and After the Spring Freshet along profile B:B' on Figure 5.3.1

D). Cross Sections Before and After the Spring Freshet along profile C:C' on Figure 5.3.1

The pattern of erosion is somewhat more consistent. There are small pockets of bank erosion along both side of the channel; bank erosion was particularly focused on the cut banks opposite bars 3 and 4. Erosion of the bed has occurred in the thalweg opposite bar 3 as well.

5.3.3) MORPHOLOGIC CHANGE IN RESPONSE TO JULY 20 EVENT

The July event has produced an entirely different pattern of net morphologic change (figure 5.3.4). At the upstream end of the reach, the only net deposition has occurred as a lobate extension at the tail of bar 1. The net volume of deposition is only 37 m³. Overall, erosion of the bed and bars has dominated the upstream end of the reach. Bar 1 has been eroded by 353 m³ and the adjacent pool has extended downstream; this is part of an overall zone of erosion in which bar 2 has been removed (see cross-section A:A' through bar 2, figure 5.3.5). This erosion, consisting of 1039 m³, extends downstream to the upstream edge of riffle 2.

Downstream and along the left bank, a net accretion of 150 m³ of sediment to the upstream edge of bar 3 has occurred, filling in the branch of the main channel that previously divided around bar 2 (figure 5.3.5). Along the cut bank opposite bar 3, erosion of both bed and bank has occurred as the pool downstream of the riffle 2 deepened and the banks retreated. The net volumetric change here is about 129 m³.

A broad band of newly deposited sediment extends from the crest of riffle 2 near the right bank across the tail of bar 3 and into the pool downstream of riffle 3 near the left bank. Deposition has also occurred near bar 4 as part of this overall zone. In all, 675 m³ have been deposited. This deposit is most likely related to the large volume of gravel mobilized in the upstream half of the reach, combined with the back water effect produced by the very sinuous channel pattern just downstream of reach 3 (figure 2.2). Bank erosion has also occurred along the left bank opposite bar 4.

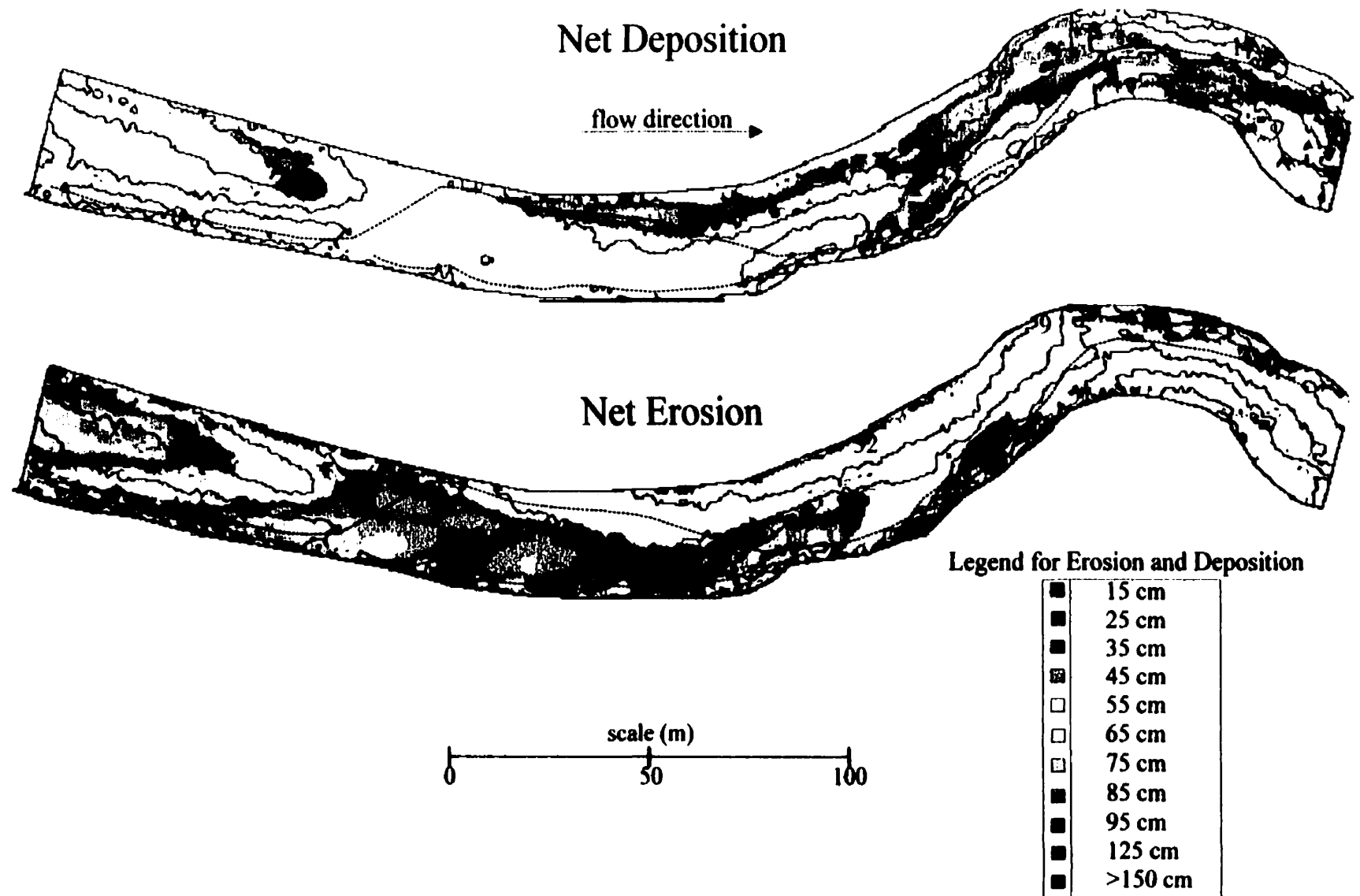


Figure 5.3.4: Net Morphologic Change, Reach 3, Resulting from July 20 Event. Volumes of change in cubic meters are shown in red. August 1996 bed contours are overlain in black. Blue dashed line indicates position of June 1996 Thalweg

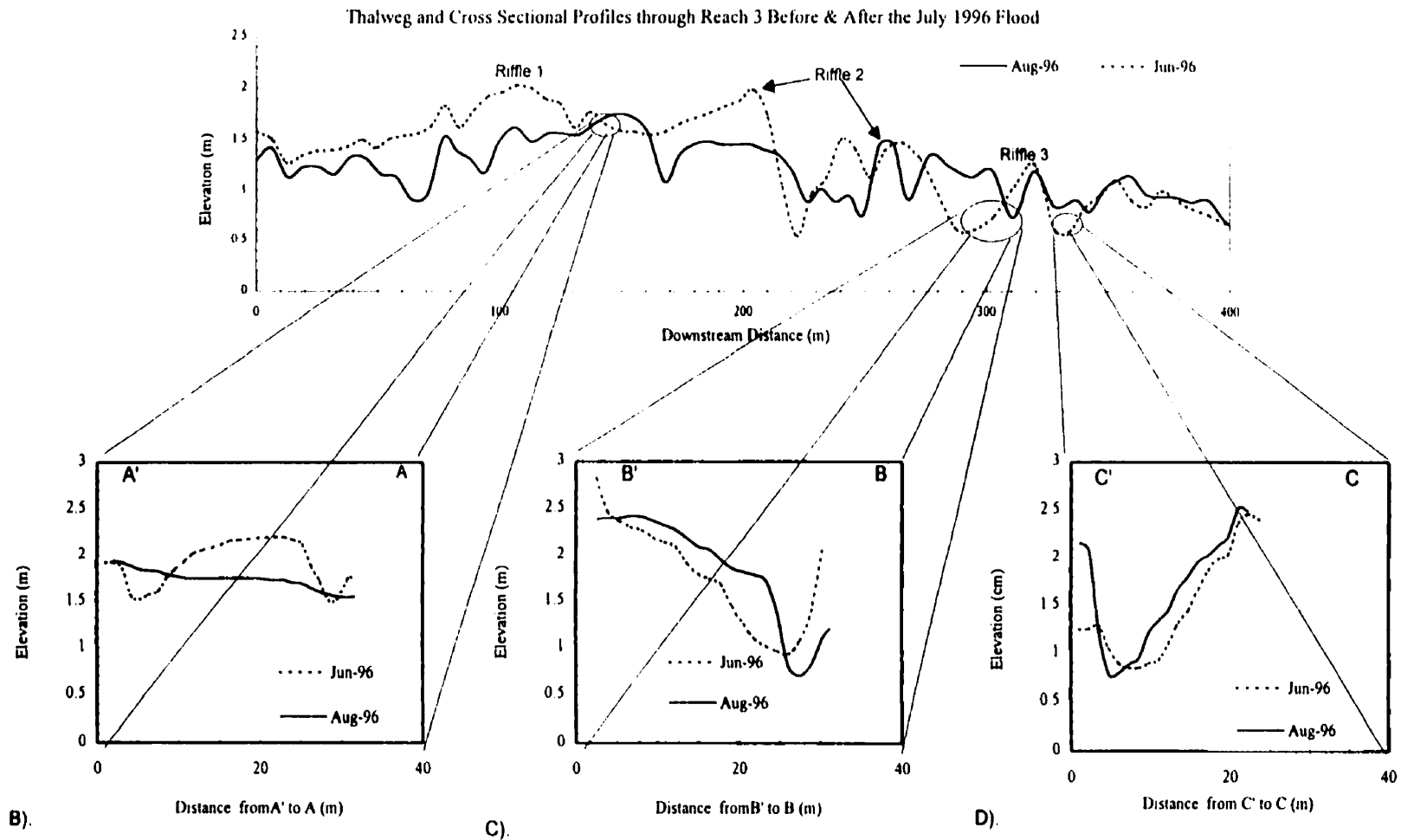


Figure 5.3.5: Thalweg and Cross Sectional Adjustments, Reach 3, caused by the July 20 Event

A). Thalweg Profiles Before and After the Spring Freshet

B). Cross Sections Before and After the Spring Freshet along profile A:A' on Figure 5.3.1

Datum of 0.0 m corresponds to an elevation of 116.3 m a.s.l.

C). Cross Sections Before and After the Spring Freshet along profile B:B' on Figure 5.3.1

D). Cross Sections Before and After the Spring Freshet along profile C:C' on Figure 5.3.1

5.3.4) SITE SPECIFIC INTERPRETATION OF MORPHOLOGIC CHANGES

The spring freshet produced little alteration of the overall morphology. There was sporadic deposition of limited volumes of sediment throughout the reach; riffle 2 underwent deposition of 45 m³ of sediment in the left branch of the channel around bar 2, and there was some overall aggradation around bar 4. Net erosion of the channel banks opposite point bars 3 and 4 occurred as well. Air photo evidence indicates that this reach has historically remained quite stable --at least in planform-- and thus the absence of channel alteration is not surprising.

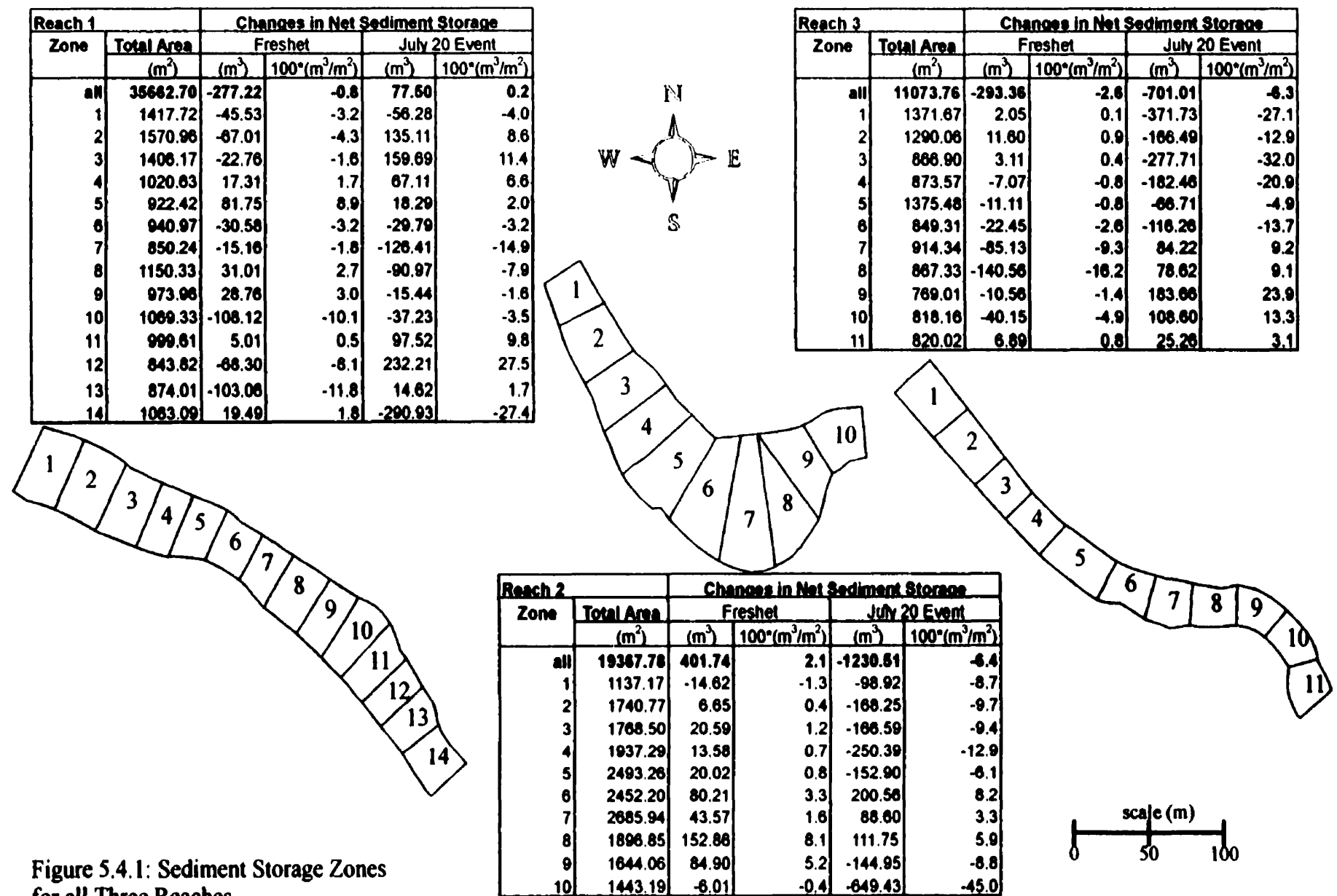
In contrast, the July 20 event altered the upstream channel bed extensively. Bar 1 was severely eroded, and bar 2 was obliterated. Bank and bed erosion also occurred opposite point bars 3 and 4. This erosion obliterated riffle 1 and caused riffle 2 to shift downstream; riffle 3 has been eroded to a degree as well. It is likely that the upstream weir is responsible for the dominance of erosion within the upper part of this reach.

There has also been a small volume of deposition along the tail of bar 1, as well as accretion of sediment to the head of bar 3. The volumes, however, are quite small in comparison with the erosion volumes. Downstream of riffle 2, a large volume of deposition has occurred, primarily of fine gravel and sand. Bar 4 has grown as a result, as has the sandy tail of bar 3. This deposition has occurred at the approximate transition from gravel bed to sand bed, and was likely the result of a significant backwater effect produced by the highly sinuous channel pattern downstream.

5.4) CHANGES IN VOLUMETRIC SEDIMENT STORAGE

5.4.1) REACH 1

The patterns of net morphologic adjustment can be analyzed in terms of the 1D change in net sediment storage within the channel along the downstream direction. This reduces the changes from a three-dimensional pattern to linear trend in the downstream direction. Changes in volumetric sediment storage were calculated for a number of discrete zones within each reach (figure 5.4.1), by defining the zones in GRASS and



calculating the total erosion and deposition volumes. These volumes were subsequently normalized by the zone area, thereby expressing changes in storage as changes in the volume per unit area, or simply, as changes in depth. Figure 5.4.2 displays the pattern of changes in sediment storage for reach 1 for both events.

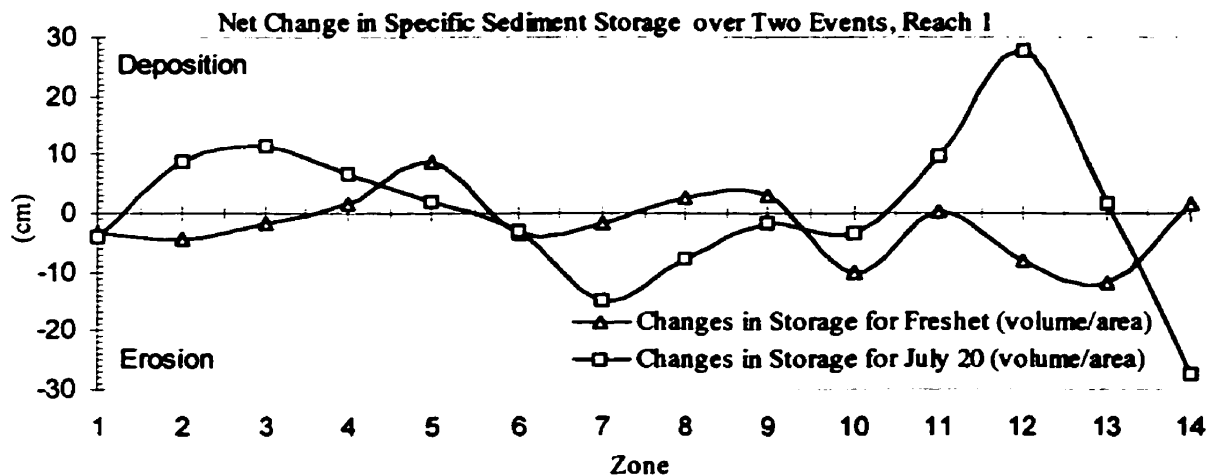


Figure 5.4.2. Net Change in Sediment Storage over Two Events, Reach 1.

During the freshet, net erosion of the channel has occurred in zones 1 through 3 -- which corresponds to the head of bar 1-- while net deposition has occurred at the tail of the bar in zone 5. There is a small amount of net erosion downstream of the bar tail, followed by deposition upon bar 2 in zones 8 and 9. The last 5 zones of reach 1 are generally marked by net erosion, which is focused on the outer bank and the adjacent bed, though zones 11 and 14 show little change in stored sediment volume.

The pattern of sediment storage is different for the July 20 event. Net deposition has occurred upon bar 1 in zones 2 to 5. Zones 6 to 10 have been eroded significantly. A large volume of sediment has been deposited in zones 11 and 12, followed by significant erosion in zone 14.

The patterns are seemingly quite dissimilar for the two events. However, if one examines bar 2 (Fig. 5.1.2 and 5.1.4), it becomes clear that the locus of deposition has merely shifted downstream from zones 8 and 9 to zones 11 and 12; the locus of erosion has likewise shifted downstream. The locus of net erosion in the vicinity of bar 1 has also

shifted downstream from zone 6 to zones 7 and 8. However, the locus of deposition has migrated upstream from zone 5 to zones 2 and 3. This is likely due to changing patterns of sediment transport across the complex point bar lying just upstream of the reach boundary during the July flood; flow likely moved more directly across the complex bar surface (Figure 2.4), supplying sediment to the secondary channel along the left bank of bar 1.

5.4.2) REACH 2

The pattern of volumetric sediment storage changes for reach 2 is presented in figure 5.4.3.

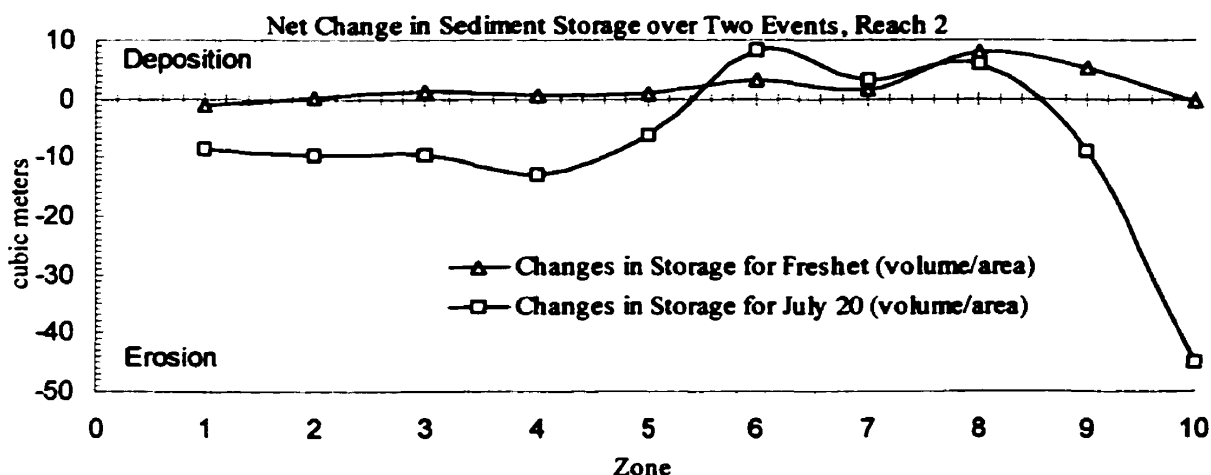


Figure 5.4.3. Net Change in Sediment Storage over Two Events, Reach 2.

Changes in sediment storage in response to the spring freshet for reach 2 are quite simple. There is little or no net change in the upstream zones. Net deposition occurs in zones 6 through 9. Zones 8 and 9 are typified by primarily sand, representing sediment likely carried in suspension, while zones 6 and 7 represent storage of bedload upon the point bar head. Notice that the largest volume of deposition is associated with zone 8.

The July 20 event produced large-scale erosion in zones 1 through 5 as the right bank was eroded and the riffle configuration altered. Net deposition occurred on the point bar top in zones 6, 7 and 8, followed by massive erosion of the bed and banks in zones 9 and 10.

During both events, sediment is stored upon the point bar, even though the cut bank opposite is not retreating due to the bank protection. During the freshet, the majority of the sediment was stored in zone 8, representing material transported in suspension, whereas during the July 20 event, the majority of the net deposition occurred at the point bar head in zone 6. However, while the spring freshet did not produce net erosion, the July 20 event produced large-scale erosion both upstream and downstream of the point bar.

5.4.3) REACH 3

The patterns of change in net sediment storage for reach 3 are presented in figure 5.4.4.

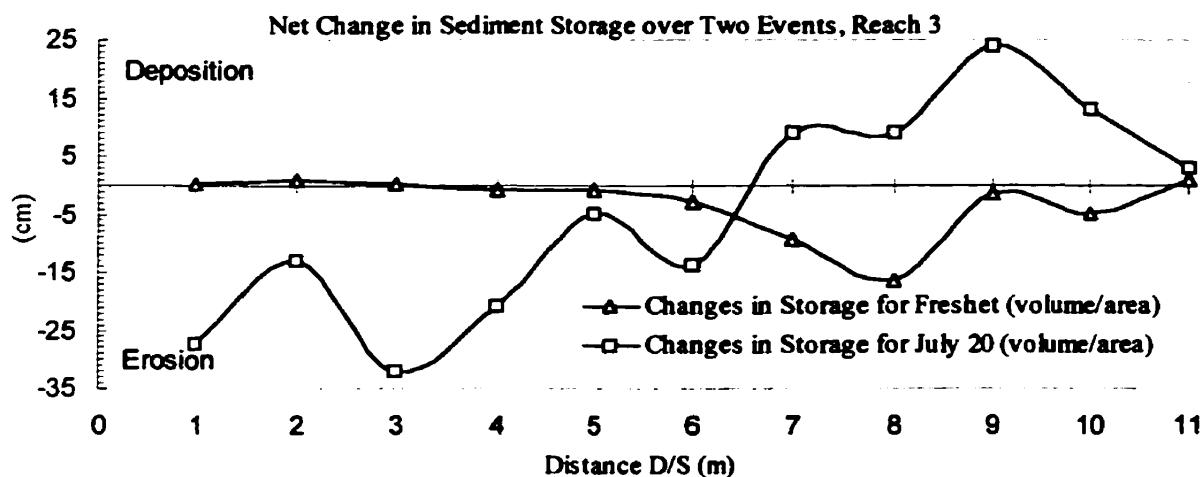


Figure 5.4.4. Net Change in Sediment Storage over Two Events, Reach 3.

Little or no change in stored sediment volumes occurred in zones 1 through 6 during the spring freshet. Some net erosion occurred in zones 7 and 8 as the cut bank opposite bar 3 retreated without the occurrence of significant deposition upon the bar. Net erosion has also occurred opposite bar 4 in zone 10 as the cut bank opposite eroded.

The July 20 event produced massive erosion in zones 1 through 6, followed by significant deposition in reaches 7 through 11. The upstream erosion is likely due to the limit on sediment transported into the reach due to the boulder weir upstream, while the downstream deposition is likely due to a backwater effect caused by the tortuous meandering channel pattern downstream of the reach.

6) PATTERNS OF CHANNEL ADJUSTMENT

6.1) CLASSIFICATION OF FLOOD SEVERITY

The question arises as to how the channel response of the Sainte Marguerite River fits into the overall framework of channel response to extreme floods. It is clear that in the study reaches neither the extreme channel widening nor the change in channel pattern observed by other researchers (Desloges and Church, 1992; Warburton, 1994; Huckleberry, 1994; Nolan and Marron, 1985; Harvey, 1984) has occurred. However, such changes have occurred on other river systems in the Saguenay region as a result of the same meteorological event. The Rivière à Mars on the other side of the Saguenay Fjord, for example, degraded significantly in several locations, and widened as well. Shifts in stream pattern from a previously sinuous single channel to a braided channel were also observed.

The Sainte Marguerite River, while undergoing mobilization of a significant proportion of its bed, did not experience the shift in regime observed on some other rivers in the region. There are several factors that may be significant in this regard. It seems clear that the distribution of precipitation was such that the southern side of the Saguenay Fjord experienced much greater amounts of precipitation than the northern side, and therefore the unit runoff magnitude was less for the Sainte Marguerite, located on the northern side of the Fjord than for other rivers. Also, the floodplain of the Sainte Marguerite is quite heavily forested, which may have been a mitigating factor.

Miller (1990) examined exactly this type of question in the Central Appalachian region. A tentative criterion for a geomorphically effective flood was derived based on the available data. Miller writes that for floodplains wider than 200 m “300 W/m² appears to be a reasonable minimum estimate of (the) threshold” (p. 132) above which floodplain scour and channel widening becomes important. Magilligan (1992) proposed this same threshold as the minimum limit for catastrophic flood effects within alluvial channels in humid environments. It should be mentioned that the threshold proposed by Miller is for

scouring of vegetation by overbank flows, and is not directly applicable to predicting within-bank scour and fill volumes.

If the unit stream power for the July 20 flood is calculated for the three reaches of the Sainte Marguerite, average values for reaches 1, 2, and 3 are 175, 105, and 85 W/m², respectively; far less than the above proposed threshold for severe channel modification. Therefore, the July 20, 1996 event could not have been expected to produce a step change in the channel pattern or significant floodplain modification.

6.2) PATTERNS EVIDENT WITHIN THE REACHES

Both clear patterns of bedform evolution as well as a sporadic distribution of local channel change were evident in the three reaches in response to the two flood events. In those locations where bedform evolution has occurred, the form of the adjustment typically followed the existing paradigm for meander development, given the existing constraints of bank protection. The degree to which the bed responded was a function of the flow conditions and the reach sediment caliber. Where there was a constraint on meander development due to bank protection, the bar evolved in accordance with this limitation. The main evolutionary patterns observed in each reach are summarized in the next paragraphs.

6.2.1) REACH 1

Deposition occurred on the left edge of bar 2 as the bank opposite retreated during both events; erosion was focused on the downstream part of the bend, and the deposition occurred in a band parallel to bank retreat, producing a net downstream component to bar growth. Point bar 1, facing a protected cutbank, responded differently. Deposition occurred along the inward avalanche face and at the bar tail; the freshet produced primarily bar tail growth while the July 20 event had a more significant lateral component of deposition. Here, erosion has been focused on the channel bed in the vicinity of riffle 2 and on the head of bar 2.

6.2.2) REACH 2

The primary form of evolution in response to the freshet within this reach was the downstream extension of the medial bar, bar 1, upstream of the bank protection. Significant deposition also occurred in the sandy deposits in the lee of the point bar (bar 2) during this event. During the July 20 event, the bank above the upstream limit of the protection measures retreated significantly; there has been a concomitant deposition of material on the opposite side of the channel, resulting in the complete absorption of bar 1 within the head of bar 2. Sediment was also deposited on top of bar 2, at its head, and along the right flank of the bar. At the downstream end of the reach --where both banks are protected-- the channel bed has scoured significantly following the July 20 event.

Various changes to the bed have occurred locally in the vicinity of the bank protection during both events; these changes are likely related to the development of vortex scour, by which a vertical vortex may scour the bed quite significantly over a very limited spatial range (Mlynarczyk and Rotnicki, 1989).

6.2.3) REACH 3

Within reach 3, little systematic change has occurred during the freshet. Some bank erosion was observed along the cut banks opposite bars 3 and 4, and generally, deposition has occurred on the point bar faces. The response of reach 3 to the July 20 event is that of overall bed degradation downstream of the weir, shifting to a pattern of aggradation downstream of riffle 2. The aggradation has resulted in a growth of bar 3; there has also been significant retreat of the adjacent cut bank.

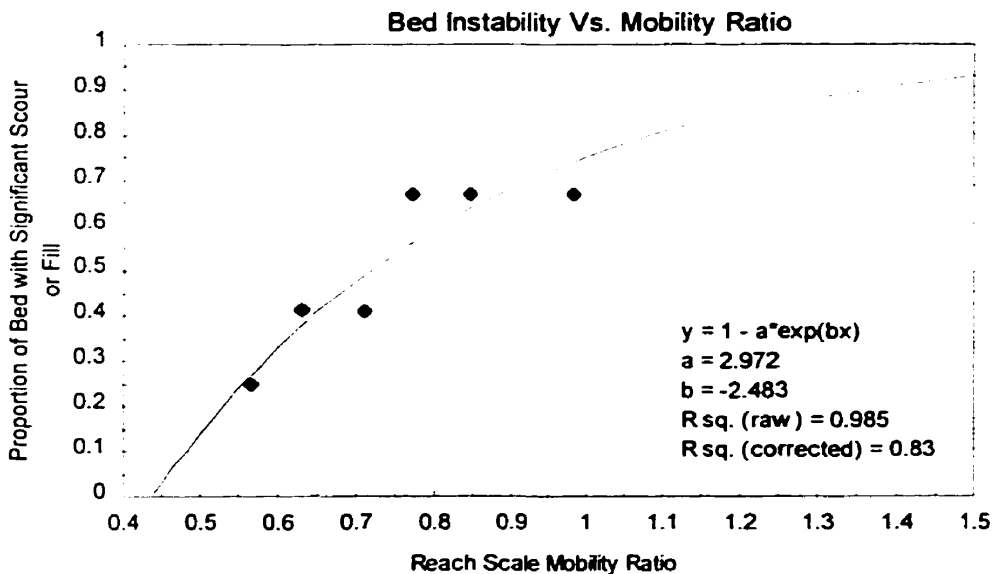
6.3) IMPACT OF FLOOD MAGNITUDE ON MORPHOLOGIC RESPONSE

The extent of bed mobilization in response to a given flood event is largely dependent upon the flow conditions and the bed material caliber. In terms of flow strength the spring freshet was comparatively large. The two upstream reaches were the most active, with 41 and 42 percent --by area-- of the bed undergoing a net change in bed elevation of greater than 10 cm (10 cm is thought to be the minimum consistently

detectable amount of net change). Reach three was much less active, and only 25 % of the bed underwent a net change of greater than 10 cm.

During the July 20, 1996 event, a larger portion of the bed was mobilized. For all three reaches, 66 percent of the bed underwent a net evolution greater than 10 cm. The proportion of bed undergoing net scour or fill greater than 10 cm was plotted in figure 6.3.1 against reach average mobility ratios calculated in Table 4.2.2. The results indicate a clear relation between these two quantities.

The strong relation between these two parameters suggests that reach scale mobility ratios are quite strongly related to the areal extent of channel disturbance.



note: significant scour is here defined to be equal to or greater than ± 10 cm

Figure 6.3.1. Bed Mobilization Versus Mobility Ratio.

A function asymptotic to 1 was fit to the data with the form

$$(9) \quad Y = 1 - 2.972 \cdot \exp(-2.483 \cdot X)$$

The non-linear regression model from which this equation was calculated had an adjusted R^2 value of 0.837. While a regression model is not strictly appropriate given the uncertainty of the estimate of the independent variable, the R^2 value does imply a relatively strong correlation between these two variables.

6.4) GENERAL PRINCIPLES OF MEANDER DEVELOPMENT

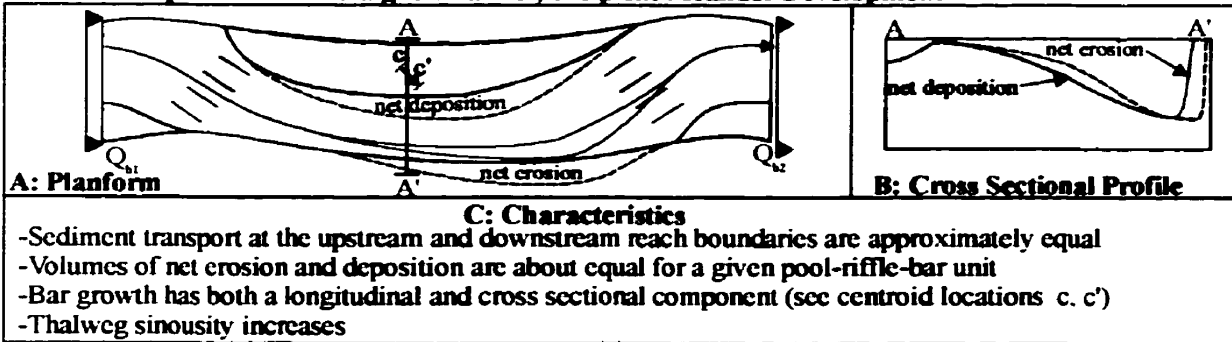
The existing body of knowledge regarding meander development indicates that a meandering stream pattern is inherently more stable than a straight one, and is thus favored in nature (Langbein and Leopold, 1968b; Hooke, 1975). There exists an interaction between the riffle-pool spacing and the meander wavelength, indicating that riffle-pool development is an integral, perhaps controlling, element in meander development (Keller and Mellhorn, 1973). Meanders develop from alternating bars by eroding the cutbank opposite and depositing sediment on the bar. A lateral growth of the bar results, coupled with a downstream component of bar growth.

The typical pattern of channel evolution for a lateral bar, based on the above understanding of channel dynamics, is presented in figure 6.4.1 part 1 (top). This model is applicable in reach 1 --for bar 2-- for both events and in reach 3 --for bars 3 and 4-- for the July 20 event. It can also be applied to the section of the bar upstream of the bank protection in reach 2 during the July 20 event.

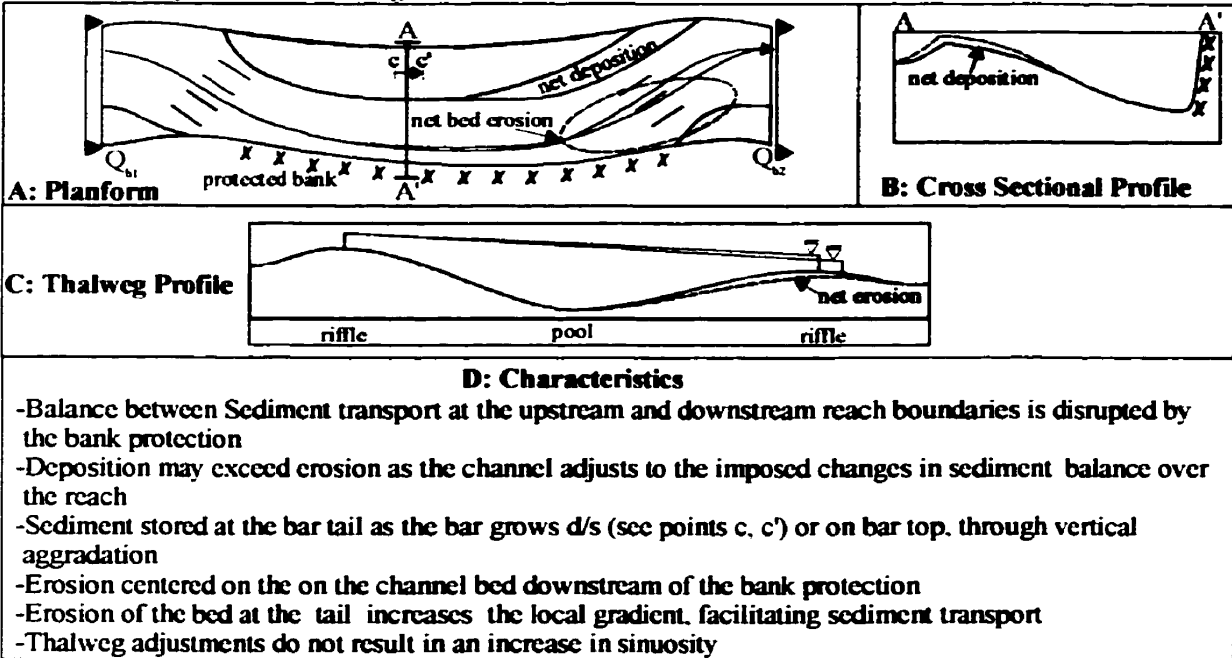
However, where bank protection prevents the erosion of the cut bank, this pattern is modified. Hooke (1975) presents a relation between bed geometry, fluid forces and sediment transport that is useful in understanding the resultant patterns. It is posited by Hooke that bed geometry is adjusted through erosion and/or deposition to produce an equilibrium between the flow conditions and the sediment transport field. Bank protection changes this equilibrium by preventing cut bank erosion. This reduces the sediment input to the channel, and also alters the sediment storage capacity of the bar opposite. Channel geometry adjusts to regain equilibrium. A schematic diagram of the adjustment of a lateral bar opposite a protected bank is presented in figure 6.4.1 (Part II, middle).

The sediment transport upstream of a protected bank (Q_{bi} , figure 6.4.1) will be unaffected by the altered bank; however, the channel morphology cannot adjust in the usual way --storing sediment upon the bar surface as the cut bank retreats-- in effect limiting the sediment storage capacity of the reach. Reach geometry will adjust to facilitate gravel transport *through* (rather than storage *in*) the reach. This may involve temporary storage upon the bar top, along the inner bank or, more commonly, at the bar

I. Channel Dynamics in a Straight Channel; Incipient Meander Development



II. Channel Dynamics in a Straight Channel with a Protected Bank



III. Channel Dynamics in a Meandering Bend with a Protected Bank

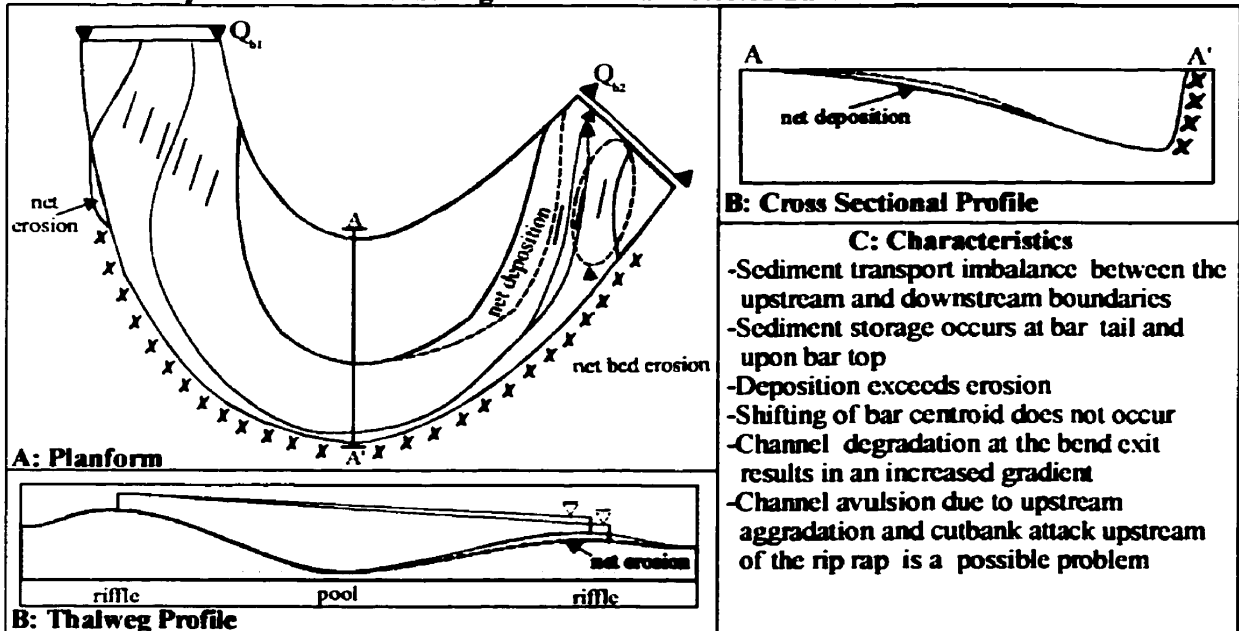


Figure 6.4.1: Channel Dynamics Moderated By Bank Protection

tail. Downstream of the protection (Q_{b2} , figure 6.4.1), the volume of sediment transport will be greatly reduced and will induce degradation of the bed. Reduced sediment transport at the downstream end of the reach is the direct corollary to protecting the cut bank, which is the normal source of sediment to the subsequent bar. This may cause the erosion of the riffle at the tail of the bar, or of the head of the next bar. Degradation of the downstream riffle may have the effect of increasing the gradient in the channel upstream and thereby increasing the rate of sediment transport *through* the reach. If it is assumed that the water surface gradient is controlled by the upstream and downstream riffles -- which act as hydraulic control points-- degradation of the downstream riffle would in effect steepen the gradient over the channel *between* the two riffles by lowering the downstream control, and possibly would increase the rate of transport through this length of channel (Figure 6.4.1, part II C.). Aggradation of the upstream riffle would have a similar effect. This would be an adjustment of geometry to produce a concomitant adjustment in the hydraulics and therefore modifying the sediment transport field, as conceptualized by Hooke (1975). However, flood hydraulics are quite complicated, and such an assertion would have to be verified experimentally. This model of channel response applies to reach 1, bar 1 for both events.

The direction bar growth shifts from primarily lateral --with a slight downstream component-- as indicated in Figure 6.4.1. part I A. (c-c') to primarily downstream growth, as indicated in part II A. This downstream migration of the bar allows the bar to eventually by-pass the bank protection, and re-attain a normal, meandering pattern.

In the case of a more acute meander bend, such as in reach 2, the effects of bank protection will be different (figure 6.4.1, part III), if the radius of curvature is sufficiently great that the point bar cannot "slide" past the bank protection. This model --a special case of that presented above-- applies to the point bar in reach 2 for both events. In a such a case, the inability of the bar to migrate past the bank protection forces the channel morphology to adapt differently. The protected cut bank may cause a general condition of aggradation upstream, as the "frozen" cut bank causes the entire system to "back up" with sediment. In these circumstances the channel may not be able to adjust its geometry to produce a balance between fluid forces and sediment transport, and aggradation of the

channel bed may continue until an avulsion is induced, thereby by-passing the bank protection. Following cut bank protection, deposition will likely occur on the downstream edge of the point bar, on the bar top and potentially on the upstream riffle as well. Degradation of the bed downstream of the bank protection will occur, for the same reasons that it would occur in the straight-channel model.

The above models are not sufficient to account for the response of bars 1 and 2 in reach 3 because of the impact of the weir upstream, which has produced a condition of channel degradation downstream. However, this is still consistent with the concepts used above to understand the impacts of bank protection.

7) SEDIMENT TRANSPORT ESTIMATES FROM MORPHOLOGIC CHANGES

Morphologic changes can be used in a number of different ways to calculate sediment transport rates using “inverse methods” (Lane *et al.* 1995; Ashmore and Church, 1996), as described in the chapter 1. These methods must be relied upon in this work for several reasons: First, the coarse nature of the substrate prevented use of small-orifice samplers such as the Helley-Smith sampler. Second, the long duration of this spring snow melt events would have made it very difficult to “catch” the event peak. Third, the exceptional conditions of the July 1996 event prevented travel to the study reaches, much less measurement of the flow and sediment transport conditions. As a result, direct sediment transport measurements are practically impossible to make in such systems.

The detailed topographic surveys of the bed allow for an estimate of the sediment transport occurring during the flood events, by comparing the spatial distribution of the sediment stored within the channel, both before and after the event. These estimates -- which admittedly may differ substantially from the “true” sediment transport rates-- are invaluable in quantifying the size of the transport event. Estimates of the water discharge at the various flood peaks has been reconstructed and indicates the size of the hydrologic event, and estimates of the *sediment* discharge will indicate the size of the geomorphic event, i.e. how much geomorphic “work” was done during the event

These “inverse methods” are limited to the transport of the bedload fraction only; sediment in transport that does not interact with the bed can obviously not be assessed using this approach. Therefore the estimates produced are only estimates of the bedload transport rate. Furthermore, the estimates of bedload transport are minimum estimates, because the net throughput of sediment, or the volume of sediment involved in scour and compensating fill at the same location (with no net bed change), cannot be accounted for (Ashmore and Church, 1996). Goff and Ashmore (1994) estimated sediment transport on the Sunwapta River --a braided proglacial stream-- with data of a similar nature to that presented herein. The approach of Goff and Ashmore was based on measured changes in sediment storage within a reach, in the absence of sediment transport input or output measurements. Three variations of the “inverse methods” (discussed below) were used,

providing a number of insights. A similar analysis has been performed upon the Sainte Marguerite River data. The results of which imply that these methods are equally applicable to single-thread, low energy meandering streams as to braided proglacial streams.

1. Paired Erosion and Deposition Approach

The most intuitive method of calculating sediment transport rates is by identifying a discrete zone of erosion and pairing it to a zone of deposition downstream. The assumption made in this method is that the volume of material eroded for one location was the source of deposition at a location further downstream. The typical distance of transport can be estimated from the distance between the centroids of erosion and deposition, which is referred to as the 'step length'. Estimation of the step length by other means, such as tracer particles, can be used to assess the validity of the pairing of a given erosion zone to a given deposition zone.

Given the event duration, the eroded volume --or the theoretically equivalent deposition volume-- and an estimate of the width of the channel active in transporting the sediment, one can calculate the event average bulk volumetric transport rate per unit width of channel. Bulk volumetric transport rates can easily be transformed to transport rates by mass by multiplying by the bulk density of the bed material, which is taken to be approximately $1,600 \text{ kg/m}^3$. The transport rates calculated in this way apply only to the bed between the identified erosion/deposition zones, not to the reach in general.

2. Total Erosion/Deposition Approach

More general reach averaged estimates can be determined in a similar fashion to that described above. The total volume of erosion (or deposition) occurring within a reach is scaled using an estimate of the reach average step length to determine the sediment transport rate. The assumption here is that all material moving within the channel moves a similar distance before deposition (step length), and therefore one can make estimates based on the sum of all the observed erosion (or deposition) within a reach without having identified paired erosion and deposition zones. The critical variable

is the step length; this can be estimated from the paired estimates of erosion and deposition made previously, or estimated by other means (e.g. tracer studies). Goff and Ashmore (1994) combined photographic evidence --in part due to limited length of their study reach-- with the observations of paired erosion and deposition zones to estimate step length. The equation summarizing this method, as presented in Ashmore and Church (1996) is

$$(10) \quad Q_b = V_e(L_s/L_r)/t$$

where Q_b is the bulk volumetric sediment transport rate (m^3/s), V_e is the total volume of erosion, L_s is the step length, L_r is the length of the reach over which V_e was determined and t is the event duration. Again, the bulk sediment density may be used to produce estimates of the transport rates by mass. Given an estimate of the average active width of the entire channel, a sediment transport rate with the units of $kg\ m^{-1}\ s^{-1}$ --which is comparable to the paired estimates-- can be calculated. This method reportedly produced lower transport rates on the Sunwapta, which was attributed to the fact that the estimates were made over the entire width of the channel which necessarily involves a degree of averaging, the possibility for compensating erosion and subsequent deposition, and to uncertainty in the step length estimates.

3. Sediment Budget Approach

The necessity of knowing the step length is circumvented by the sediment budget approach. The basis for this method is the continuity equation, which, according to Ashmore and Church (1995) can be written in finite difference form as

$$(4) \quad \Delta V = V_i - V_o$$

where ΔV is the net change in sediment storage within the reach and V_i and V_o are volumetric sediment inputs to, and outputs from, the reach in question. Therefore, given either sediment input or equally output, the total volumetric transport at the opposite boundary can be calculated given surveys of intervening storage change. This can be applied to a number of consecutive reaches, though a measured sediment transport rate at some point is required. In the absence of actual measurements, a zero transport condition must be assumed at a given point, which is the method adopted by Goff and Ashmore

(1994). This is a questionable though necessary assumption, the validity of which can be assessed by comparing it to results produced by the other methods (Goff and Ashmore, 1994).

7.1) SEDIMENT TRANSPORT ESTIMATES ALONG THE SAINTE MARGUERITE RIVER

7.1.1) PAIRED EROSION AND DEPOSITION APPROACH

Sediment transport rates were estimated using three paired erosion/deposition zones in reach 1 and one paired erosion/deposition zone in reach 2 for the spring freshet. No clear pairings were evident in reach 3, which has much finer substrate. During the July 20 flood, there is evidence that the step length equaled or exceeded the scale of the reach length, and no convincing pairs could be identified in any reach. Therefore, paired calculations were only made in the first two reaches for the spring freshet. In several cases, discrete patches of net erosion or net deposition in close proximity were treated as a single erosion or deposition zone; the individual patch volumes shown on Figures 5.1.2 and 5.2.2 are listed in the summary table 7.1.1. No quantitative information is available with which to judge accurately the event duration of the spring freshet, due to the lack of stream gauge information for the spring peak flow period.

Table 7.1.1. Sediment Transport Estimates for the Spring Freshet Based on Paired Erosion/Deposition Zones.

Pair	Reach 1			Reach 2
	1	2	3	1
Step Length (m)	82	86	64	58
Active Channel Width (m)	18	14	9	40
Total Erosion (m ³)	148 + 12	102	34 + 10	76.337
Total Deposition (m ³)	168	107	38 + 7	30 + 25 + 14
Transport Rate (kg m ⁻¹ event ⁻¹)	15241	12131	7625	3053

7.1.2) TOTAL EROSION/DEPOSITION WITH TYPICAL STEP LENGTH APPROACH

Only pairs 1 and 2 for reach 1 represent transport occurring within the main channel near the thalweg; pair 3 in reach 1 is associated with the back channel behind bar

1, while pair 1 in reach 2 is associated with transport of sediment across the bar head rather than along the thalweg. Thus, the typical step length which was subsequently applied to the total net erosion and deposition occurring with each of the three reaches is based on pairs 1 and 2 from reach 1 (Table 7.1.1). The gravel/cobble transport within reach 1 has a typical step length on the order of 80 meters. In reach 2, the somewhat shorter step length (58 m) is associated with erosion at the bar head followed by deposition on the bar top, rather than transport along the thalweg and thus cannot be considered to be representative of the reach as a whole. An assumed step length of 80 m also seems to be reasonable for this reach during the spring freshet. There are no convincing pairs of erosion and deposition within reach 3; a nominal step length of 80 m was also applied there.

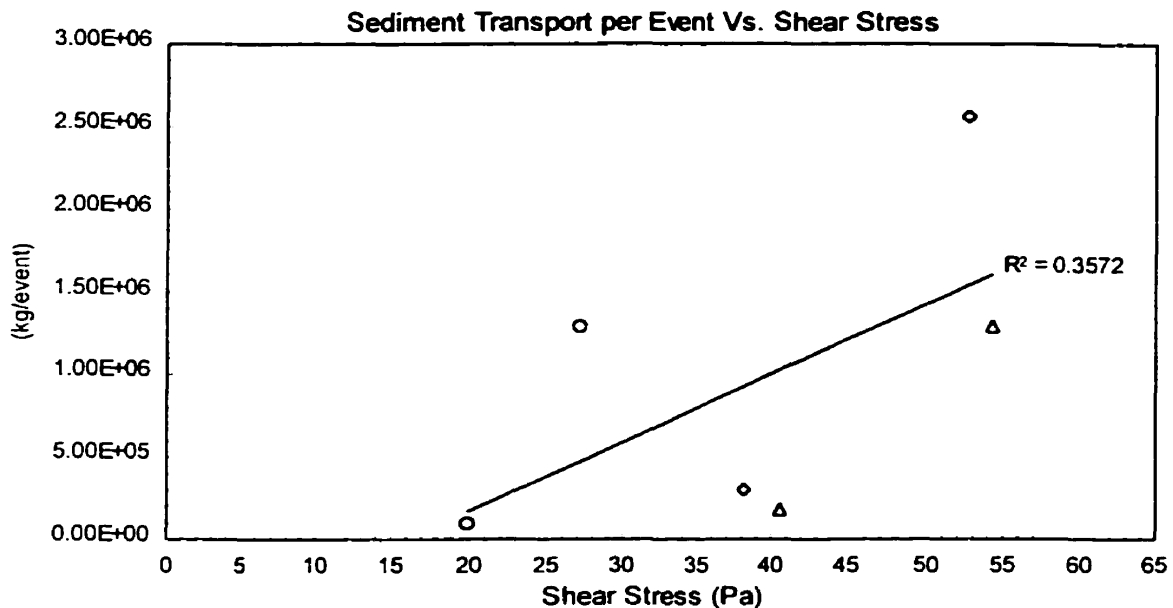
As mentioned previously, no convincing pairs of erosion and deposition were identified for the July 20 flood. The discrepancy in reach 1 (Figure 5.1.4) between the volume of deposition on bar 2 ($769 + 10 = 779 \text{ m}^3$) and the total erosion upstream ($32 + 6 + 9 + 525 + 14 = 586 \text{ m}^3$) indicates that the step length cannot be reliably resolved given the limited size of the reach for an event of this magnitude. An alternate approach was used for this flood, whereby the step length was estimated from the distance between consecutive loci of deposition; in this case, the distance between the centroids of deposition on bar 1 and bar 2 in reach 1 was taken to be a typical step length (given the current theoretical model of meander development, this should be an equivalent measure of the typical transport distance). This distance is approximately 200 m. This is thought to be a conservative estimate of the step length. This value was then applied to all three reaches for the July 20 flood. Table 7.1.2 presents the step length values applied in each of the reaches for both flood events.

Table 7.1.2. Step Lengths Applied to Erosion Volume Estimates of Sediment Transport.

	Reach 1	Reach 2 ¹	Reach 3 ¹
	Step Length (m)		
Freshet	84	80	80
July 20 Flood	200 ²	200	200

1: estimate of step length based on values calculated for the given flood in reach 1

2: based on distance between consecutive loci of deposition, rather than paired erosion/deposition zones



Note: Estimates from reach 1 are indicated with an open triangle, from reach 2 with a diamond and from reach 3 with a circle.

Figure 7.1.1. Sediment Transport per Event *versus* Peak Shear Stress.

Figure 7.1.1 displays the estimates of sediment transport based on the above step length estimates and equation (10) for the three reaches for both flood events using the total volume of erosion or deposition; the larger of the two values was chosen, given the negative bias inherent in these methods. The transport estimates were plotted against the estimated peak shear stress during the event, presented in Table 4.2.1; shear stress estimates have an uncertainty of between 13 and 20%.

There is a definite relation between peak shear stress and the sediment transport, though considerable scatter exists. Sediment transport rates depend on the applied shear stress and the caliber of bed material. The scatter may be in part due to the variations in substrate texture between the three reaches. In figure 7.1.2, the data were subsequently re-plotted against the reach average mobility ratios, defined in section 4.2.1, which are a reach-scale index of flow stress normalized by the critical entrainment stresses for the reach substrate.

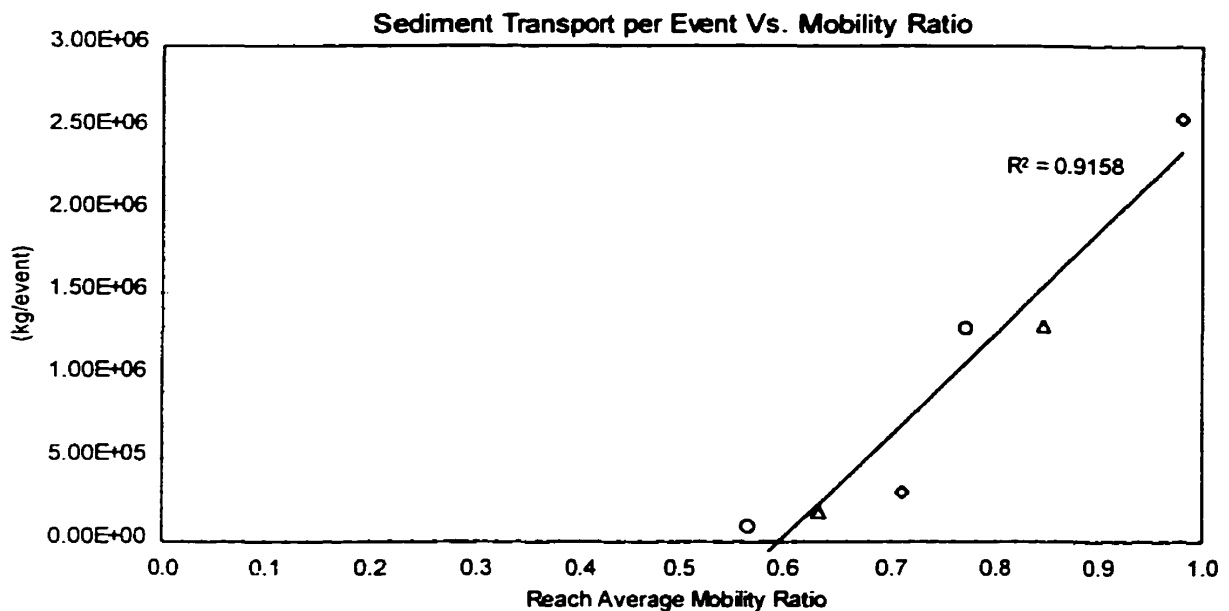


Figure 7.1.2. Sediment Transport per Event *versus* Mobility Ratio.

Accounting for the variable sediment texture using the reach average mobility ratios dramatically reduces the scatter in Figure 7.1.2. Given the morphologic and sedimentologic contrasts between the three reaches, such a strong relation is quite striking. Over 90% of the variation in transport rates can be explained by variations in reach scale mobility ratio for the transport events. The remaining variability is likely the product of the duration of the transport event, which has not been accounted for in the estimates presented above.

Estimates of sediment transport made by this “typical step length” method involve greater uncertainty than the paired zone method, because of the application of a typical step length to all zones of erosion/deposition. However, these estimates also produce reach average estimates and therefore better represent the reach average response than a single erosion/deposition pair would. While the intuitive simplicity of the paired erosion/deposition zone approach is appealing, it is not possible to identify appropriate pairs for all zones of erosion/deposition, which limits the applicability of this method to the reach as a whole. The strong relation between the total erosion/deposition estimates

and the reach average mobility ratios suggest that this is the most appropriate method to characterize reach average transport rates.

7.1.3) SEDIMENT BUDGET APPROACH

The sediment budget approach requires that the net changes in sediment storage be calculated to allow for a propagation of a known transport rate in either the upstream or downstream direction. As such, this method is most profitably applied to situations where a measured sediment transport rate is available at one cross-section, or where one can be certain that a zero transport rate is applicable somewhere (for example, a delta front). In this study, it will be necessary to identify a zero transport cross-section --through which one has to assume that negligible transport has occurred-- due to the lack of direct sediment transport measurements.

Typically, changes at monumented cross-sections are used to calculate the net change in sediment storage, requiring some sort of extrapolation between successive cross-sectional profiles. In this work, however, the detailed surveys and digital elevation models produced from them allow for the direct calculation of the net change in sediment storage within various segments of the channel. Reach 1 was divided into 14 segments for which changes in sediment storage were calculated; reach 2 was divided into 10 segments and reach 3 into 11 (Figure 5.4.1). Volumetric sediment transport into and out of each segment was calculated by specifying a zero transport condition between two successive segments at an appropriate location, allowing some estimate of sediment transport to be made. The zero transport plane was located so as to produce no negative transport rates.

The designation of a zero transport plane in reaches 1 and 2 is somewhat arbitrary; in reach 1 the zero transport plane was set at the upstream edge of zones 1 and 14 for the spring and July events, respectively, and in reach 2 at the upstream edge of zones 10 and 1, respectively (Figure 5.4.1). In reach 3, the zero transport plane location reflects the effect of the weir upstream of the reach; the zero transport plane is located at cross-sections 4 and 1, for the spring and July events, respectively (see Figure 5.4.4). The

resultant transport rates for each zone boundary were averaged to produce a reach estimate, as per the other approaches. In addition, the maximum transport rates were calculated, indicating the peak within-reach transport rate. The results are presented below in Table 7.1.3.

Table 7.1.3. Sediment Budget Estimates of Average and Maximum Sediment Transport Rates.

Reach	Event	Average Transport Rate (kg/m/event)	Maximum Transport Rate (kg/m/event)	Zone
1	Spring Freshet	4,752	12,493	14
	July 20, 1997	8,675	17,883	2
2	Spring Freshet	7,509	11,651	2
	July 20, 1997	14,428	33,945	10*
3	Spring Freshet	6,534	17,798	11
	July 20, 1997	43,736	66,322	7

* max. transport rate for this zone is at the downstream boundary. It is at the upstream boundary for all other zones

The maximum transport rates are substantially higher than the reach average transport rates, and represent the peak within-reach transport rate, similar to the paired erosion zone rates. The maximum transport rates occurred at various locations in the three reaches for the two events; the zone for which the maximum transport rate occurs (as calculated at the upstream edge of the zone) is also included in Table 7.1.3.

In reach 1, the peak transport rate, based on the sediment budget approach, occurs at the upstream boundary of zone 14, i.e. along the downstream edge of bar 2, where cut-bank retreat has supplied a large volume of sediment to the stream channel. During the July 20, 1997 event, the peak transport rate in reach 1 occurred at the upstream boundary of zone 2, which corresponds to the middle of bar 1. However, the peak transport rates in reach 1 for the spring and July 20 events are not substantially different, indicating that there is likely a very significant through-put component during the July 20 event, thereby producing a significant underestimation of the transport rate in this reach for the July 20 event.

In reach 2, the peak transport rate occurred at the upstream edge of zone 2, corresponding to the upstream edge of bar 1 (the mid-channel bar) during the spring

freshet. During the July 20 event, the peak transport rate occurred at the downstream edge of zone 10; the transport rate is nearly twice that of peak rate in reach 1.

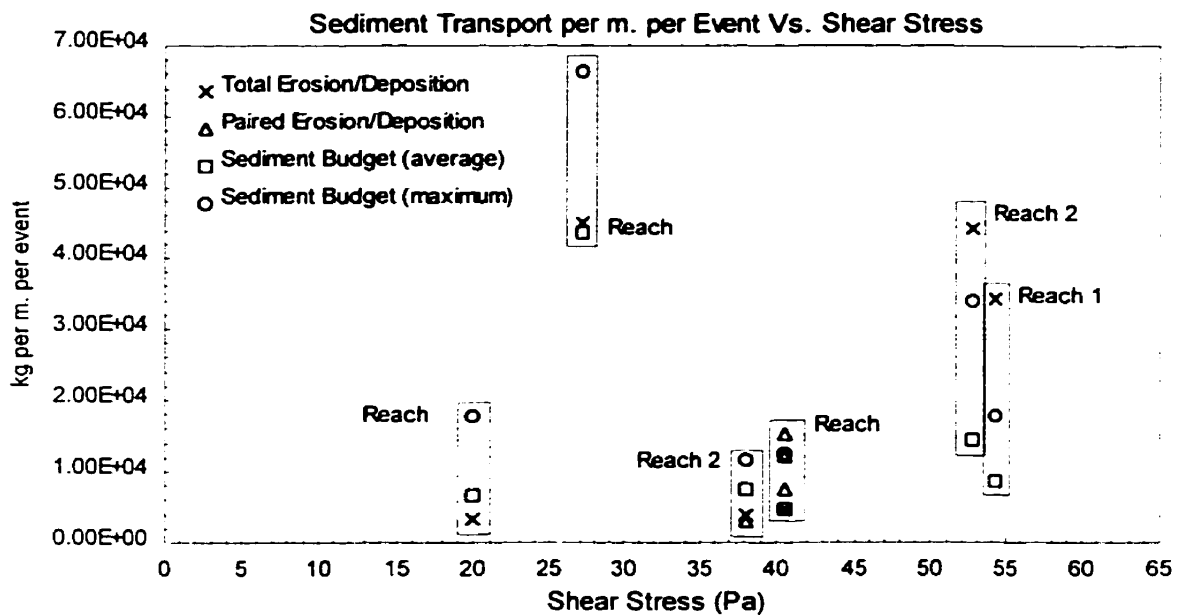
The peak transport rate occurred in reach three at upstream boundary of zone 11, near the transition from a predominantly gravel-bed channel substrate to a sand-bed substrate. During the July 20 event, the peak transport rate occurs at the upstream boundary of zone 7 during the spring freshet, corresponding to the head of bar 3. These data are also presented graphically below in figure 7.1.3.

7.1.4) SUMMARY OF TRANSPORT ESTIMATES

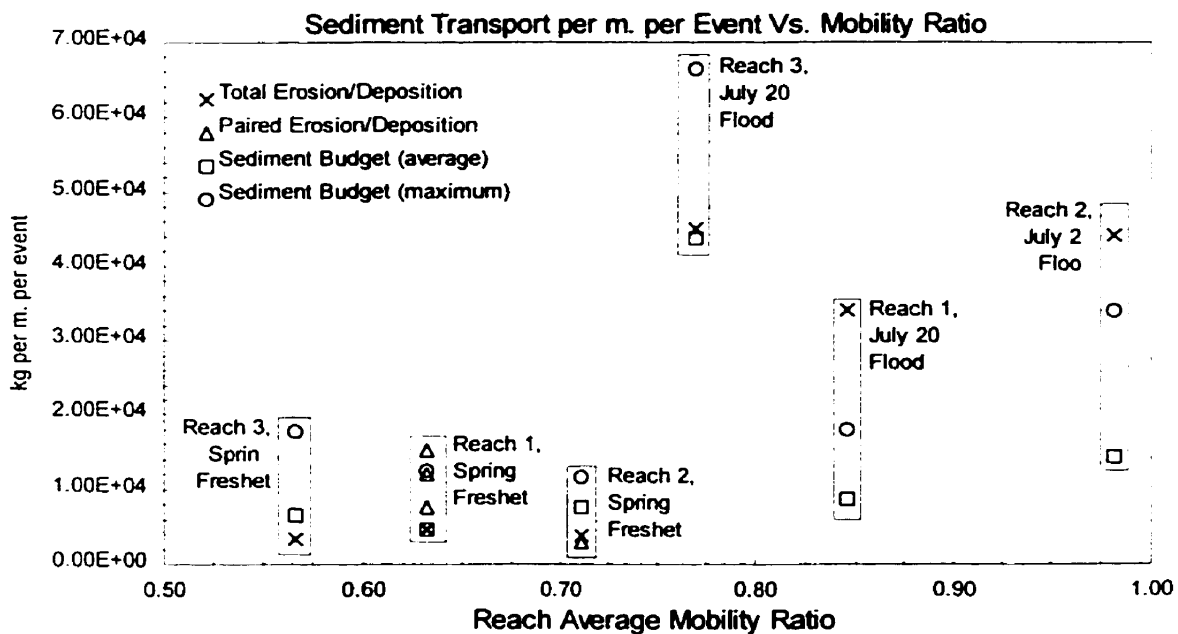
All the estimates made by the various techniques are presented below, in figure 7.1.3. These are minimum estimates of sediment transport because they are all based on net scour and fill occurring during a flood event. Note that the average sediment budget estimates correspond rather well with the total erosion/deposition estimates for all three reaches during the spring freshet (points with lower shear stress). In fact, the sediment budget approach produces reach average transport rates that exceed the total erosion/deposition rates in reaches 2 and 3, and which correspond almost exactly with the total erosion/deposition rates in reach 1. Maximum sediment budget estimates made for reach 3 are higher than those made based on typical step length estimates and equation (1).

However, there is a large discrepancy between both the average and the maximum sediment budget and total erosion/deposition approaches for reaches 1 and 2 for the July flood. Here, the sediment budget approach (both average *and* maximum estimates) underestimates the transport rate produced by the total erosion/deposition method significantly, reflecting a significant sediment throughput component for this event.

For reach 3, where the weir upstream may have produced a zero transport condition at the upstream boundary of the reach during the two transport events, there is a close agreement between the average sediment budget transport estimates and the total erosion/deposition estimates; the maximum sediment budget estimates are significantly higher for both events in reach 3.



A) Sediment Transport per Meter of Width per Event *versus* Shear Stress (Pa)



B) Sediment Transport per Meter of Width per Event *versus* Reach Average Mobility Ratio

Figure 7.1.3. Sediment Transport per Meter of Width per Event - All Data.

As expected, the paired erosion/deposition estimates are higher than the total erosion/deposition rates in reach 1, where the pairs were adjacent to the thalweg, and slightly less than the erosion/deposition zone rates in reach 2, where transport was occurring over the bar head rather than the thalweg. The maximum sectional transport rates calculated using the sediment budget approach for the spring freshet correspond with the paired erosion/deposition estimates in reach 1 for the same event; during the spring freshet, the maximum sediment budget transport rate in reach 2 exceeded both the paired erosion/deposition and the total erosion/deposition estimates.

It should be reiterated at this point that the above estimates are by necessity minimum transport rates, and that the 'true' transport rates (including suspended and bedload through put) are likely larger than all the above estimates. However, the methods applied produced consistent, coherent results. Where discrepancies exist, they can be understood in terms of the assumptions made in each approach or in terms of reach specific conditions. While the planimetric changes occurring in each of the reaches are not overwhelming, especially for the spring freshet, it is quite possible that most sediment transport occurring within such low energy channels does produce net changes in sediment storage, and would therefore be reflected by the types of sediment transport calculations made above. Detailed bed surveys are capable of resolving these changes, and can be used to produce consistent estimates of bedload transport in the same way as coarser surveys can be used to produce transport estimates in the presence of more striking planimetric adjustments occurring in braided channels.

7.2) COMPARISON OF TRANSPORT ESTIMATES FROM THE SAINTE MARGUERITE AND SUNWAPTA RIVERS

To make comparisons of the average transport rates between these two very different systems, it is necessary to make some assumptions about the duration of the transport events. Goff and Ashmore (1994) have estimated that the duration of transport events in their study of the Sunwapta River is typically about 6 hours. For the Sainte Marguerite River, there is no data from any source on the likely duration of the flow during the spring freshet; the spring freshet in fact encompasses more than one peak.

During the July 20 event, stage data on the North-East branch indicates that the flow was at bankfull stage or higher for three days; thus, the event duration can be estimated to be 72 hours.

For the July 20 event, calculations of the sediment transport rate in $\text{kg m}^{-1} \text{s}^{-1}$ were made for the erosion/deposition zone method and the sediment budget method in all three reaches. The results of these calculations and a summary of rates reported by Goff and Ashmore (1994) are presented in table 7.2.1.

Table 7.2.1. Sediment Transport Estimates on the Sainte Marguerite July 20 Flood and Sunwapta Rivers.

Sainte Marguerite River ¹			Sunwapta River ²		
Reach	Erosion/Deposition Zone kg/m/s	Sediment Budget kg/m/s		Erosion/Deposition Zone kg/m/s	Sediment Budget kg/m/s
1	0.132	0.033		0.018 - 0.213 ³	0.0076 - 0.2263
2	0.170	0.056		0.035 - 0.394 ⁴	.
3	0.174	0.169	Ave	0.083 ²	0.066
				0.165 ³	

1: Based on a sediment transport event of 72 hours duration 2: Source: Goff and Ashmore (1994) 3: based on a step length of 40 m 4: based on a step length of 80 m

The estimates of the sediment transport rates during the July 20 event in all three reaches using the erosion/deposition zone method are comparable to the estimates made on the Sunwapta River with a step length of 80 m. This indicates that the level of activity during the July 20 event approached those typical of a proglacial braided system. The sediment budget estimate for the Sainte Marguerite likewise corresponds well with that of the Sunwapta.

Given appropriately detailed survey techniques, it thus seems that the inverse method is capable of producing reliable transport rates in lower energy gravel-bed systems such as the Sainte Marguerite River, as well as in braided systems. While the planimetric channel adjustments --even during exceptional events such as the July 20 event-- are not nearly so striking as those occurring in a typical braided system, low amplitude vertical adjustments can be resolved using the appropriate survey techniques,

from which transport estimates can be derived. It should be noted that braided rivers exhibit substantial vertical adjustment as well, which increases the likelihood of missing real scour and fill.

8) IMPLICATIONS FOR SALMONID SPAWNING HABITAT STABILITY

The stability of spawning zones is a key factor in the success of salmonid stocks. Mobilization of the bed can improve spawning habitat by flushing excess fine particles from the gravel matrix (Adams and Beshta, 1980; Carling, 1987), or it may adversely affect habitat by introducing fines to lower levels in the substrate (Lisle, 1989; Nawa and Frissell, 1993). Given that the burial depth of the salmonid eggs is typically between 10 and 50 cm (Milhous, 1982; Lisle, 1989; Montgomery *et al.* 1996; DeVries, 1997), bed scour can pose a direct threat to egg survival if a sufficient thickness of the bed is mobilized during the incubation period (Lisle, 1989; Nawa and Frissell, 1993). Net deposition --especially of fine sediment-- upon spawning beds can also have detrimental effects on the eggs by inhibiting fry emergence or by reducing the inter-gravel flow, which maintains the appropriate dissolved oxygen concentrations while also removing waste product produced by developing eggs (Vaux, 1962; Phillips, 1971; Koski, 1972; Beshta and Jackson, 1978; Carling and McCahon, 1987). While the important question of spawning zone sedimentology must be left to a further study, the available data shed light on scour and fill patterns over spawning beds.

Given the importance of spawning beds to salmon production in river systems, an examination of the impacts of the two flood events of 1996 upon the stability of potential spawning zones was thus undertaken. Potential spawning zones were defined as the zone upstream of the riffle crest of a well-developed riffle, where salmon are normally expected to spawn (Stuart, 1953; Milhous, 1982). The maximum width of the zone was taken to be the estimated water surface width during low to moderate flows (in this case, corresponding to a discharge of about 10 m³/s, roughly corresponding to the flows occurring during spawning in October). Although the distribution of redds depends on adult salmon densities in the system, downwelling zones coming up to the riffle crest are thought to be preferred habitat. Here, the streamwise length of the potential spawning zone was taken to be one channel width from the middle of the riffle crest. Two potential spawning zones were identified in this way in each of the three reaches (figures 5.1.1, 5.2.1, 5.3.1). Scour exceeding various threshold values was tabulated for all such zones

and for both floods. The results are presented in table 8.1, for threshold scour of 10, 20 and 40 cm.

Table 8.1. Percent of Designated Spawning Zones Subject to Net Erosion, 1996.

Reach 1	Spring Freshet			July 20 Flood		
	≥ 10 cm	≥ 20 cm	≥ 40 cm	≥ 10 cm	≥ 20 cm	≥ 40 cm
average ¹	22%	11%	3%	38%	23%	10%
zone 1	46%	23%	0%	85%	63%	15%
zone 2	40%	30%	16%	37%	27%	15%
Reach 2						
average ¹	16%	8%	4%	28%	17%	6%
zone 1	1%	0%	0%	28%	10%	5%
zone 2	15%	2%	0%	48%	32%	10%
Reach 3						
average ¹	10%	4%	2%	42%	34%	14%
zone 1	1%	0%	0%	85%	81%	47%
zone 2	5%	0%	0%	26%	18%	1%

¹: refers to percent of entire reach subject to net erosion within each depth class

Given that egg burial depths range between 10 and 50 cm, it is clear that a substantial proportion of the potential spawning zones in reach 1 underwent significant detrimental scour during both events. According to DeVries (1997) any scour exceeding 20 cm would begin dislodging Atlantic salmon eggs, while scour exceeding 30 cm would generally remove all eggs present. Consider, too, that net scour depth (the result of scour and subsequent fill) is likely to be less than the maximum scour depth, which is the critical measure for egg survival. In reach 1, during the freshet, nearly 1/4 of the potential spawning zone in zone 1 was scoured to a depth of 20 cm or more, while in zone 2 nearly 1/3 of the zone was similarly affected; the reach average (including all bed areas) was only 11%. Scour was concentrated along the thalweg. The degradation of riffle 2 and the extension of the pool upstream of riffle 4 affected the spawning zones in reach 1. In the other two reaches, the potential spawning zones were substantially more stable during the spring freshet (Table 8.1).

During the July 20 event, significant impacts occurred to all spawning zones in all reaches. In reach 1, fully 63% of zone 1 was scoured to a depth of 20 cm or more, while in zone 2, 27 % scoured to 20 cm or more. The exact distribution of scour and fill for all identified potential zones in all reaches for both events is shown in figure 8.1. Both

values exceed the areal average value of 23%. In reach 2, the scour depths were somewhat less on average, though 28% of zone 1 scoured to a depth of 10 cm or more, which is equal to the areal average. Forty-eight per cent of zone 2 scoured to a depth of 10 cm or more, indicating above average bed scour. In Reach 3, 47% of zone 1 was scoured to a depth in excess of 40 cm; 81% of zone 1 scoured to a depth greater than or equal to 20 cm. Zone 2 was less drastically affected, with only 26% of the zone undergoing scour of 10 cm or more.

Scour continued to be focused on the thalweg, with both riffle degradation and pool extension processes. Lateral migration of the thalweg --as the cut banks retreated-- was important in controlling the distribution of spawning zone scour. Sediment supply limitations due to the weir upstream of reach 3 also contributed to the overall degradation of the spawning zones, as did the protected cut bank upstream of zone 1 in reach 1, which was responsible for the degradation of riffle 2.

In summary, it is clear, that significant proportions of all the spawning zones were negatively impacted by erosion during the July 20 event, while only the zones in reach 1 were affected detrimentally during the spring flood.

In the above analysis, the component of net deposition on top of spawning zones has been ignored. Presented below is the total area of potential spawning habitat which underwent either net erosion or net deposition, by greater than various specified threshold amounts.

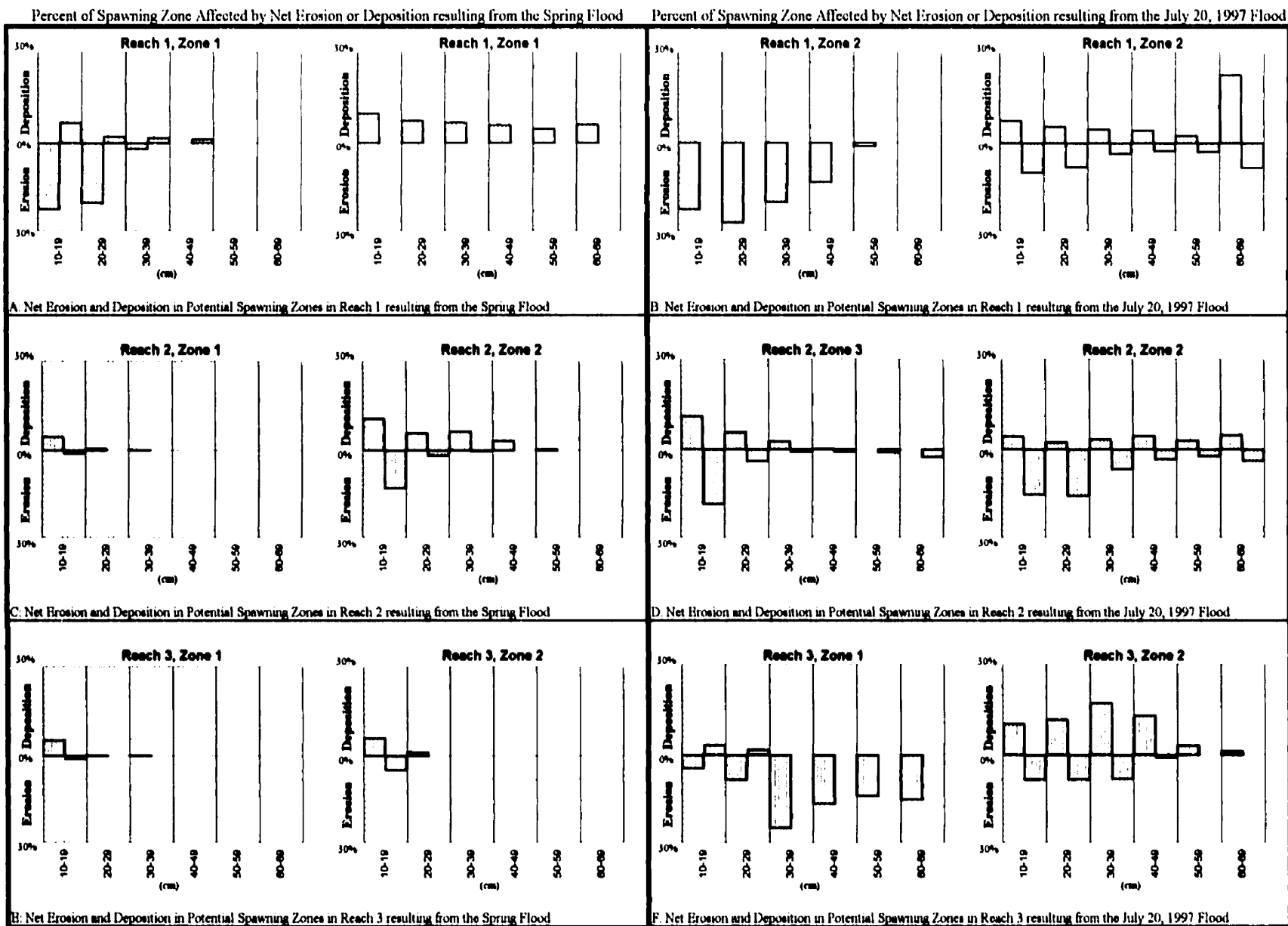


Figure 8.1 Distribution of Net Scour and Fill in Potential Scour Zones in All Three Reaches

Percentages refer to the proportion of the zone subject to scour or fill of the magnitude indicated, size classes are expressed in cm.

Table 8.2. Percent of Designated Potential Spawning Zones Affected by Erosion or Deposition, 1996.

Reach 1	Spring Freshet			July 20 Flood		
	>10 cm	>20 cm	>40 cm	>10 cm	>20 cm	>40 cm
average	42%	19%	3%	67%	45%	25%
zone 1	57%	28%	1%	85%	63%	15%
zone 2	40%	30%	16%	83%	65%	44%
Reach 2						
average	41%	21%	10%	66%	44%	21%
zone 1	6%	0%	0%	48%	18%	5%
zone 2	42%	18%	3%	71%	50%	22%
Reach 3						
	25%	9%	2%	66%	50%	21%
zone 1	7%	0%	0%	90%	82%	47%
zone 2	12%	1%	0%	83%	64%	18%

Note that, during the spring freshet, 42% of zone 2 in reach 2 underwent a net change of 10 cm or more, which likely represents a significant detrimental effect. Eighteen per cent of this zone underwent a net change of 20 cm or more. The zones in reach 3 were not significantly impacted during the spring freshet.

During the July 20 event, more than 80% of zones 1 and 2 in reach 1 underwent a net change of 10 cm or more, while more than 60% of these two zones underwent a net change of 20 cm or more. In zone 2, fully 44% of the bed underwent a net change of 40 cm or greater. In reach 2, 48% of zone 1 underwent a net change of 10 cm or more, while 71% of zone 2 underwent a similar change. Half of zone 2 underwent a net change of 20 cm or greater. In reach 3, both reaches were significantly impacted; 82% of zone 1 underwent a net change of 20 cm or more, while 64% of zone 1 underwent a similar net change. Clearly, significant detrimental changes to the riffle environments occurred during this event, which --had there been eggs in the substrate-- would likely have severely depleted the salmon stocks.

In the study reaches, an important control on the spatial distribution of deposition in spawning zones was the abandonment of one branch of the main channel surrounding a medial bar. In both reaches 2 and 3, the July 20 event has caused the left branch of the

main channel to fill as the thalweg shifted towards the outer bank. This mechanism was responsible for the preponderance of the observed fill in riffle environments.

The observed impacts on spawning zones were related to channel morphology, channel alterations and event magnitude. Within reach 1, important impacts occurred in both spawning zones during both events. The relatively straight channel pattern allows for a greater downstream component of bar movement, which by necessity involves net scour of the riffle environment as the riffle crest shifts downstream with the bar. This process was exacerbated by the bank protection measures, which forced the channel to maintain its straight pattern. In addition, the presence of bank protection cut off the sediment supply from the cut bank which, resulting in a corresponding net erosion of the channel bed in the vicinity of the riffle just downstream of the protected bank. Zone 1 in reach 1 was subject to net erosion of 10 cm or greater over 46% of the area, which is likely a direct result of the bank protection upstream.

In reach 2, erosion was not a significant threat to the spawning zones during the freshet. However, significant deposition occurred within zone 2 during this event. This deposit is likely related to the bank protection measures. The bank protection has halted the natural retreat of the cut bank, which normally occurs to accommodate deposition on the point bar face. However, the bank protection has caused significant deposition to occur where otherwise it might not.

Event magnitude controls the severity of these problems as well. It is clear that the July 20 event, which was the largest recorded flood on the North-East branch of the Sainte Marguerite River, had dramatic effects on all the zones in all the reaches, where between 48% and 90% of the bed in the potential spawning zones underwent a net change of 10 cm or more. The spring freshet resulted in changes of 10 cm or more to between 6% and 57% of the bed in the potential spawning zones.

9) CONCLUSIONS

The present work has identified clear patterns of morphologic adjustment in response to two distinct flood events. The resultant patterns were broadly consistent with the existing paradigm of meander development and maintenance. Where bank protection measures existed, the patterns of channel response -- although different from the usual pattern of meander development-- were predictable given the concepts embodied in the existing paradigm of meander development. The channel response to the second flood was consistent with that to the first, despite the different event magnitudes. The primary difference was the extent of the channel over which bedform evolution occurred, as opposed to bedform change. No shift in channel pattern occurred during the flood of July 20, despite its exceptional size.

Several techniques were used to calculate sediment transport rates based on the observed spatial arrangement of net changes in sediment storage. The results are consistent with those reported by Goff and Ashmore (1994) on the braided Sunwapta River. Sediment transport per event was found to be strongly related to reach scale mobility ratio, despite the different patterns of channel response in the three reaches in response to the two flood events. The average rates of transport during the July 20 event were of the same magnitude as those reported by Goff and Ashmore (1994) for a braided system, indicating the exceptional size of this event.

The effect of such channel mobility on potential spawning habitat was quite significant. Large portions of the potential spawning zones underwent either net fill or net scour during both events. Bank protection measures seem to have contributed to the most severe case of spawning zone erosion 46% of a spawning riffle site immediately downstream of a recent bank revetment underwent detrimental net scour of 10 cm or more during the spring freshet while fully 85% of the zone was similarly affected during the July 20 event. Such severe disturbance was not observed for the three spawning zones downstream of unprotected banks.

REFERENCES

- Adams, J.N. and R.L. Beschta. 1980. Gravel bed composition in Oregon Coastal Streams. *Can. J. Fish. Aquat. Sci.* vol. 37: 1514-1521.
- Andrews, E.D. 1979. Scour and fill in a stream channel, East Fork River, Western Wyoming. *USGS Professional Paper* 1117, 49p.
- Andrews, E.D. 1983. Entrainment of gravel from naturally sorted riverbed material. *Geol. Soc. Am. Bull.* vol. 94: 1225-1231.
- Andrews, E.D. 1984. Bed material entrainment and hydraulic geometry of gravel bed rivers in Colorado. *Geol. Soc. Am. Bull.* vol. 95: 371-378.
- Andrews, E.D. and G. Parker. 1987. Formation of a coarse surface layer as the response to gravel mobility. in *Sediment Transport in Gravel-bed Rivers*. ed(s) C.R. Thorne, J.C. Bathurst and R.D. Hey. p.269-325.
- Andrus, C.W., Long, B.A. and H.A. Froehlich. 1988. Woody debris and its contribution to pool formation in a coastal stream 50 years after logging. *Can. J. Fish. Aquat. Sci.* vol. 45: 2080-2086.
- Ashmore, P.E. 1991. Channel morphology and bed load pulses in braided, gravel-bed streams. *Geografiska Annaler.* vol 73: 37-52.
- Ashmore, P.E. 1991. How do gravel-bed rivers braid. *Can. J. Earth Sci.* vol. 28: 326-341.
- Ashmore, P.E. and M. Church. 1995. Sediment transport and river morphology: a paradigm for study. *prepared for Gravel-bed Rivers IV Workshop*.
- Baker, V.R. 1977. Stream-channel response to floods, with examples from central Texas. *Geological Survey Bulletin.* vol. 88: 1057-1071.
- Bathurst, J.C., Thorne, C.R. and R.D. Hey. 1979. Second flow and shear stress at river bends. *J. Hydraul. Div. HY10.* vol. 105: 1277-1295.
- Begin, Z.B. 1981. Stream curvature and bank erosion: a model based on the momentum equation. *Journal of Geology.* vol. 89: 497-504.
- Bencala, K.E. 1984. Interactions of solutes and streambed sediment. 2. A dynamic analysis of coupled hydrologic and chemical processes that determine solute transport. *Water Resources Research*, vol. 20 (12):1804-1814.
- Bencala, K.E., V.C. Kennedy, G.W. Zellweger, A.P. Jackman and R.J. Avanzino. 1984. Interactions of solutes and streambed sediment. 1. An experimental analysis of cation and anion transport in a mountain stream. *Water Resources Research*, vol. 20 (12):1797-1803.
- Beschta, R.L. and W.L. Jackson. 1978. The intrusion of fine sediments into a stable gravel bed. *J. Fish. Res. Board Can.* vol. 36: 204-210

- Beschta, R.L. and W.S. Platts. 1986. Morphologic features of small streams: significance and function. *Water Resources Bulletin*. vol. 22(3): 369-378.
- Carling, P.A. 1987. Bed stability in gravel streams with reference to stream regulation and ecology. In: K. Richards (ed.), *River Channel, Environmental Process*. Blackwell Oxford, p. 272-294.
- Carling, P.A. 1991. An appraisal of the velocity-reversal hypothesis for stable pool-riffle sequences in the River Severn, England. *Earth Surface Processes and Landforms*. vol. 16: 19-31.
- Carling, P.A. and C.P. McCahon. 1987. Natural siltation of brown trout spawning gravels during low-flow conditions. *in Regulated Streams: advances in ecology*. J.F. Craig and J.B. Kemper, (ed.s). Plenum Press, New York. pp. 229-244.
- Carson, M.A. and G.A. Griffiths, 1989. Gravel transport in the braided Waimakariri River: mechanisms, measurements and predictions. *J. Hydrology*. vol 109: 201-220.
- Church, M. 1983. Pattern of instability in a wandering gravel bed channel. *Spec. Publ. int. Ass. Sediment*. vol. 6: 169-180.
- Church, M. 1994. Channel morphology and typology. *in The Rivers Handbook*. P. Callow and G.E. Petts (ed.s). Blackwell Publ. Oxford.
- Church, M. and Jones, D. 1982. Channel bars in gravel-bed rivers. *in Gravel-bed Rivers*. R.D. Hey, J.C. Bathurst and C.R. Thorne (ed.s). pp. 291-324.
- Church, M. and M.A. Hassan. 1992. Size and distance of travel of unconstrained clasts on a streambed. *Water Resources Research*. vol. 28(1): 299-303.
- Church, M., McLean, D.G. and Wolcott, J.F. 1987. River bed gravels: sampling and analysis. *in Sediment Transport in Gravel-Bed Rivers*. Thorne, C.R., Bathurst, J.C. and Hey, R.D. (ed.s).
- Church, M. Miles, M.J. and K.M. Rood. 1987. Sediment transfer along Mackenzie River: a feasibility study. Environment Canada, Inland Waters Directorate, Western and Northern Region, Sediment Survey Section, Report IWD-WNR(NWT)-WRD-SS-87-1.
- Clifford, N.J. and Richards, K.S. 1992. The reversal hypothesis and the maintenance of riffle-pool sequences: a review and field appraisal. *in Lowland Floodplain Rivers: Geomorphological Perspectives*. P.A. Carling and G.E. Petts (ed.s).
- Colby, B.R., 1964. Scour and fill in sand bed rivers. USGS Professional Paper 462-D, 32p.
- Desloges, J.R. and M. Church. 1992. Geomorphic implications of glacier outburst flooding: Noeick River valley, British Columbia. *Can. J. Earth Sci.* vol. 29: 551-564.
- DeVries, P. 1997. Riverine salmonid egg burial depths: review of published data and implications for scour studies. *Can. J. Fish. Aquat. Sci.* vol. 54: 1685-1698.
- Dietrich, W.E., Kirchner, J.W., Ikeda, H. and Iseya, F. 1989. Sediment supply and the development of the coarse surface layer in gravel-bedded rivers. *Nature*, vol. 340: 215-216.

- Dinehard, R.L. 1992. Gravel-bed deposition and erosion by bedform migration observed ultrasonically during storm flow, North Fork Toutle River, Washington. *J. Hydrology*. vol. 136: 51-71.
- Ferguson, R. and P. Ashworth. 1991. Slope-induced changes in channel character along a gravel-bed stream: the Alt Dubhaig, Scotland. *Earth Surface Processes and Landforms*. vol. 16: 65-82.
- Ferguson, R.I. 1993. Understanding braiding processes in gravel-bed rivers: progress and unsolved problems. *in Braided Rivers*. Best, J.L. and Bristow, C.S. (ed.s). Geological Society Special Publication No. 75. pp. 73-87.
- Foley, M.G. 1978. Scour and fill in steep, sand bed ephemeral streams. *Bull. Geol. Soc. Am.* vol. 89: 559-570.
- Gilvear, D.J. and Harrison, D.J. 1991. Channel change and the significance of floodplain stratigraphy: 1990 flood event, Lower River Tay, Scotland. *Earth Surface Processes and Landforms*. vol. 16: 753-761.
- Goff, J.R. and P.E. Ashmore. 1994. Gravel transport and morphological change in braided Sunwapta River, Alberta, Canada. *Earth Surface Processes and Landforms*. vol. 19: 195-212.
- Gomez, B. 1994. Effects of particle shape and mobility on stable armour development. *Water Resources Research*. vol. 30(7): 2229-2239.
- Gomez, B. and Church, M. 1989. An assessment of bed load sediment transport formulae for gravel bed rivers. *Water Res. Res.* vol. 25(6): 1161-1186.
- Gupta, A. 1983. High-magnitude floods and stream channel response. *Spec. Publs. int. Ass. Sediment.* vol. 6: 219-227.
- Harvey, A.M. 1984. Geomorphological response to an extreme flood: a case from southeast Spain. *Earth Surface Processes and Landforms*. vol. 9: 267-279.
- Harvey, J.W. and K.E. Bencala. 1993. The effect of streambed topography on surface-subsurface water exchange in mountain catchments. *Water Resources Research*, vol. 29 (1): 89-98.
- Hassan, M.A. 1990. Scour, fill and burial depth of coarse material in gravel bed streams. *Earth Surface Processes and Landforms*. vol. 15: 341-356.
- Hassan, M.A. and M. Church. 1992. Virtual rate and mean distance of travel of individual clasts in gravel-bed channels. *Earth Surface Processes and Landforms*. vol. 17: 617-627.
- Hey, R.D. 1976. Geometry of river meanders. *Nature*. vol. 262: 482-484.
- Hickin E.J. 1974. The development of meanders in natural river-channels. *American Journal of Science*. vol. 274: 414-442.
- Hooke, R. 1975. Distribution of sediment transport and shear stress in a meander bend. *The Journal of Geology*. vol. 83(5): 543-565.

- House, P.K. and P.A. Pearthree. 1995. A geomorphic and hydrologic evaluation of an extraordinary flood discharge estimate: Bronco Creek, Arizona. *Water Resources Research*. vol. 31(12): 3059-3073.
- Hubbel, D.W. 1964. Apparatus and techniques for measuring bedload. *USGS Water Supply Paper*. 1748: 74 pp.
- Huckleberry, G. 1994. Contrasting channel response to floods on the middle Gila River, Arizona. *Geology*. vol. 22: 1083-1086.
- Jackson, R.G. 1975. Velocity-bedform-texture patterns of meander bends in the lower Wabash River of Illinois and Indiana. *Geol. Soc. Am. Bull.* vol. 86: 1511-1522.
- Keller, E.A. 1971. Areal sorting of bed-load material: the hypothesis of velocity reversal. *Geol. Soc. Am. Bull.* vol. 82: 753-756.
- Keller, E.A. and Brookes, A. 1973. Consideration of meandering in channelization projects: selected observations and judgments. *in River Meandering, Proc. Conf. Rivers*, 1983. ASCE. New Orleans. 384-397.
- Keller, E.A. and J.L. Florsheim. 1993. Velocity-reversal hypothesis: a model approach. *Earth Surface Processes and Landforms*. vol. 18: 733-740.
- Keller, E.A. and Swanson, F.J. 1979. Effects of large organic material on channel form and fluvial processes. *Earth Surf. Processes* vol. 4: 361-380.
- Keller, E.A. and W.N. Melhorn. 1973. Bedforms and fluvial processes in alluvial stream channels: selected observations. *in. Fluvial Geomorphology*. M. Morisawa (ed.). London. George Allen & Unwin.
- Keller, E.A. and W.N. Melhorn. 1978. Rhythmic spacing and origin of pools and riffles. *Geol. Soc. Am. Bull.* vol. 89: 723-730.
- Koski, K.V. 1972. Effects of sediment on fish resources. *Fish. Res. Instit., Univ. Washington*, Seattle, Wash, 36 p.
- Lane, S.N., Richards, K.S. and J.H. Chandler 1995. Morphological estimation of the time-integrated bed load transport rate. *Water Resources Research*. vol. 31(3): 761-772.
- Langbein, W.B. and Leopold, L.B. 1968. River channel bars and dunes-theory of kinematic waves. *USGS Prof. pap.* 422-L.
- Langbein, W.B. and Leopold, L.B. 1968. River meanders-theory of minimum variance.. *USGS Prof. pap.* 422-H.
- Laronne, J.B. and M.J. Duncan. 1989. Constraints on duration of sediment storage in a wide, gravel-bed river, New Zealand. *IAHS Publication* 184: 165-172
- Laronne, J.B., D.N. Outhet, P.A. Carling and T.J. McCabe. 1994. Technical Note: Scour chain employment in gravel bed rivers. *Catena*, vol. 22: 299-306.
- Leeder, M.R. 1983. On the interactions between turbulent flow, sediment transport and bedform mechanics in channelized flows. *Spec. Publ. Int. Ass. Sediment.* vol. 6:5-18.

- Leopold, L.B. and W.W. Emmett. 1984. Bedload movement and its relation to scour. in Elliot, C.M. (ed.) *River Meandering, Proceeding of the Conference Rivers 83*, Publ. by Am. Soc. Civil. Eng. 640-649.
- Leopold, L.B. and Emmett, W.W. 1984. Bedload movement and its relation to scour. in *River Meandering; Proceedings of the 1983 Conference on Rivers, ASCE*. C.M. Elliot (ed.) 640-649.
- Leopold, L.B., W.W. Emmett and R.M. Myrick. 1966. Channel and hillslope processes in a semi-arid are, New Mexico, USGS Professional Paper 352-G: 193-253.
- Leopold, L.B., Wolman, M.G. and J.P. Miller. 1964. *Fluvial Processes in Geomorphology*. W.H. Freeman and Co. San Francisco.
- Leviasky, S. 1955. An introduction to fluvial hydraulics. Constable, London. pp. 257.
- Likens, G.E. and R.E. Bilby. Ref. 38. Development, maintenance, and role of organic-debris dams in New England Streams.
- Lisle, T. 1979. A sorting mechanism for a riffle-pool sequence: Summary. *Geol. Soc. Am. Bull.* vol. 90: 616-617.
- Lisle, T. 1989. Sediment transport and resulting deposition in spawning gravels, North Coastal California. *Water Resources Research.* vol. 25(6): 1303-1319.
- Magilligan, F.J. 1992. Thresholds and the spatial variability of flood power during extreme floods. *Geomorphology*, vol. 5: 373-390.
- Milhous, R.T. 1982. Effect of sediment transport and flow regulation on the ecology of gravel-bed rivers. in *Gravel-bed Rivers*. R.D. Hey, J.C. Bathurst and C.R. Thorne (ed.s). pp. 819-842.
- Miller, A.J. 1990. Flood hydrology and geomorphic effectiveness in the Central Appalachians. *Earth Surface Processes and Landforms.* vol. 15: 119-134.
- Mlynarczyk, Z. and Rotnicki, K. 1989. Flood and vortex scour of the channel bed of the Prosna River, and their depth range. *Earth Surface Processes and Landforms.* vol. 14: 365-373.
- Montgomery, D., J. Buffington, N. Peterson D. Schuett-Hames and T. Quin. 1996. Stream-bed scour, egg burial depths and the influence of salmonid spawning on bed surface mobility and embryo survival. *Can. J. Fish. Aquat. Sci.* vol. 53: 1061-1070.
- Mosley, M.P. 1981. The influence of organic debris on channel morphology and bedload transport in a New Zealand forest stream. *Earth Surface Processes and Landforms.* vol. 6: 571-579.
- Mosley, M.P. 1981. The influence of organic debris on channel morphology and bedload transport in a New Zealand forest stream. *Earth Surf. Processes and Landforms.* vol. 6.: 571-579.
- Nanson, G.C. and E.J. Hickin. 1983. Channel migration and incision on the Beaton River. *J. Hydraul. Eng.* vol. 109(3): 327-337.

- Nawa, R.K. 1993. Measuring scour and fill of gravel streambeds with scour chains and sliding bead monitors. *N. Am. J. Fish. Man.* vol. 13: 634-639.
- Neill, C.R. 1969. Bedforms in the Lower Red Deer River, Alberta. *J. Hydrol.* vol. 7: 58-85.
- Neill, C.R. 1971. River bed transport related to meander migration rate. *Am. Soc. Civil Eng. Proc. J. Waterways, Harbours and Coastal Eng. Div.* vol. 97: 783-786.
- Neill, C.R. 1987. Sediment balance considerations linking long-term transport and channel process. *in* *Sediment Transport in Gravel-bed Rivers.* C.R. Thorne, J.C. Bathurst and R.D. Hey. (ed.s). pp. 225-240.
- Nicholas, A.P., Ashworth, P.J., Kirkby, M.G. and Murray, T. 1995. Sediment slugs: large-scale fluctuations in fluvial transport rates and storage volumes. *Prog. in Phys. Geog.* vol. 19(4):500-519.
- Nolan, K.M. and Marron, D.C. 1985. Contrast in stream-channel response to major storms in two mountainous areas of California. *Geology*, vol. 13: 135-138.
- O'Neill, M.P. and A.D. Abrahams. 1984. Objective identification of pools and riffles. *Water Resources Research.* vol. 20(7): 921-926.
- Parker, G. 1976. On the cause and characteristics scales of meandering and braiding in rivers. *Journal of Fluid Mechanics.* vol. 76(3):457-480.
- Parker, G., P.C. Klingeman and D.L. McLean. 1982. Bedload size and distribution in paved gravel-bed streams. *J. Hydraul. Div. Am. Soc. Civ. Eng.* vol. 108(HY4): 544-571.
- Phillips, R.W. 1971. Effects of sediment on the gravel environment and fish production, p. 64-74. *in* *Forest land uses and stream environment.* J.K. Krygier and J.D. Hall (ed.s).
- Popov, I.V. 1962. A sediment balance of river reaches and its use for the characteristics of the channel process. *Transactions of the State Hydrologic Institute.* vol. 94: 3-21. Translated in *Soviet Hydrology 1962*: 249-267.
- Prus-Chacinski, T.M. 1954. Patterns of motion in open-channel bends. *Assoc. Int. d'Hydrologie, Publ.* 38. vol. 3: 311-318.
- Reid, I. and L.E. Frostick. 1994. Fluvial sediment transport and deposition. *in* *Sediment Transport and Depositional Processes.* K. Pye (ed). 89-192.
- Reid, I. Frostick, L.E. and Layman, J.T. 1985. The incidence and nature of bedload transport during flood flows in coarse-grained alluvial channels. *Earth Surface Processes and Landforms.* vol. 10: 33-44.
- Richards, K.S. 1976a. The morphology of riffle-pool sequences. *Earth Surface Processes.* vol. 1: 71-88.
- Richards, K.S. 1976b. Channel width and the riffle-pool sequence. *Geol. Soc. Am. Bull.* vol. 87: 883-890.

- Richards, K.S. 1978. Channel geometry in the riffle-pool sequence. *Geografiska Annaler*. vol. 60: 23-27.
- Sear, D.A. 1996. Sediment transport processes in pool-riffle sequences. *Earth Surface Processes and Landforms*. vol. 21: 241-262.
- Stuart, T.A. 1953. Spawning, migration, reproduction and young stages of loch trout. *Freshwater and Salmon Fisheries Res. Sta. H.M. Stationary Off. Edinburgh*. pp. 39.
- Thorn, C.R. and Hey, R.D. 1979. Direct measurements of secondary currents at a river inflection point. *Nature*. vol. 280(19): 226-228.
- Tinkler, K.J. 1970. Pools, riffles and meanders. *Geol. Soc. Am. Bull.* vol. 81: 547-552.
- Turnpenny, A.W.H. and R. Williams. 1980. Effects of sedimentation on the gravels of an industrial river system. *J. Fish. Biol.* vol. 17: 681-693.
- Vaux, W.G. 1962. Interchange of stream and intergravel water in a salmon spawning stream. *U.S. Dept. Int. fish Wildl. Serv., Spec. Sci. Rep., Fish.* 405: 11p.
- Walder, J.S. and Driedger, C.L. 1994. Rapid geomorphic change caused by glacial outburst floods and debris flows along Tahoma Creek, Mount Rainier, Washington, U.S.A. *Arctic and Alpine Research*. vol. 26(4):319-327.
- Warburton, J. 1994. Channel change in relation to meltwater flooding, Bas Glacier d'Arolla, Switzerland. *Geomorphology*. vol. 11:141-149.
- Wilcock, P.R. 1996. Estimating local bed shear stress from velocity observations. *Water Resources Research*. vol. 32(11):3361-3366.
- Wolman, M.G. and L.B. Leopold. 1957. River flood plains: some observations on their formation. *USGS Prof. Pap.* 282-C.

APPENDIX A: SEDIMENT TEXTURE VARIATIONS

A.1) REACH 1

Samples of the surface and subsurface material were made at three bar heads before and after the July 1996 flood. The first two bars are completely within the reach, while the third bar head is located on the downstream boundary of the reach in June 1996, and beyond it in August. Bulk samples were taken of the surface and the underlying subsurface material at each location. Wolman type grid-by-number samples were also taken at each of the above sample points as well as at various points along the bar surface for the two bars within the reach (locations shown on figure 5.1.1).

The surface and subsurface distributions, based on the bulk sampling techniques, are shown on figure A.1. From these distributions, the D50 and D85 have been extracted in Table A.1 to illustrate any changes in sediment texture over the course of the flood.

Table A.1. Bed and Surface D50 and D85, Reach 1, Prior to and Following July 20, 1996.

	June D ₅₀ (mm)	Aug. D ₅₀ (mm)	June D ₈₅ (mm)	Aug. D ₈₅ (mm)
Bar 1, Subsurface	33	39	69	80
Bar 1, Surface	41	49	75	89
Bar 2, Subsurface	27	31	68	77
Bar 2, Surface	64	62	102	101
Bar 3, Subsurface	25	19	74	70
Bar 3, Surface	54	59	85	100

From this data, it is clear that some pattern of textural evolution seems to have occurred. The percentage change in the above parameters is presented below. Changes less than 10% were given a value of zero, or no change, given sampling uncertainties (Church *et al.*, 1987).

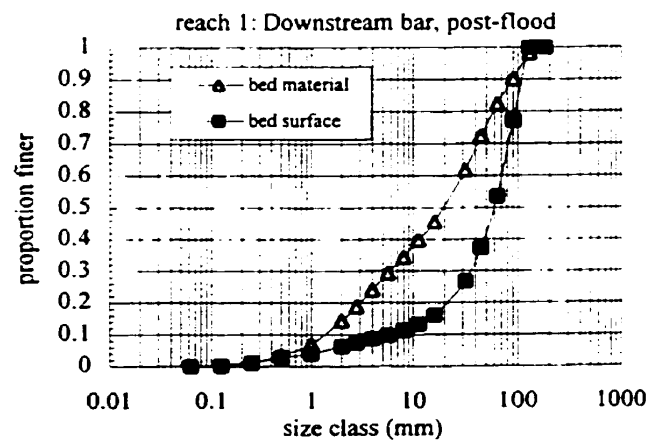
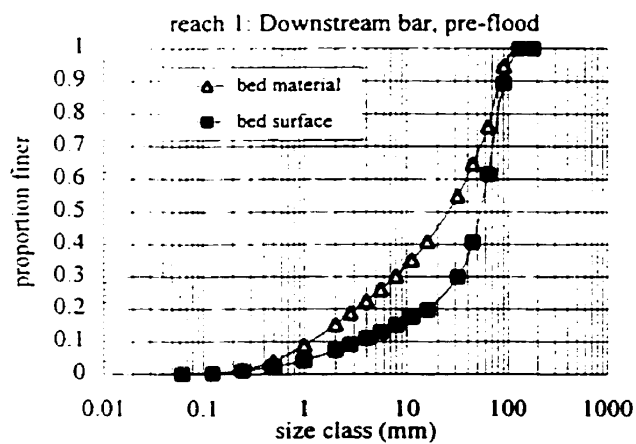
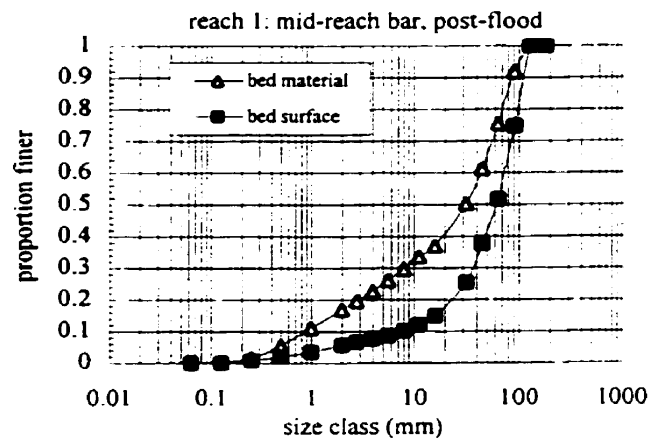
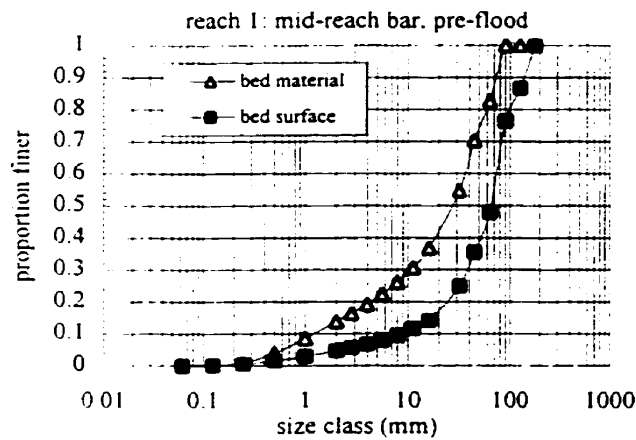
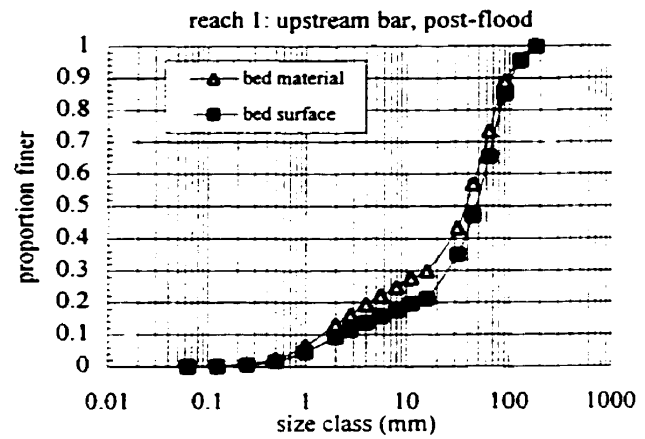
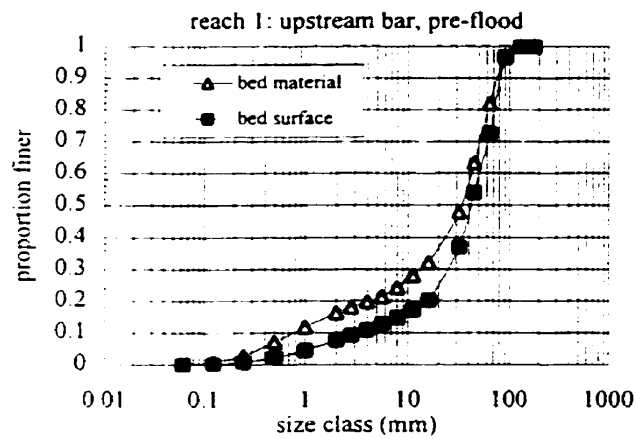


Figure A.1: Surface and Subsurface Sediment Texture Distribution, Reach 2, Based on Bulk Sediment Samples, Prior to and Following July 20 flood. Sample located on figure 5.1.1

Table A.2. Textural Modifications occurring in Reach 1 during the July 20 Flood Event.

	ΔD_{50} Subsurface	ΔD_{50} Surface	ΔD_{85} Subsurface	ΔD_{85} Surface
Bar 1	+18%	+20%	+16%	+19%
Bar 2	+15%	0	+13%	0
Bar 3	-24%	0	0	+18%

A net coarsening of the sediment texture following the flood is evident for bars 1 and 2, while the downstream bar exhibits no change or possible fining of the bed material. This suggests that there has been a net export of the finer fraction of sediment from the reach, which thereby implies a degree of size selective transport. However, the data are not extensive enough to draw general conclusions about the nature of the sedimentological changes that may have occurred.

A calculation of the armor ratio before and after the flood reveals that there has been no consistent direction for net change in the ratio. The armor ratio is simply the ratio of the median size of the surface to that of the underlying subsurface; it describes the coarseness of the surface relative to the underlying parent material (Dietrich *et al.*, 1989). It seems that at the bar head, there has been little alteration of the character of the armor surface (Table A.3). This does suggest, however, that the falling limb of the flood hydrograph was gradual enough to allow a reformation of the armor layer in the fashion described by Gomez (1994). Alternatively, it may be taken to indicate that the armor is not destroyed during a flood but remains, playing an integral role in the modification of the sediment entrainment thresholds as Andrews and Parker (1987) contend.

Table A.3. Armor Ratio, Reach 1, Based on Surface Texture and Bar Head Bed Material.

	U/S bar	Mid. bar	D/S bar
Arm. Ratio (June)	1.24	2.37	2.16
Arm. Ratio (August)	1.26	2.00	3.11

The Wolman sample distributions are shown in figure A.2. While the three Wolman samples taken on each of the bars within the reach are different following the flood, there is no consistent trend to this pattern of change. On the first bar, there has generally been a reduction in the range of sediment textures, that is, the typical pattern of downstream fining is not observed after the flood. This is likely due to the fact that all the sediment was deposited as a single unit --during the advance of avalanche face, both laterally and downstream, during the July flood-- as opposed to being the product of a number of floods and depositional units. The second bar has exhibited little systematic textural adjustment.

A.2) REACH 2

Three bulk samples of the surface and subsurface were taken on various bars within reach 2 preceding the July 1996 flood. At the same time, the surface at each of these locations by a Wolman type grid-by-number sample. The sample locations are shown on figure 5.2.1. In addition, grid by number samples were also taken at various other points on the point bar.

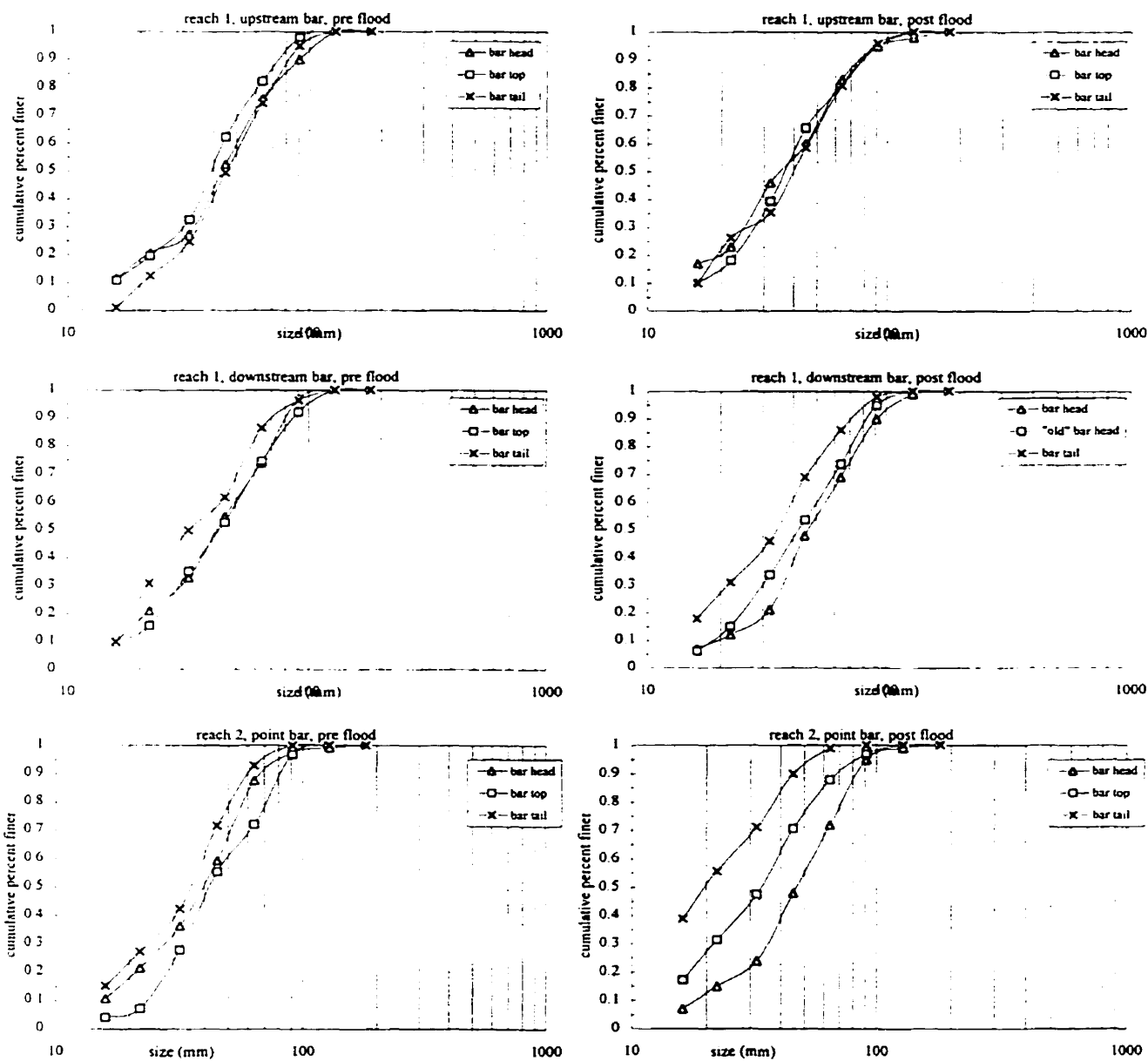


Figure A.2: Surface Texture Distributions, Reach 1 & 2, Based on Wolman Samples, Prior to and Following July 20 Flood

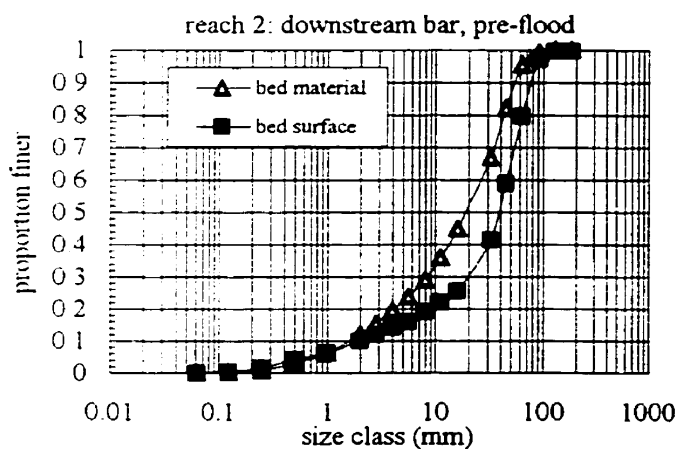
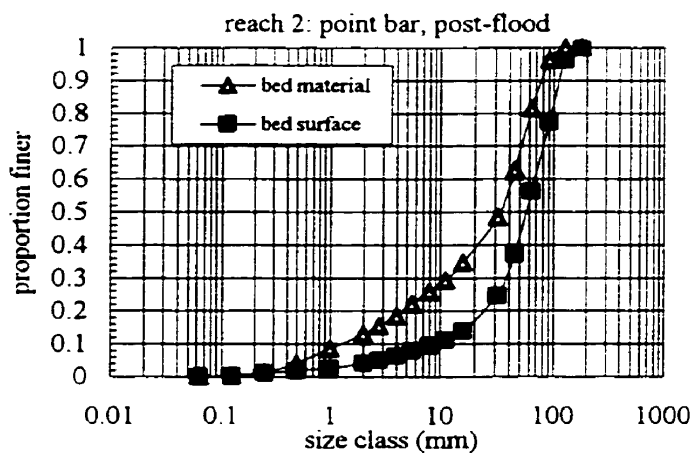
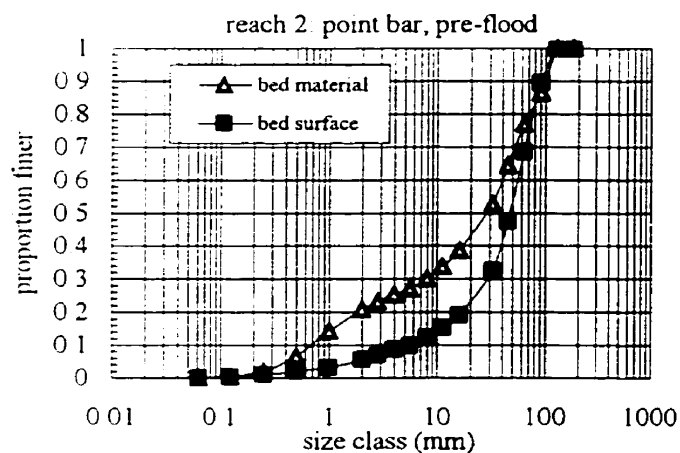
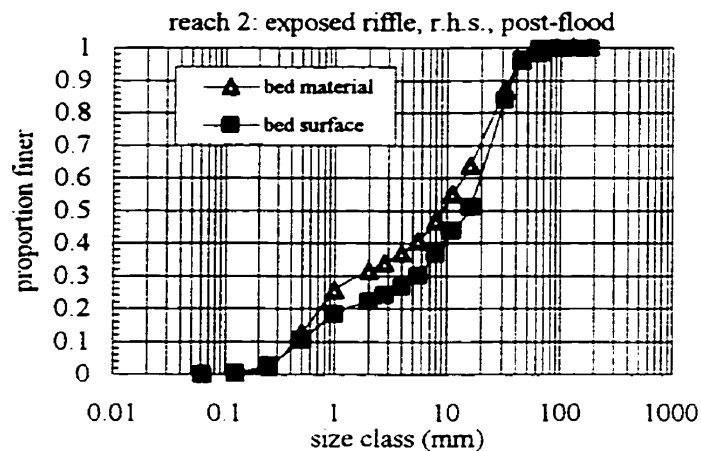
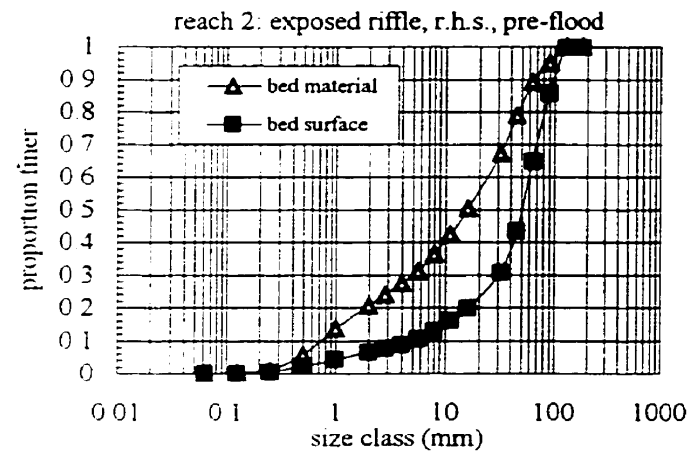


Figure A.3: Surface and Subsurface Sediment Texture Distribution, Reach 2, Based on Bulk Sediment Samples, Prior to and Following July 20 flood. Sample located on figure 5.2.1

Following the July flood, re-sampling in the same locations was attempted. However, two of the three initial sites were located on bedforms that had disappeared during the flood, and thus no re-sampling was possible. The only true paired, before and after sample in this reach is that of the point bar head. The point bar sample locations were based on morphologic association, and were in fact quite distant from each other. This could not be avoided, and was the direct result of the unusual amount of morphologic change occurring during the July flood. A sample was taken on the exposed riffle along the right bank after the flood, but it is not believed to represent an analogous deposit to that taken before the flood. The bar at the end of the reach that was sampled before the July flood was no longer present afterwards, and no sample was taken in August. The Wolman samples were repeated following the July flood, in approximately the same locations.

The distributions for the bulk surface and subsurface samples are shown in figure A.3. The Wolman samples for reach 2 are presented in figure A.2. The two samples of the point bar head can be compared, noting the direction of sedimentological change (though the limitations of having only one sample are obvious).

Table A.4. Bed and Surface D50 and D85 and Textural Modifications, Reach 2, Prior to and Following July 20.

	D50 (June)	D85 (June)	D50 (August)	D85 (August)
Subsurface	29	91	32	69
Surface	46	84	59	101
	D50 (b.m.)	D50 (Surf.)	D85 (b.m.)	D85 (Surf.)
Net Change	+10%	+28%	-24%	+20%

The data is very limited, and there are no conclusions that may be drawn from it. However, there may be a pattern of surface and subsurface coarsening at the point bar head following the July flood. The only discrepancy is the 24% decrease in the D85 of the bed material. Considering that the coarsest fraction of the sample is that which is most prone to error, this decrease may be an artifice of sample site selection and or size.

The Wolman samples, taken before and after the flood show a trend of increased variability in sediment texture following the flood (figure A.2). Most noticeable is the

much finer distribution found at the point bar tail. Also significant is the finer material found upon the point bar top following the flood. Where, before the July flood, the bar top and bar head had similar distributions, following it there is a very pronounced difference.

This illustrates a significant component of downstream fining, unlike that which occurred on the upstream bar in reach 1, where the post flood Wolman samples were much less different than before the flood. In part, the downstream fining noted on the point bar may be due to the upstream migration of the bar head as sediment has accumulated, thereby shifting the zone over which downstream fining can be expected to occur. In addition, increased supply of fine sediment from the upstream terrace may have caused the widening of the size distributions that were observed. It can be expected that subsequent, lower flows will progressively winnow fine material from the bar top surface, possibly returning the range of observed distributions to that formerly observed.

A.3) REACH 3

Sampling of the reach sediment texture was not possible prior to the July 20 flood. Persistently high flows covered the bars in this reach for a significant portion of the month of July. Following the July 20 event, the sediment texture was sampled using the bulk sampling techniques for the surface and subsurface material. Wolman samples were not used here, because the substrate was too fine for this method to be effective. The relevant parameters for the substrate in reach 3 is presented in figures 2.4.1 and 2.4.2, including a general map of the distribution of sediment textures within the reach.